CHARACTERIZING AND TARGETING THE JAK/STAT PATHWAY IN LGL LEUKEMIA

T. Tiffany Wang

Chapel Hill, NC

BS, Biology, University of North Carolina at Chapel Hill, 2009

MS, Biological and Physical Sciences, University of Virginia, 2016

A dissertation presented to the Graduate Faculty at the University of Virginia in Candidacy for the degree of Doctor of Philosophy

Department of Microbiology, Immunology and Cancer Biology

University of Virginia

April 2020

ABSTRACT

LGL leukemia is a rare hematological malignancy that typically runs an indolent course, but all patients eventually require treatment. LGL leukemia encompasses three subtypes; T-cell, chronic NK-cell and aggressive NK-LGL leukemia. Current LGL leukemia therapy includes utilization of broad immunosuppressants including Methotrexate, Cyclophosphamide and Cytoxan. While these drugs show efficacy in reducing symptoms, none of them are curative, and may cause adverse effects and higher susceptibility to infections. A central goal of the Loughran lab is to identify better therapeutics for LGL leukemia.

Genomic analysis of cancer offers the hope of identifying new treatments or aiding in the selection of existing treatments. Rare leukemias pose additional challenges in this regard as samples may be hard to acquire and the underlying pathway found may not be attractive to drug development since so few individuals are affected. The aim of this thesis is to further characterize the JAK/STAT signaling pathway in LGL leukemia. By using a combination of genomic and molecular biology methods, we can better understand what role this dysregulated pathway plays in the pathogenesis of LGL leukemia.

Whole genome sequencing was used on both a rat NK-LGL leukemia model (Chapter 2) and on T-LGL leukemia patient samples (Chapter 3). In both of these chapters, we discovered novel JAK1 and STAT3 mutations that were functionally characterized. First, a novel mutation in JAK1 was found in a spontaneously occurring LGL leukemia rat model cell line, RNK-16. This significant discovery revealed several things. This confirmed the significance of JAK/STAT pathway in a spontaneous LGL leukemia model and this activating mutation increased downstream STAT signaling. Interestingly, this mutation was the only oncogene mutation confirmed in *ex vivo* RNK-16 leukemia material, meaning this mutation was there from the beginning and may explain in part, why it is more aggressive than the other strains.

Lastly, we tested the efficacy of a peptide that blocks IL-15 signaling pathway (Chapter 4). Our pre clinical data showed the induction of apoptosis in LGL leukemia cells and the reduction of downstream pathways relevant to the pathogenesis of LGL leukemia.

This resulted in the start of a phase 1/2 clinical trial that enrolled 20 LGL leukemia patients spanning four medical centers across the US. This trial showed clinical efficacy in a few patients, indicating a need for further studies and to continue the fight for a cure for LGL leukemia.

ACKNOWLEDGEMENTS

First and foremost, I would like to thank my thesis advisor, Dr. Tom Loughran, who has helped me to succeed in graduate school. I am inspired by your passion in caring for your patients and your dedication to your research lab. Thank you for being my advocate and I am grateful to have had the opportunity to work in your lab.

I would also like to thank Dr. Dave Feith for his mentorship and leadership in lab. Without you, I know I would not be the scientist or writer that I am today. Thank you for your encouragement and patience with my manuscript writing, and your time and energy in helping everyone succeed in lab. I am truly lucky to have had your support and guidance.

Dr. Tom Olson, thank you for guidance in helping me learn the language of DNA. I started graduate school not really knowing much about chromatin and now I've written a chapter on ATAC-seq. Without your mentorship, my projects would not have progressed to where it is now.

Thank you to the members of my thesis committee (Dr. David Brautigan, Dr. Tim Bender, Dr. Jim Casanova, and Dr. Mitch Smith) for your time and guidance during my committee meetings. Thank you for making my meetings enjoyable and for your feedback and questions that have pushed me to become a better scientist.

I have been fortunate to work in a fun and supporting lab environment and I thank everyone that has been a part of the Loughran lab. Jennifer, thank you for being there with me through thick and thin and for being my lunch and shopping bestie. I suppose I am lucky that you wanted to sabotage me in our first rotation as graduate school would not have been as fun or entertaining without you by my side. Su-Fern and Wendy, thank you welcoming me to the other (AML) side of the Loughran Lab. I truly enjoy and appreciate our chats and you guys always give the best advice. Thank you to everyone else in the Loughran lab for making my time in graduate school a pleasant experience.

Lastly, I would like to thank my family. Since the start of graduate school, my family has tripled in size. I am so grateful to my new family for their support and for

welcoming me in with open arms. In particular, thank you to David Hawks for believing in me and being by my side. Graduate school would have been more tough without your support. Finally, I would like to thank my parents for their many sacrifices in order to give my brother and I the best opportunities. Most importantly, thank you to my mom for all the home cooked meals she sent me home with.

Thank you to Kayla Friedman and Malcolm Morgan of the Centre for Sustainable Development, University of Cambridge, UK for producing the Microsoft Word thesis template adapted to produce this document.

T. Tiffany Wang - April 2020

CONTENTS

LIST OF TABLES

LIST OF FIGURES

1 INTRODUCTION

1.1 LARGE GRANULAR LYMPHOCYTE LEUKEMIA

Large granular lymphocyte (LGL) leukemia is a rare chronic disorder that typically results from clonal expansion of $CD3^+CD8^+$ cytotoxic T-lymphocytes or $CD3^-$ natural killer (NK) cells that are localized to the blood, spleen and liver [1–4]. It is characterized by an infiltration of clonally expanded large granular lymphocytes, which are a distinct subset of normal circulating blood cells. In healthy adults, LGLs represent 10-15% of peripheral blood mononuclear cells (PBMCs). LGLs become activated through antigen interaction, resulting in expansion followed by death by apoptosis after antigen clearance. LGL leukemia cells are activated cytotoxic cells characterized by profoundly dysregulated apoptosis, resulting in leukemic LGL survival and expansion. These expanded leukemic LGL can take over 50-90+% of patient PBMCs, causing neutropenia, anemia and other symptoms. The median survival is 9-10 years [5] and patients typically die from severe infections.

CLINICAL ENTITIES

LGL leukemia was first described in 1985 as a disorder involving clonal invasion of the blood, marrow and spleen [6]. In 1999, the World Health Organization (WHO) classification recognized T- and NK-cell LGL leukemia as separate entities [2], and in 2008, added an additional chronic NK-cell LGL leukemia as a provisional entity to distinguish from the more aggressive form [7]. Most recently in 2016, WHO classification recognized mutational subsets [8].

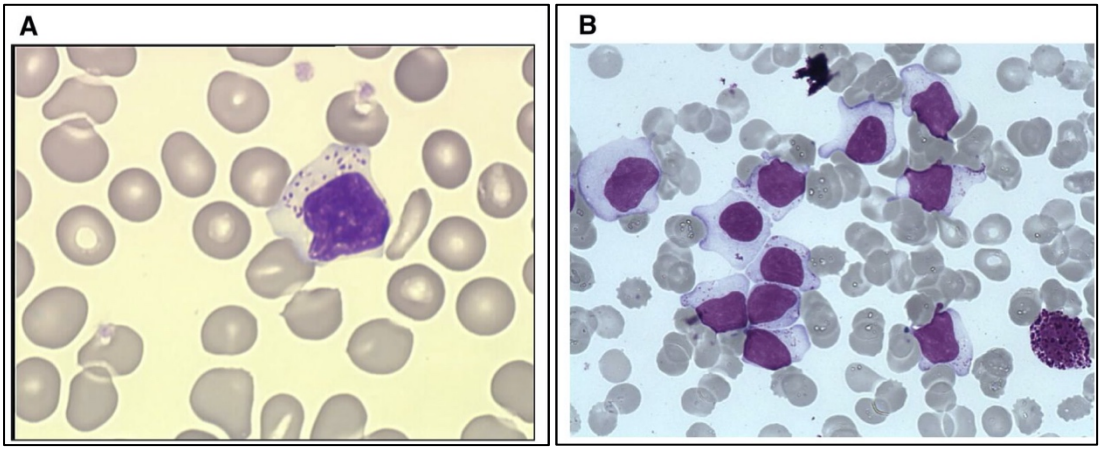

Figure 1.1: Blood smears of normal and leukemic cells

[A] Blood smear showing normal LGL. [B] Blood smear showing expansion of LGL characteristic of leukemia [1].

CHRONIC LGL LEUKEMIA

Chronic LGL leukemia can be of T-cell or NK-cell origin. Chronic T-LGL leukemia is the most common entity, accounting for 85% of all cases. The median age of diagnoses is 66.5, affecting both men and women equally. Cell surface markers of T-LGL leukemia are typically $CD3^{+}CD8^{+}CD56^{-}CD57^{+}CD28^{-}TCR\text{-}\alpha\beta^{+}$. On the other hand, chronic NK-LGL leukemia is typically $CD3^{-}CD8^{+}CD56^{+}CD16^{+}$ [9]. Chronic NK-LGL leukemia makes up about 10% of cases and shares many of the clinical and molecular features with chronic T-LGL leukemia.

AGGRESSIVE NK-LGL LEUKEMIA

This subset of NK-LGL leukemia is the most rare subtype, representing 5% of cases, and is the most aggressive. Patients are typically younger with a median age of 39 with poor prognosis. It is associated with Epstein-Barr virus and most patients are of Asian descent [1].

DIAGNOSIS AND SYMPTOMS

Blood and bone marrow smears (**Figure 1.1**) are used to diagnose LGL patients. Criteria for LGL leukemia includes elevated number of circulating LGL cells (Figure 1.1b). Normal levels of circulating LGL in peripheral blood is 0.25×10^9 LGL/Liter. Patients are diagnosed with LGL leukemia when sustained counts of LGL are at or above $0.4 - 2 \times 10^9$ LGL/Liter present with symptoms such as fever, fatigue, frequent infections and unexplained weight loss [9]. These symptoms are reflective of underlying issues like anemia and neutropenia [10]. to examine relative quantity and morphology of cells, and presence of at least 20% blasts generally constitutes diagnosis with acute leukemia. [11]. At diagnosis, flow cytometry is performed to calculate percentage of $CD3^+$, $CD16^+$, $CD8^+$, and $CD57^+$ cells. Additionally, sequencing of the T-cell receptor (TCR) is used to determine clonality of leukemic cells. In T-LGLL, clonality can be tracked via the unique T-cell receptor (TCR) gene rearrangement that happens during T-cell maturation. As this is a permanent and irreversible genetic event, it may be used as a unique genetic barcode. The TCR is composed of two chains, either α and β or γ and δ, and its unique rearrangement is detectable by standard clinical methods to determine the presence of a clonal expansion without necessarily yielding information about the sequence [12,13]. In NK-LGLL or CLPD-NK, clonality is harder to assess since a unique receptor rearrangement is not part of the normal biology. Instead, a restricted pattern of killer immunoglobulin-like receptor (KIR) expression by immunophenotyping has been used as a surrogate of clonality, though it is difficult to say whether the same receptor expression corresponds to the same genetic clone.

TREATMENT

Currently there is no cure for LGL leukemia. While the majority of patients follow an indolent disease progression, LGL is typically treated with broad immunosuppressants. At time of diagnosis, ~45% of patients require treatment for symptoms. The first line of treatment is Methotrexate (MTX) and if no response is observed, then administration

of cyclophosphamide is used [14]. These immunosuppressants help in achieving a 50% complete response. However, immunosuppressants like MTX are associated with increased infection rates and other toxicities[15]. There is a desperate need to develop new therapeutic options for LGLL, which can provide patients with a better quality of life.

1.2 PATHOGENESIS

The current understanding of pathogenesis of LGL leukemia begins with unknown chronic antigen activation of LGLs [1]. (**Figure 1.2**) These activated T-cells undergo clonal expansion that result in production of inflammatory cytokines, followed by evasion of apoptosis through a resistance to Fas [14,16]. Neutrophils are sensitive to the increase of soluble Fas and undergo apoptosis, causing neutropenia and other cytopenias. To date, the etiology of LGL leukemia has not been fully established. There are several hypothesized theories under investigation: viral transformation, chronic antigen-driven stimulus, and somatic oncogenic mutation. It is important to note that these mechanisms are not mutually exclusive; thus, one or more may be relevant in a given patient and the LGL leukemia patient population as a whole.

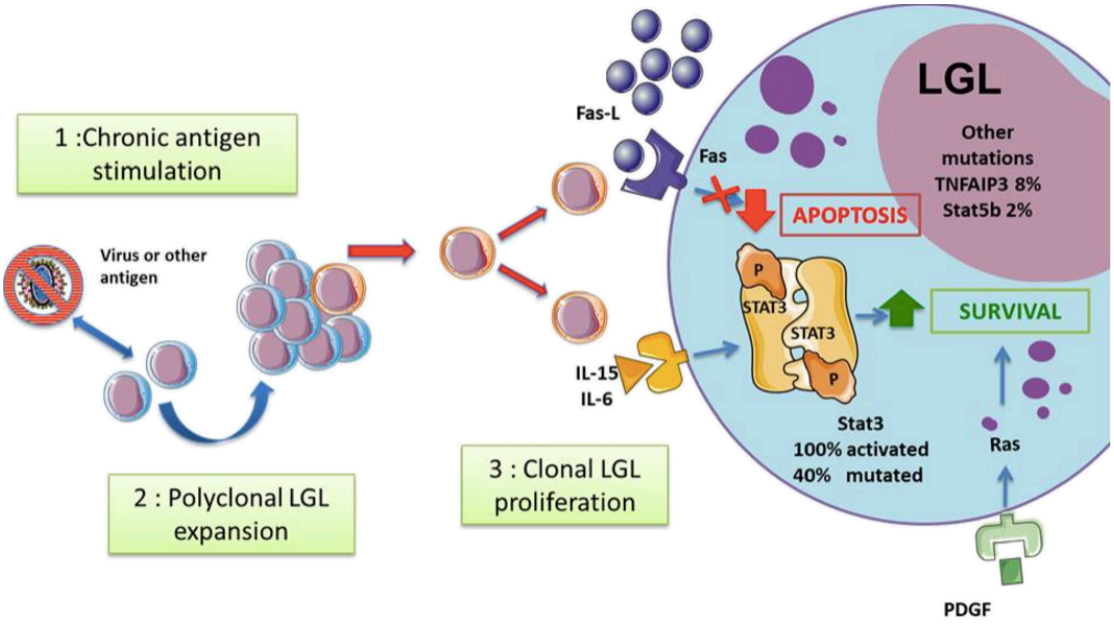

Figure 1.2 Current model of pathogenesis of LGL leukemia [17].

The initiating step of pathogenesis of LGL leukemia is a chronic antigen stimulation leading to a sustained clonal proliferation. Evasion of activated induced cell death is promoted by resistance to Fas and an increase of cytokine (IL-15) and growth (PDGF) factors. Sustained STAT3 activation is explained, in part, by external stimuli and also in part by STAT3 somatic activating mutations.

CHRONIC ANTIGEN STIMULATION

The terminal effector memory ($CD45RA^{+}/CD62L^{-}$) phenotype of T-LGLL cells suggests the possibility of chronic antigen exposure as a driver of LGL expansion [16]. Compatible with this hypothesis, several studies examining the antigen-specific sequence of the T-cell receptor or its combinatorial rearrangements in the variable region have found a nonrandom distribution [18–21]. It is hypothesized that these restricted clonotypes may predispose an individual toward the extreme monoclonal expansions commonly found in T-LGL leukemia [22]. However, whether the observed restricted clonotypes may be a cause (for example, a restricted repertoire that prevents clearance of antigen) or an effect (for example, the result of a chronic antigen, such as cytomegalovirus (CMV) [23] or HTLV [24]) remains inconclusive, with some studies only finding clonotype restriction in T-LGLL subtypes [25] and all studies lacking in large sample size. In the NK-LGL leukemia subtype, killer immunoglobulin-like (KIR) receptors play an analogous role to the activation of T-cell receptors in T-LGL

leukemia. Several studies [26–29] have found a skewing of the ratio of activating to inhibitory KIR receptors in favor of activation. Interestingly, expansion of T cell clones has also been detected in half of a cohort of chronic NK-LGL leukemia patients, with some of these patients progressively switching to T-LGL leukemia [30]. Activating KIRs have also been found in other autoimmune diseases, suggesting that this phenotype may contribute to the pathogenesis of the disease. Moreover, the HLA associations with HLADR4 [31], HLA-DR15 [32], and HLA B7 [22] suggests a possible autoimmune predisposition, blurring the lines between autoimmune disorders and leukemia.

VIRAL TRANSFORMATION IN LGL LEUKEMIA

The etiology of viral transformation has been explored in all forms of LGL leukemia. A documented association of Epstein-Barr virus (EBV), a known oncogenic initiator, with the aggressive form of NK-LGL leukemia was shown in several Japanese studies [33,34]. However, this contrasts with a failure to find EBV DNA in NK-LGL leukemia patients of Western Europe and the United States [35], which may explain the differences in clinical presentation (EBV-associated LGL leukemia in Asia is more aggressive and invasive). In addition to EBV, human T-lymphotropic virus (HTLV), also known to be oncogenic, has been explored as a causative agent in LGL leukemia. Retroviral infection has been only rarely documented in LGL leukemia [36], however some studies have shown a higher prevalence of seroreactivity to human HTLV-1 envelope protein in LGL leukemia patients [37,38] and in patients with NK-cell variant LGL leukemia or CLPD of NK [39], compared to reference cohorts. Although not linked to disease, the HTLV tax protein has been successfully employed to create experimental model systems [40,41]. More recently, studies from our lab confirmed seroreactivity with HTLV-1/2 transmembrane envelope protein, BA21 and found that family members sharing the same environment with a patient had elevated LGL counts and increased seroreactivity [42], providing evidence suggesting a common viral pathogen in the initiation of LGL leukemia.

DYSREGULATED SURVIVAL PATHWAYS

Dysregulated apoptosis has been shown to be an important mechanism in the pathogenesis of LGL leukemia. Based on their expression of Fas (CD95) and Fas-Ligand (CD178) [43,44], leukemic T cell LGLs are activated cytotoxic cells that escaped Fas-mediated activation-induced cell death (AICD) [16,45]. In addition, soluble Fas in patient sera [46], may act as a decoy receptor that negates Fas-induced AICD. The expansion of leukemic T and NK LGL cells may result from constitutive activation of one or several survival pathways: JAK/STAT3/Mcl-1 [45], Ras/MEK/ERK [46,47], SFK/PI3K/AKT [48–50], and sphingolipid signaling [51,52]. The activating mutations in signal transducer and activator of transcription 3 (*STAT3*) in particular have been a major focus in recent research and will be discussed in more detail in the subsequent sections. A summary of these studied pathways is shown in **Figure 1.3.**

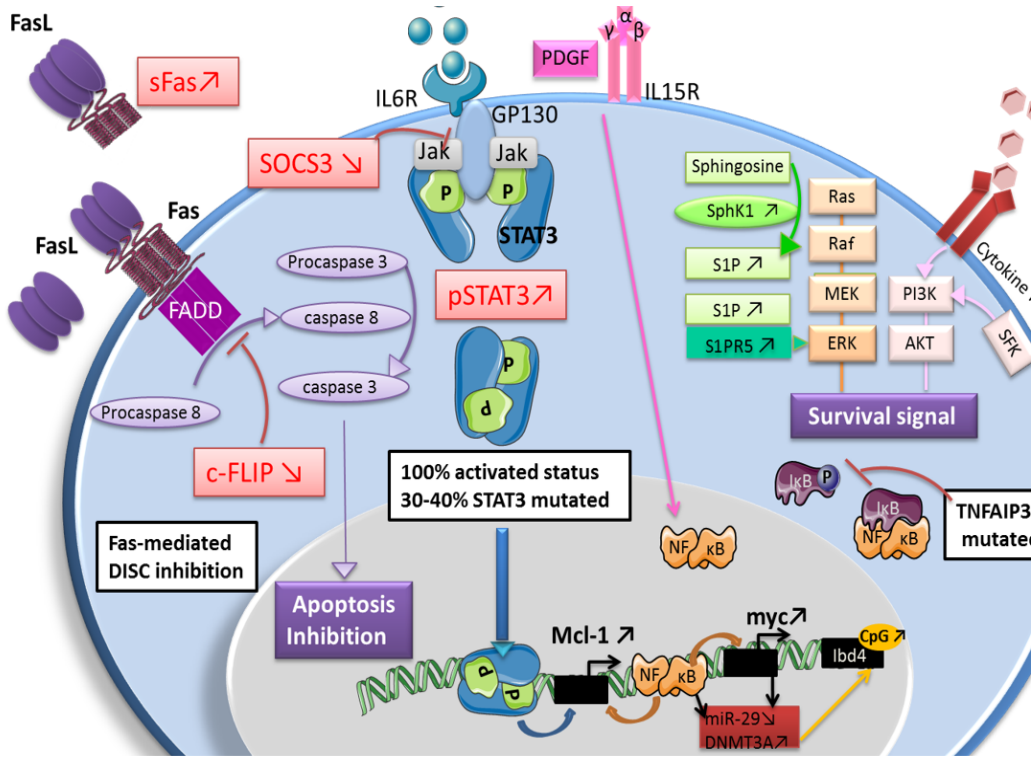

Figure 1.3: Aberrant signaling pathways in LGL leukemia adapted from [1]

IL-15 IN LGL LEUKEMIA

Interleukin 15 (IL-15) is a proinflammatory cytokine that has been implicated in the pathogenesis of LGL leukemia [53]. IL-15 is a member of the common gamma chain (γc) family and is proven to promote survival and proliferation of T-cells [54,55]. IL-15 binding to its receptor complex causes induction of several survival pathways such as JAK/STAT, Akt, and ERK pathways. Significantly elevated levels of IL-15 mRNA and IL-15Rα are found in patient PBMCs [56,57]. Using a systems biology approach, IL-15 was identified as one of two master regulators of the disease [53], making IL-15 an attractive target for therapies, which will be studied in Chapter 4.

JAK/STAT PATHWAY

JAK/STAT signaling pathway is essential for cell proliferation and survival. Extracellular signals transmit their messages through membrane bound receptors that activate this pathway. Ligand binding to its membrane bound receptor such as IL-15 to the IL-15 receptor complex phosphorylate the intracellular tail of the receptor complex that results in the activation of downstream pathways. The constitutive activation of this pathway in LGL leukemia is a hallmark of this disease.

Janus kinase (JAK) is a family of four tyrosine kinases that transduce signals from membrane bound receptors to downstream proteins. This family consists of JAK1, JAK2, JAK3 and TYK2. JAKs are activated by phosphorylation after ligand binding to the receptor. Phosphorylated JAKs then recruit downstream proteins such as STATs.

Signal transducer and activator of transcription (STAT) is a family of seven members: STAT1, STAT2, STAT3, STAT4, STAT5A, STAT5B, and STAT6. The STATs have similar domain structure with STAT3 being depicted in Fig. 1. STATs are cytoplasmic transcription factors that are activated by tyrosine phosphorylation and mediate cellular responses downstream of cytokine signaling. STAT3 regulates cell growth, differentiation and survival and is involved in cellular responses through cytokines

including interferons, interleukin (IL)-6 family and the common gamma chain family ILs, and growth factors [10]. Cytokine binding to receptors causes phosphorylation of Janus kinases (JAK), which in turn phosphorylate the intracellular tail of the receptor and create a docking site for STAT3. Once bound to the receptor, STAT3 becomes phosphorylated, dimerizes and translocates to the nucleus to bind directly to DNA, resulting in activation of multiple cellular pathways [11]. Both activating and dominant negative germline mutations in STAT3 cause a number of immune disorders [12], underlining its importance in multiple immune cell types.

1.3 GENOMICS OF LGL LEUKEMIA

Next-generation sequencing (NGS) methods such as whole-genome sequencing (WGS) and whole-exome sequencing (WES) have been shown to be more sensitive and quantitative for detection of mutations in peripheral blood samples [58] than traditional Sanger sequencing. With decreasing sequencing costs and increasing availability of bioinformatic approaches, WGS and WES have been utilized as relatively unbiased and powerful methods for high-resolution detection and quantification of genetic alterations in disease. While WGS is more expensive than WES, it has the advantage of detecting regulatory alterations such as in enhancers and non-coding regions which may be missed by WES, gene array, and targeted studies. Among leukemias, such approaches have already been applied in examples such as acute myeloid leukemia [59,60], chronic lymphocytic leukemia [61,62], multiple myeloma [63] and hairy cell leukemia [64]. The findings in these cases range widely from a single, causative mutation in almost all patients to multiple heterogeneous contributory mutations in a variety of pathways. Although genome-wide sequencing studies in LGL leukemia have been relatively small in scale, there is sufficient evidence from both WES and targeted studies for the role of activating STAT mutations in ~40% of patients. Most of the larger studies have been conducted on T-LGL leukemia as the NK-type is much rarer. Nevertheless, existing studies in NK-LGL leukemia have also found *STAT* mutations at a similar proportion

[25,65], which helps unify the two disease subtypes under a common molecular pathway. Even in patients without activating *STAT* mutations, the similarity of their leukemic gene expression profile, with a constitutively active STAT3 pathway, suggests other mutations may also activate the same pathway [66], supporting the role of a more comprehensive genome-wide characterization.

STAT3 MUTATIONS

Of perhaps the most significance, *STAT3* has been found to be the most prevalent mutated gene in T and NK cell LGL leukemia patients (reviewed in [67]). *STAT3* signaling controls the induction of downstream genes that are important for cell survival. *STAT3* is constitutively active in T-LGL leukemia patients, regardless of *STAT3* mutation status [53]; therefore, its pathway is expected to be important in the pathogenesis of this disease. Somatic *STAT3* mutations in any human cancer were first reported in 40% of T-LGL leukemia patients using next-generation exome sequencing of a cohort of 77 patients [68]. In a separate group of 120 T-LGL leukemia patients, Jerez et al. found *STAT3* mutations in 27% of those patients [65]. A total of 7 mutations were found; all of which are located a few codons apart in the dimerization interface of the Src Homology 2 (SH2) domain of *STAT3* as viewed in **Figure 1.4**. These mutations include Y640F, D661V, D661Y, D661H, K658N, N674I and Y657_K658insY. Among the 31 patients with *STAT3* mutations, Y640F and D661Y were the most prevalent, found in 17% and 9% of *STAT3*-mutated patients, respectively. Using luciferase reporter constructs, all mutations were found to be activating mutations, resulting in increased STAT3 activity [68]. *STAT3* mutations were also found in 30% of a group of 50 NK-LGL leukemia patients, showing a similarity in the pathogenesis of T cell and NK cell derived LGL leukemia [65].

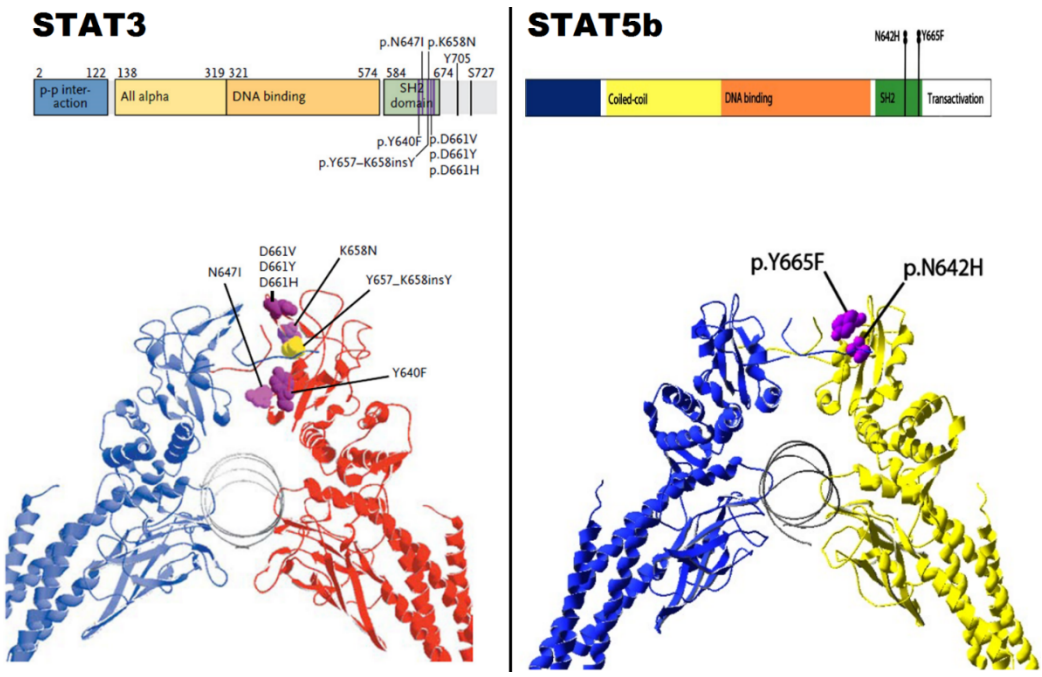

Figure 1.4: STAT mutations

Mutations on *STAT3* (left) and *STAT5b* (right), which localize to the SH2 domain at the dimer interface. These were the first detected and most common. Figure adapted from [68].

More recently, novel activating mutations in *STAT3* outside the SH2 domain have been found in three T-LGL leukemia patients; two being missense mutations H410R and S381Y located in the DNA binding domain and another F174S located in the coiled-coil domain [69]. This cohort included 88 T-LGL and 18 NK-LGL leukemic patients with no STAT3 or STAT5 mutations in known sites within the SH2 domain. Instead, the authors found the new mutations H410R and F174S to also be activating mutations that exhibited increased STAT3 phosphorylation and increased expression of STAT3 responsive genes. While these studies demonstrated the occurrence of STAT3 mutations, a subsequent study found that 22% (18 of 82) of T-LGL leukemia patients labeled as STAT3 mutants harbored two or up to four STAT3 mutations [67]. These findings further support the pathogenic capabilities of STAT3 and highlight the need to sequence the full-length STAT3 gene.

CLINICAL IMPLICATIONS OF STAT3 MUTATIONS

Initial data suggest that somatic *STAT3* mutations are correlated with one large immunodominant clone, a higher association with neutropenia and the need for therapeutic treatment [65]. Not only is *STAT3* mutation associated with both T-LGL and NK-LGL leukemia subtypes, it also appears to be correlated with frequently co-occurring clinical disorders such as pure red cell aplasia (PRCA), myelodysplastic syndrome (MDS), and aplastic anemia (AA) [70–72]. The best established clinical association is with rheumatoid arthritis (RA), with up to 38% of *STAT3*-mutated patients having RA compared to 6% of patients with wild-type STAT3 [67]. However, *STAT3* mutation comorbidity with PRCA has been controversial. The initial study of *STAT3* mutations reported no association with PRCA, while others such as a study of 36 patients from China showed about 50% of those with *STAT3* mutations to also have PRCA [71]. Lastly, T-LGL leukemai patients with *STAT3* mutations have a higher probability of smaller sized leukemic LGL [73], though whether *STAT3* mutation is the causative mechanism remains unclear.

The Eastern Cooperative Oncology Group 5998 (ECOG) trial, which was the first prospective clinical trial for T-LGL leukemia, showed that patients with the Y640F *STAT3* mutation had a more favorable response to methotrexate (MTX) treatment [15]. This highlights the potential diagnostic and therapeutic significance of STAT3 mutations in LGL leukemia, although additional studies in larger patient cohorts are needed to confirm these initial observations. Since the initial discovery of activating *STAT3* mutations in T-LGL leukemia, similar mutations have been recognized in other T cell malignancies [74–76]. In the proper clinical setting a positive activating *STAT3* mutation adds additional specificity to the diagnosis of T-LGL leukemia and offers a sensitive way of tracking minimal residual disease through methods such as ddPCR [77].

STAT5B MUTATIONS

Emphasizing the significance of STATs in the pathogenesis of LGL leukemia, four mutations in *STAT5b* were discovered in a group of 211 *STAT3* mutation-negative T

and NK cell LGL leukemia patients, with a total frequency of 2%. This was the first evidence of mutated *STAT5b* in any human disease. Perhaps not surprisingly, just as in *STAT3*, the *STAT5b* mutations N642H and Y665F are both located in the SH2 domain (**Figure 1.4**) and increase the transcriptional activity of STAT5b [78]. Leukemic LGL from mutated *STAT5b* patients show increased phosphorylation of *STAT5b* in the nucleus, however, unlike with *STAT3* mutants, patients with wild-type *STAT5b* do not show increased *STAT5b* activity [79]. Both patients with the *STAT5b* N642H mutation had a more aggressive form of LGL leukemia, a stark contrast to the typical indolent form of LGL leukemia [78]. Subsequent analyses (unpublished data) of two patients reported to have a previously described [80] aggressive $CD3^+CD56^+$ phenotype also demonstrated presence of the *STAT5b* N642H mutation. More recently, activating *STAT5b* mutations have been found to occur with higher frequency in the rarer CD4+ subtype of T-LGL leukemia [81]. At the very least, these findings highlight the importance to further investigate the molecular implications and therapeutic targeting of *STAT5* mutations in LGL leukemia.

While mutations of *STAT3* and *STAT5b* are prevalent and likely contribute to the pathogenesis of LGL leukemia, *STAT* mutations alone cannot explain the entirety of this disease because the frequency of these mutations is less than 50%. Patients without *STAT3* mutations have constitutively active *STAT3* expression, along with very similar global gene expression patterns [65,68] implying that there are other mechanisms that induce *STAT3* activation such as upstream mutations [15]. Exome sequencing of patients with both wild-type *STAT3* and *STAT5b* uncovered other somatic mutations in *PTPRT* [66], *TFNAIP3* [82], *BCL11B* [66], *TET2* [66], *DNMT3A* [83], *SLIT2* [66], and *NRP1* [66]. Selected somatic mutations detected in LGL leukemia are summarized in **Table 1.1.**

Table 1.1: Summary of mutations found in LGL leukemia

Gene	Mutation	Pathway affected	% mutated	ref
STAT3	F174S, S381Y, H410R, S614R, Y640F, N647I, Y657_K658insY, K658N, D661Y, D661V, D661H	JAK/STAT	27-43	[65,68,69,84]
STAT5b	N642H, Y665F, S715F	JAK/STAT	2	[78,81]
TFNAIP 3 (A20)	F127C, E630X, A717T	NF-κB	8	[82]
DNMT3A	E907del	DNA methylation	<1	[83]
TET2	E1144K	DNA methylation	<1	[83]
PTPRT	V995M	JAK/STAT	<1	[66]
SLIT2	W647	Tumor suppressor	<1	[66]
NRP1	V391M	T-cell activation	<1	[66]
BCL11B	H126R	T-cell proliferation	<1	[66]

OTHER MUTATIONS IN THE JAK/STAT PATHWAY

Protein tyrosine phosphatase, receptor type T (PTPRT) plays a role in the *STAT3* signaling cascade as a phosphatase, acting as a negative regulator of *STAT3*. PTPRT dephosphorylates *STAT3* at Y705 and is shown to be a tumor suppressor in several cancers [85]. A V995M mutation in the *PTPRT* gene was found in a single patient diagnosed with T-LGL leukemia. This novel mutation occurs in the active phosphatase

domain and is hypothesized to render PTPRT inactive [66]. Reduced phosphatase activity of PTPRT would allow *STAT3* to remain phosphorylated and hence activated longer, contributing to the perpetuation of oncogenesis.

Tumor necrosis factor, alpha-induced protein 3 (*TNFAIP3)* is a known tumor suppressor that encodes for A20, a negative regulator of NF-κB signaling, which is also deregulated in T-LGL leukemia [85][82]. Out of 39 patients, three patients were found harboring mutations in the A20 gene, two were nonsynonymous and the third was a missense mutation. Interestingly, a correlation of *TNFAIP3* mutation and *STAT3* mutations was observed in an independent group of 34 T-LGL leukemia patients as three out of the four patients with a *TNFAIP3* mutation also harbored a *STAT3* mutation [85]. Deregulation of both JAK/STAT and NF-κB signaling pathways are key features that contribute to the pathogenesis of T-LGL leukemia [41], and both pathways can be constitutively activated by somatic mutation.

Most recently in a single case study, mutations in *TET2* and *DNMT3A* were found in the leukemic clone of a T-LGL leukemia patient also harboring the Y640F *STAT3* mutation [83]. *DNMT3A* encodes for a DNA methyltransferase, and mutations in this gene have also been found in acute myeloid leukemia (AML) and result in decreased gene expression [86]. In addition, *TET2* mutations have also been detected in AML, and this gene is involved in the demethylation of DNA, which modulates chromatin structure [87]. Indeed, this may be related to a previous exploration [88] of two upstream regulators of *STAT3*: interleukin 6 (IL-6) and suppressor of cytokine signaling 3 (SOCS3), which induce and inhibit *STAT3*, respectively. In particular, the demethylating agent 5-Aza-2'-Deoxycytidine (DAC) restored SOCS3 expression and reduced *STAT3* activity, although the authors were not able to localize the causative region of demethylation in the specific SOCS3 region tested. Collectively, these findings underscore the importance of epigenetic modifiers and the need for additional studies to clarify the epigenome's role in the pathogenesis of LGL leukemia.

MUTATIONS ASSOCIATED WITH T-CELL ACTIVATION AND PROLIFERATION

B-cell lymphoma/leukemia 11B (*BCL11B*) is a transcription factor that regulates the expression of genes important for T cell development such as IL-2 [89], NF-κB and TCRβ [90]. An H126R mutation in the *BCL11B* gene was found only in the leukemic CD8+ cells of a single T-LGL leukemia patient [66]. In T-cell acute lymphoblastic leukemia, *BCL11B* deletions and missense mutations were found in 10-15% of patients [91]. In AML, *BCL11B* was identified as an oncogene as mutations in *BCL11B* increased expression of BCL11B protein, resulting in increased expression of T-cell associated genes [40]. For LGL leukemia, it is hypothesized that increased expression of BCL11B may increase T-cell activation and proliferation [82].

Slit homolog 2 protein (*SLIT2)* plays a role as a tumor suppressor and can be methylated, or silenced, in chronic lymphocytic leukemia and acute lymphoblastic leukemia [94][92]. The mutation found in a T-LGL leukemia patient is a W674 stop mutation, suggesting that this novel mutation may lead to loss of function and play a role in cancer development.

Lastly, neuropilin-1 (*NRP1*) is a receptor that participates in the communication between dendritic cells and T cells, which is important in initiating an immune response. A V391M *NRP1* mutation found in a single LGL leukemia patient may affect the interaction between dendritic and T cells, which would affect their activation and proliferation [66].

These somatic mutations, while rare, are associated with either the STAT3 pathway or T-cell activation and proliferation and may be important in the clonal expansion in T-LGL leukemia. These findings emphasize the need to sequence a larger cohort of patients and characterize the biochemical effects of mutations on pathways vital to the survival of leukemic LGL. This will identify possible therapeutic vulnerabilities dependent on certain mutations and may facilitate personalized treatment options based upon gene mutation status.

1.4 CONCLUSIONS

These studies so far have been encouraging and offer many follow-up questions for subsequent investigation. Past [15,93,94] clinical trials have focused on immunosuppressive therapies, which are the mainstream of therapeutic approaches for LGL leukemia. Despite the high frequency of activating mutations in *STAT3*, no clinical trials of rationally designed STAT inhibitors have been conducted to date in LGL leukemia, in part due to the lack of clinical advancement and success for these molecules thus far. However, a recent study suggests that JAK/STAT pathway inhibition is at least one mechanism of action for the currently used first-line treatment, methotrexate [95]. In the absence of a curative treatment, further molecular characterization is needed to define additional targets.

In this thesis, we aim to further analyse the implications of JAK/STAT pathway mutations in LGL leukemia. This body of work improves the current understanding of how JAK1 and STAT3 mutations affect downstream signaling and STAT activation. We discovered novel mutations within this pathway using whole genome sequencing methods in both T- and NK-LGL leukemia models. Finally, we used a novel peptide inhibitor to block upstream of JAK/STAT activation and showed its preclinical success leading to induction of leukemic cell death.

2 DISCOVERY AND CHARACTERIZATION OF NOVEL JAK1 MUTATION IN A RAT NK-LGL LEUKEMIA MODEL

This chapter is adapted from:

Wang, T.T.; Yang, J.; Dighe, S.; Schmachtenberg, M.W.; Leigh, N.T.; Farber, E.; Onengut-Gumuscu, S.; Feith, D.J.; Ratan, A.; Loughran, T.P., Jr.; Olson, T.L. Whole Genome Sequencing of Spontaneously Occurring Rat Natural Killer Large Granular Lymphocyte Leukemia Identifies JAK1 Somatic Activating Mutation. Cancers 2020, 12, 126.

Conceptualization, T.L.O.; data curation, T.T.W., J.Y., S.D., E.F., S.O.-G., A.R. and T.L.O.; formal analysis, T.T.W., J.Y. and A.R.; funding acquisition, T.P.L.J.; investigation, T.T.W. and S.O.-G.; methodology, T.T.W.; project administration, T.T.W., D.J.F. and T.L.O.; resources, T.P.L.J.; supervision, D.J.F. and T.P.L.J.; validation, T.T.W., M.W.S. and N.T.L.; visualization, T.T.W. and S.D.; writing—original draft, T.T.W.; writing—review and editing, T.T.W., J.Y., D.J.F., A.R., T.P.L.J. and T.L.O.

ABSTRACT

Large granular lymphocyte (LGL) leukemia arises spontaneously in elderly Fischer (F344) rats. This rodent model has been shown to emulate many aspects of the natural killer (NK) variant of human LGL leukemia. Previous transplantation of leukemic material into young F344 rats resulted in several strains of RNK primary leukemic cells. One strain, RNK-16, was adapted into the RNK-16 cell line and established as an aggressive NK-LGL leukemia model. Whole genome sequencing of the RNK-16 cell line identified 255,838 locations where the RNK16 had an alternate allele that was different from F344, including a mutation in *Jak*1. Functional studies showed *Jak*1 Y1034C to be a somatic activating mutation that mediated increased STAT signaling as assessed by phosphoprotein levels. Sanger sequencing of *Jak*1 in RNK-1, -3, -7 and -16 found only RNK-16 to harbor the Y1034C *Jak*1 mutation. *In vivo* studies revealed that rats engrafted with RNK-16 primary material developed leukemia more rapidly than those engrafted with RNK-1, -3, and -7. Additionally, *ex vivo* RNK-16 spleen cells from leukemic rats exhibited increased STAT1, STAT3, and STAT5 phosphorylation compared to other RNK strains. Therefore, we report and characterize a novel gain-of-function *Jak*1 mutation in a spontaneous LGL leukemia model that results in increased downstream STAT signaling.

2.1 INTRODUCTION

Large granular lymphocyte (LGL) leukemia is a lymphoproliferative neoplasm characterized by uncontrolled clonal expansion of LGLs of T-cell or natural killer (NK) cell origin, which causes anemia, neutropenia, and splenomegaly [96]. The World Health Organization classified LGL leukemia into three subtypes: T-cell LGL leukemia, chronic lymphoproliferative disorder of NK cells, and aggressive NK-cell leukemia [8]. The aggressive NK-cell leukemia is distinct from its indolent counterparts, affecting younger individuals with a higher prevalence in Asia and South America [1,34]. While the etiology of LGL leukemia is not well understood, LGL leukemia is characterized by multiple aberrant signaling pathways, including the Janus kinase/signal transducers and activators of the transcription (JAK/STAT) signaling pathway [96,97].

The JAK/STAT pathway relays extracellular signals from cytokines and other factors to intracellular factors to control nuclear transcription. This pathway is essential for various intracellular processes, including apoptosis, immune response, and differentiation. JAKs are non-receptor tyrosine kinases that interact with the intracellular tail of membrane-bound receptor complexes. JAK proteins consist of four domains; an N-terminal FERM (F for 4.1 protein, E for ezrin, R for radixin and M for moesin) domain, an SH2 domain, a pseudokinase domain, and a C-terminal protein tyrosine kinase (PTK) domain. Within the PTK domain lies an activation loop housing two highly conserved adjacent tyrosine residues. JAK signaling is well studied, and mutations in the JAK family are clearly implicated in the pathogenesis of hematological disorders [98,99]. JAK1 mutations have been reported in various hematological malignancies, including 7–27% of T-cell acute lymphoblastic leukemia (ALL) [100–104], 8–12% of T-cell prolymphocytic leukemia [105,106], 1.5% of B-ALL [102], and a small percentage of acute myeloid leukemia [107]. Subsequently, JAK1 mutations have been linked to solid tumor cancers, including Hepatitis B-associated hepatocellular carcinoma [108] and gynecological tumors [109].

JAK signaling phosphorylates downstream STAT proteins, important in regulating the transcription of genes involved in cell differentiation, survival, and proliferation [99,100]. Dysregulated STAT1, STAT3, and STAT5 signaling is well documented in LGL leukemia [45]. All patients exhibit constitutive STAT1 and STAT3 phosphorylation, and the occurrence of *STAT5B* [67,81,110] and *STAT3* [67–69,110] somatic activating mutations are a hallmark of LGL leukemia. Taken together, perturbations in the JAK/STAT pathway are well documented in hematological malignancies.

Fischer 344 rats are an inbred strain of rats that were used for decades as a primary in vivo model for cancer and toxicology studies [111]. Large granular lymphocyte (LGL) leukemia spontaneously occurs in 30–50% of Fischer 344 rats over 18 months of age [112–114]. Presentation of the disease in rats include anemia, splenomegaly, and leukemic cell infiltration of the spleen, liver, and lungs. [115]. Morphologically, these leukemic cells resemble LGLs with cytoplasmic granules. Functional studies using cytotoxicity and cell marker assays characterized these leukemic cells as being of NK cell origin and labelled as rat natural killer (RNK) cells [116]. Transplantation of primary RNK material induces leukemia, and has been utilized to establish 15 RNK strains. Of all strains, RNK-16 was characterized as a highly cytotoxic variant [116,117] and adapted into the RNK-16 cell line [118,119]. While high prevalence of disease and slight variations in features differ from the human counterpart, the morphological, functional, and clinical similarities established RNK-16 as a model of the human aggressive form of natural killer LGL leukemia (NK-LGL leukemia) [115,120,121].

The goal of the present study was to further characterize the RNK-16 cell line through whole genome sequencing (WGS). The results will aid interpretation of future LGL leukemia therapy response studies by our lab and others who use this model. Whole genome sequences from the RNK-16 cell line were compared to the F344 genome to reveal variants in several oncogenes. This led to the discovery of a novel *Jak*1 Y1034C mutation, which was also validated in ex vivo primary spleen material from leukemic rats. This allowed us to identify the mutated JAK1 as the putative leukemic driver JAK1, as well as mutations that occurred during adaptation to culture. Functional assays

showed that *Jak1* Y1034C increased downstream STAT1, STAT3, and STAT5 phosphorylation in both the cell line and the primary RNK material. Characterization of this mutation may have a larger impact in future studies as more JAK1 mutations are uncovered in other diseases.

2.2 MATERIALS AND METHODS

ACQUISITION OF SEQUENCING DATA

Paired-end Illumina short read sequences were downloaded for the F344/NCrl sample from the European Nucleotide Archive (ENA; Run: ERR224448). The RNK-16 cell line was kindly provided by Drs. Craig Reynolds and Howard Young (National Cancer Institute, Bethesda, MD, USA). DNA was isolated by AnaPrep (BioChain Institute, Newark, CA, USA) and quantified by Qubit (Thermo Fisher (Waltham, MA, USA). A sequencing library was prepared with a Nextera (San Diego, CA, USA) kit, using half the recommended DNA input and paired-end sequenced on the NextSeq 500 (Illumina (San Diego, CA, USA)) at the Center for Public Health Genomics at the University of Virginia.

ALIGNMENTS

Illumina short-read sequences from the RNK-16 cell line and the F344 sample were aligned to the *Rattus norvegicus* reference sequence (rn6) with BWA mem [122], using the default parameters. Putative PCR duplicates were flagged using SAMBLASTER [123], which was also used to add MC and MQ tags to all the output paired-end alignments, and separate the split-reads, the discordant pairs, and the unmapped sequences from the resulting output (Table S3). The SAM outputs were converted to BAM format and sorted by chromosomal coordinates using SAMTools [124]. All BAM files for the same samples were merged using SAMTools, and BAMreport

(https://github.com/aakrosh/BAMreport) was then used to generate the alignment statistics and metrics.

CNV MAP

Evidence of GC bias were found in both sequence datasets **(Table S3)**, and the same diagnostic plots also revealed evidence of large copy number aberrations in the RNK-16 sample that could confound variant calls. From there, a copy number variant map was created to define the non-uniform ploidy variation in the RNK-16 sample by binning the aligned fragments into intervals of 10 kb mappable bases. Then, a locally weighted linear regression modeled the relationship between GC content and coverage in those intervals. This LOWESS fit was then used to scale the coverage in each bin, based on the mean coverage in bins with the same GC content. Circular binary segmentation (CBS) [125] identified bins that shared the same copy number state, and a Gaussian mixture model was used to genotype the segments and calculate their copy number state.

IDENTIFICATION OF VARIANTS

FreeBayes [126] identified the variants in the samples, requiring that the allele fraction in at least one sample be 0.1 and supported by two reads. The CNV map was provided as an input, and required that the Phred scaled probability of a polymorphism at the loci be greater than 5. The following additional options were used: —pooled-discrete, —pooled-continuous, —genotype- qualities, —report-genotype-likelihood-max and —allele-balance-priors-off.

ANNOTATION AND FILTERING OF VARIANTS

Variants where the F344/NCrl sample was homozygous for the reference were labelled, and an alternate allele in RNK-16 was observed as somatic, using filters implemented

similar to SpeedSeq [127]. To start, genotype likelihoods were extracted from the output of FreeBayes. For RNK-16, we retrieved the best likelihood to not be the reference, and for F344/NCrl, the best likelihood was to be the reference. We required that (a) both the retrieved likelihoods be above a minimum threshold, and (b) we filtered to remove any low-frequency variants in RNK-16 that were also present in the F344/NCrl sample at low frequencies. We then used SnpEff [128] to annotate these labeled variants, using dbSnp and the variant calls from Hermsen et al. [129]. This left us with 255,838 positions, with evidence of an alternate allele in RNK-16 (**Table 2.1**).

Table 2.1: Alignment statistics for the RNK-16 and F334/NCrl samples.

Sample	Reads	Aligned (%)	Duplicates (%)	Properly paired (%)
RNK-16	657,092,472	96.02	2.73	93.46
F344/NCrl	807,260,796	99.18	5.55	95.59

GENE ENRICHMENT ANALYSES

Genes with variants were filtered for a Z score of >20 and those labelled with a medium or high impact. Homolog analysis of these gene variants was performed using DAVID (Database for Annotation, Visualization, and Integrated Discovery), resulting in a list of 458 human genes, of which 157 did not have the same name. Variant genes were queried in the CGC (Cancer Gene Census) to determine which were implicated in cancers.

SANGER SEQUENCING TO VALIDATE WHOLE GENOME SEQUENCING RESULTS

Sequencing primers from Eurofins for eight oncogenes identified in COSMIC were designed using Primerblast [130] (**Table 2.2**). Bulk DNA from RNK-1, -3, -7, and -16 was sent to Eurofins for Sanger sequencing to determine oncogene mutation status.

Table 2.2: List of sequencing primers used for validation of mutations found in RNK-16 cell line.

Primer No.	Sequencing Range		Start Site	5'- sequence-3'	Tm (°C)	Length	GC Content
FOR_1	701	1400	654	AGATGCAGTTGCCAGAGCTT	60.164	20	50
FOR_2	1401	2100	1347	TACAGAATGGCTGTCACGGT	59.165	20	50
FOR_3	2101	2800	2056	GCCATTGGATCTCTTCATGC	60.579	20	50
FOR_4	2801	3500	2756	GTCAAGTCCCTGAAGCCTGA	60.386	20	55
REV_1	700	1	756	CGCATCCTGGTAAGAAGATT	56.909	20	52.2
REV_2	1400	701	1442	TCCACCTCAGCACGTACATC	59.707	20	55
REV_3	2100	1401	2156	CTTCCAAGTAACTCAGGGCG	59.869	20	55
REV_4	2800	2101	2844	TTCTCGTGGTAGAGGTTCCG	60.246	20	55
brd3 forward	6002298		6002318	AAGCAACAGATGCCTCCCTC	60.03	20	55
brd3 reverse		6002779	6002799	CCGCTTAGCTGCTTGCTTTT	59.76	20	50
DDR forward	88342294		88342314	CAGCATAGGGTACCAAGCCC	60.18	20	60
DDR2 reverse		88342867	88342891	CATGAATGAGGAACAAAGTGTCCA	59.48	24	41.67
Fat1 forward	50398179		50398202	AGCATCCTTAGCCATTAAACGGA	60.12	23	43.48
Fat1 reverse		50398634	50398655	AGTACTCCAGCCTGTCTAGGT	60	21	52.38
Ncor2 forward	37032405		37032425	GGTCCTGAGGTGGCTACTTG	60	20	60
Ncor2 reverse		37032852	37032872	GATGCCAGCTCTGGATGGAC	60	20	60
Nono forward	71341038		71341061	CCTGTAGTGGGAAGACCTTTGAG	60.31	23	52.17
Nono reverse		71341526	71341549	ACCAGACAGACTTTAACGCACTA	59.68	23	43.48
Stag1 forward	109202303		109202326	GGCATATGGACAGTATTTCATGG	57.37	23	43.48
Stag1 reverse		109202963	109202985	TCCACTCTCAGCCACTTCTACA	60.49	22	50
Thrap3 (1) forward	144180643		144180666	TCCATAAACTGACTTAGCCCTCC	59.55	23	47.83
Thrap3 (1) reverse		144181150	144181172	TGGGAGACAACTTTCCATTCCC	60.23	22	50
Thrap3 (2) forward	144180693		144180716	TCCATAAACTGACTTAGCCCTCC	59.55	23	47.83
Thrap3 (2) reverse		144181150	144181172	TGGGAGACAACTTTCCATTCCC	60.23	22	50
Thrap3 (3) forward	144180715		144180738	TCCATAAACTGACTTAGCCCTCC	59.55	23	47.83
Thrap3 (3) reverse		144181160	144181182	TGGGAGACAACTTTCCATTCCC	60.23	22	50

JAK1 MUTAGENESIS

A full-length clone of the rat JAK1 sequence (XM_006238453.1) in the pCMV3 vector was purchased from Sinobiological (Cat. RG81640-UT), as was the pCMV3 empty vector (Cat. CV011) and pCMV3–GFP (Green Florescent Protein) control vector (Cat. CV026). A JAK1 Y1034C mutation was introduced into the rat JAK1 pCMV3 using an In-Fusion HD Site-directed Mutagenesis kit (Takara (Kusatsu, Shiga Prefecture, Japan), Cat. 638909), with primers acquired from Eurofins

(F: 5' AGACCGATAAGGAGTACTACAGT 3',

R: 5' GGAGTACTACACAGTCAAGGATGAC 3').

Primers were designed to overlap by 15 bp at the 5', ends with a GC content of 40–50%. The mutant DNA was transformed into Stellar Competent cells, and plasmid DNA was isolated. Insertion of only the desired Y1034C mutation and presence of a full-length JAK1 were confirmed by Sanger sequencing.

CELL CULTURE

RNK-16 cell line (kindly provided by Dr. Craig Reynolds, NCI) was cultured in RPMI 1640 supplemented with 10% Fetal Bovine Serum (FBS), non-essential amino acids (Sigma (St. Louis, MO, USA)), 1% sodium pyruvate (Sigma), and 25 μM 2-mercaptoethanol. HEK293-FT (human embryonic kidney) cells (kindly provided by Kenichiro Doi and H.G Wang, PSU College of Medicine) were cultured in DMEM with 10% FBS.

TRANSFECTION AND WESTERN BLOT ANALYSIS

The empty vector, GFP, WT JAK1, or mutant JAK1 cDNA was transfected using Lipofectamine 3000 (Invitrogen (Carlsbad, CA, USA), Cat. L3000008) into HEK293-FT cells. High transfection efficiency was determined via GFP transfection control. Whole cell lysates were prepared in RIPA buffer (ThermoFisher (Carlsbad, CA, USA))

72 h post-transfection; proteins were electrophoresed on a 4–12% acrylamide gel (ThermoFisher) and subsequently transferred to a Polyvinylidene fluoride (PVDF) membrane. Membranes were blocked and incubated with varying antibodies. Cell signaling technology primary antibodies used in this study included Phospho-STAT3 (Y705, Cat #9131), STAT3 (Cat #9139), Phospho-STAT1 (Y701, Cat #&649), STAT1 (CAT #9175), Phospho-STAT5 (Y694, Cat #9351), STAT5 (Cat #9363), Phospho-JAK1 (Y1034/1035, Cat #3331), and JAK1 (Cat# 3344). After incubation overnight at 4 ◦C with a primary antibody, blots were incubated with a secondary antibody (anti-rabbit IgG–HRP (Horseradish Peroxidase) linked (Cat #7073) or anti-mouse IgG–HRP linked (Cat #7076)) for one hour, and washed before treating with Clarity enhanced chemiluminescence (ECT; Biorad) reagent. Membranes were imaged using a ChemiDoc MP instrument and analyzed using ImageLab (Biorad (Hercules, CA, USA)).

ANIMAL STUDY

Animal experimentation was performed according to protocols approved by the Institutional Animal Care and Use Committee at the University of Virginia (Protocol # 4014-05-17). Male F344 rats of approximately 5 weeks of age were obtained from Charles River Laboratory. After one week of conditioning to our vivarium, one million viable RNK-1, RNK-3, RNK-7, or RNK-16 primary cells were transplanted intraperitoneally into F344 rats in triplicate for all groups, except for RNK-1, where there were not enough viable cells to engraft three animals. Peripheral blood samples were collected weekly to monitor leukemia development after RNK cell engraftment. Rats losing 20% body weight most likely developed NK-LGL leukemia and were euthanized. At necropsy, rat spleens were harvested. Splenocytes were isolated using s Ficoll–Hypaque density gradient centrifugation and cryopreserved in liquid nitrogen for future use. Rat blood was collected using Becton Dickinson (BD) (Franklin Lakes, NJ, USA) microcontainers with K2EDTA (BD 365974). Blood smears were prepared using a standard technique, and staining was done using a VWR (Radnor, PA, USA) Hematology Quick stain kit (VWR#10143-224). Slides were examined (Olympus

(Shinjuku, Tokyo, Japan) BX51) using immersion oil. Frozen splenocytes were taken from liquid nitrogen, and protein harvested for western blotting analysis, as described above.

STATISTICAL ANALYSIS

Statistical analyses for all in vitro systems utilized unpaired Student's *t*-test, with $p < 0.05$ considered statistically significant. Analyses were performed in both Microsoft Excel and GraphPad Prism.

2.3 RESULTS

IDENTIFICATION AND VALIDATION OF MUTATIONS IN THE RNK-16 CELL LINE AND RNK-16 PRIMARY SPLEEN MATERIAL

Whole genome sequencing (WGS) was successfully performed on the RNK-16 cell line in an effort to identify variants that contribute to NK cell leukemogenesis (**Figure 2.1**). After filtering for quality control parameters and removing variants also seen in F344 genome, we were left with 255,838 variants. Variants were annotated for their impact on the canonical transcripts using SnpEff. Restriction of genes with variants of a Phred quality score of over 20 and labelled as high or moderate impact resulted in 498 genes. Using the Homologene database, these 498 genes were mapped to 457 human genes, of which 157 did not have the same names. Those with matched gene names were queried in the COSMIC Cancer Gene Census, which classifies genes into two tiers based on the extent of evidence that variants in those genes drive oncogenic transformation [131]. Eight genes with mutations in RNK-16 were labelled as having oncogenic transformative potential, including *Brd*3, *Ddr*2, *Fat*1, *Jak*1, *Ncor*2 *Nono*, *Stag* and *Thrap*3 (**Table 2.3**).

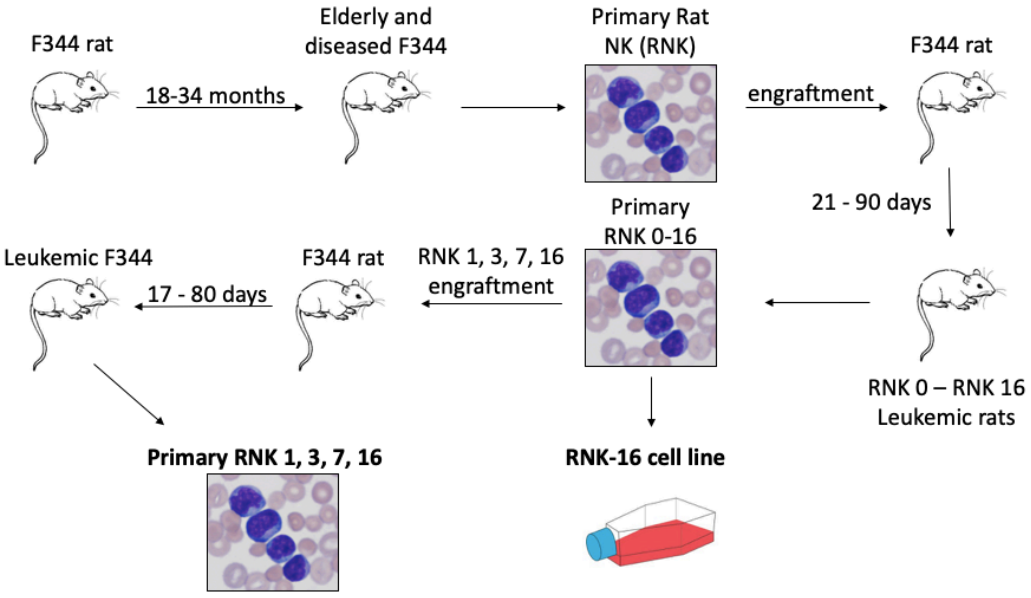

Figure 2.1: Diagram of RNK material.

Aging F344 rats naturally develop LGL leukemia. Leukemic cells were transplanted back into young F344 rats to produce several strains of RNK [114]. RNK-16 cells were adapted into a cell line. Transplantation of RNK-1, -3, -7, and –16 into young F344 rats generated ex vivo spleen samples and those samples in bold were used in these studies.

Table 2.3: Cancer Gene Census (CGC) query revealed genes mutated in RNK-16 cell line that are implicated in cancer.

Tier levels are assigned by CGC and indicate depth of evidence of mutations in those genes having oncogenic transformative potential. Variants in *Ddr*2, *Fat*1, *Jak*1, *Ncor*2, and *Stag* were confirmed using Sanger sequencing in RNK-16 cell line. Only mutation in *Jak*1 was confirmed in RNK-16 primary spleen cells.

Gene symbol	Tier level	RNK-16 Cell Line WGS	RNK-16 Cell Line Validation	RNK-16 primary spleen cells
Brd3	1	✓	×	×
Ddr2	1	✓	✓	×
Fat1	1	✓	✓	×
Jak1	1	✓	✓	✓
Ncor2	1	✓	✓	×
Nono	1	✓	×	×
Stag	1	✓	✓	×
Thrap3	2	✓	×	×

SEQUENCING STRATEGIES WERE DESIGNED TO VALIDATE THE VARIANTS BY SANGER SEQUENCING IN THE RNK-16 CELL LINE.

Out of the eight genes, variants were confirmed in five including *Ddr2*, *Fat1*, *Jak1*, *Ncor2* and *Stag*. As RNK-16 cell line was adapted to *in vitro* culture from *ex vivo* RNK-16 material, validation of these mutations was necessary to demonstrate that mutations were not the result of cell line transformation. Sanger sequencing of *ex vivo* RNK-16 spleen cells (**Figure 2.1**) confirmed only the *Jak*1 variant **(Figure 2.2A),** indicating the adaptation of RNK-16 primary cells into the RNK-16 cell line may have resulted in the gain of mutations in *Ddr2*, *Fat1*, *Ncor2* and *Stag*, but not *Jak1*. JAK1 is a tyrosine kinase involved in cytokine signaling that results in downstream activation of STATs. This *Jak1* mutation is found in the PTK domain and is located within the activation loop that contains two tyrosine phosphorylation sites, 1033 and 1034 (**Figure 2.2B**). Results of WGS as well as Sanger validation of cell line and primary splenocyte material are summarized in **Table 2.3**.

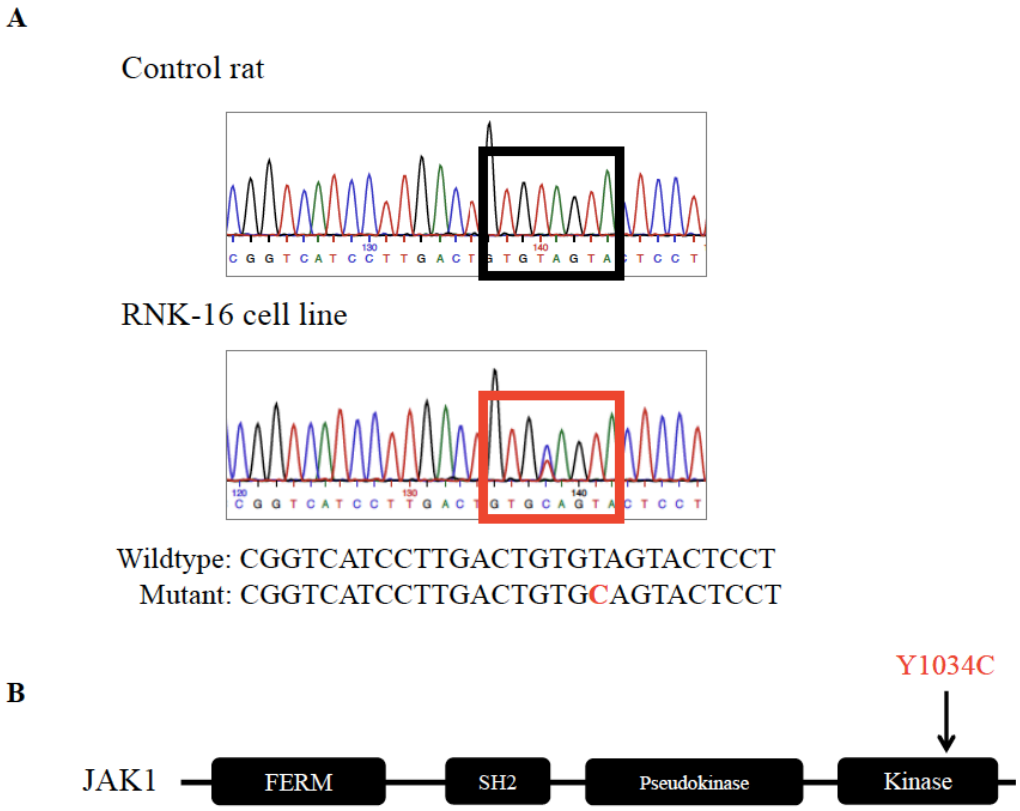

Figure 2.2: Validation of JAK1 variant by Sanger sequencing.

Validation of JAK1 variant by Sanger sequencing. **[A]** Sequencing chromatographs from Sanger sequencing validate JAK1 mutation in RNK-16 cell line. [**B**] JAK1 variant occurs in the kinase Sanger sequencing validate JAK1 mutation in RNK-16 cell line. JAK1 variant occurs in the kinase domain at Y1034, resulting in a change from tyrosine to cysteine. It sits within the activation loop, adjacent to another phosphorylation site at Y1033.

JAK1 MUTATION INCREASED DOWNSTREAM STAT SIGNALING

To examine the effects of Y1034C *Jak1* mutation on protein function, we transiently expressed WT *Jak1* or *Jak1* Y1034C in HEK293-FT cells. Western blotting demonstrated constitutive phosphorylation of downstream STAT targets including STAT1, STAT3 and STAT5 (**Figure 2.3**). The epitope of the phosphorylated JAK1 antibody recognizes the dual tyrosine phosphorylation in the activation loop (1033/1034), which is altered in the mutant, therefore it was unable to recognize the mutant phosphorylated protein even though mutant overexpression was confirmed by the total JAK1 antibody. Total JAK1 protein levels were unchanged, indicating that mutation did not increase production of total JAK1. Low levels of all phosphoprotein targets were observed when transfected with WT *Jak1*, drastically different from the large increase of phosphorylation with transfection of *Jak1* Y1034C. Thus, insertion of *Jak1* Y1034C induced constitutive activation of STAT signaling independent of exogenous cytokine signaling.

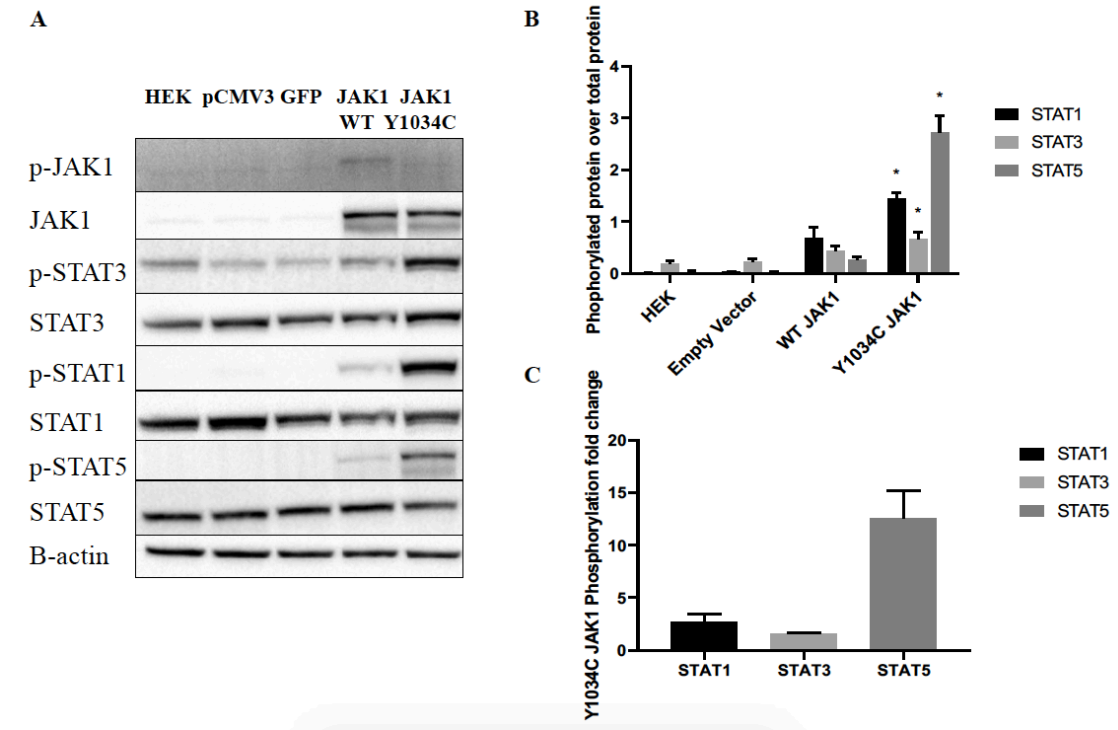

Figure 2.3: *Jak1* Y1034C mutation increased STAT protein phosphorylation in HEK293FT cells.

HEK293FT cells were transfected with pCMV3 vectors containing no insert, GFP, WT rat JAK1, or rat JAK1 Y1034C. 72 hours post transfection, cells were harvested and protein lysates were analyzed by western blotting. Membranes were probed with phosphorylated and total antibodies of JAK1, STAT3, STAT1 and STAT5. Representative western blot shown in [A], quantification of all replicates (n=4) with SEM graphed in [B], and calculation of fold change in JAK1 Y1034C phosphorylated proteins over WT JAK1 phosphorylated proteins from all replicates with SEM graphed in [C]. Statistics were performed for mutant JAK1 relative to WT JAK1. * = $p < 0.05$.

IN VIVO AND EX VIVO CHARACTERIZATION OF PRIMARY RNK MATERIAL SHOWS AN AGGRESSIVE DISEASE COURSE AND INCREASED STAT SIGNALING WITH MUTANT JAK1.

Previous characterization of primary *ex vivo* RNK material reported RNK-16 to have high cytotoxicity compared to RNK-1 and RNK-7 [116,117]. Characterization of RNK-3 was not previously published, although all of the RNK material was isolated together. Additionally, our Sanger sequencing of *ex vivo* RNK-1, -3, -7, and -16 spleen material detected *Jak1* Y1034C only in RNK-16 (**Figure 2.4A**). To further characterize these RNK strains, one million viable primary RNK-1, -3, -7, and -16 cells were injected i.p. into young F344 rats to study leukemia onset of RNK-16 compared to other strains. Rats engrafted with RNK-16 showed significantly shorter time to disease onset, as determined by absolute white blood count and weight loss. (**Figure 2.4B**) Average time to disease onset for RNK-16 was 17.7 days, less than half the time for rats injected with RNK-1 to develop leukemia and less than a quarter of the time for rats transplanted with RNK-3 and RNK-7 to develop disease. Protein extracts from spleen cells harvested from leukemic rats were run on western blots and probed for downstream STAT phosphorylation (**Figure 2.4C**). RNK-16 spleen cells had increased STAT1 and STAT3 phosphorylation relative to all other RNKs and similar levels of STAT5 phosphorylation to RNK-7. Taken together, these studies provide molecular and biochemical data to complement the previously published functional characterization of RNK primary material.

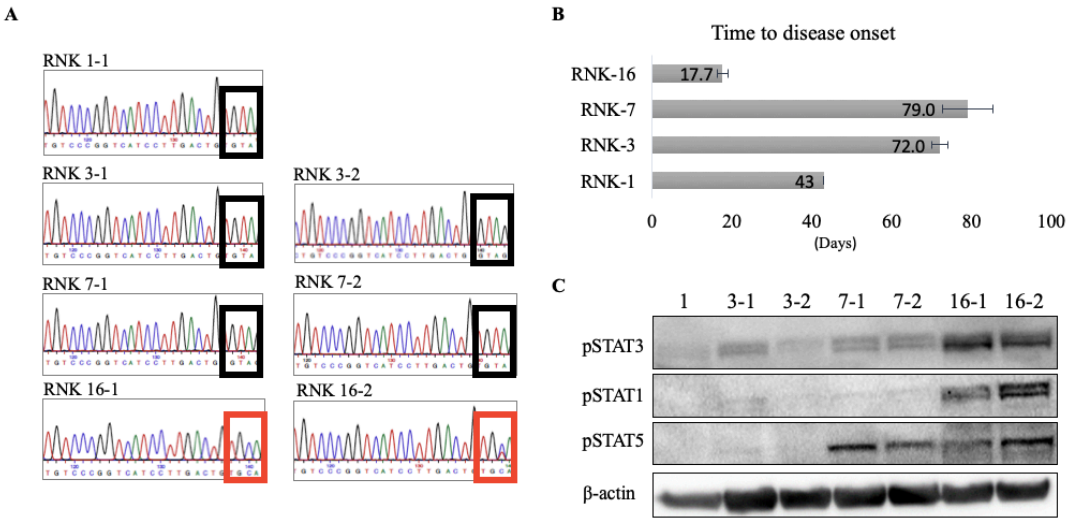

Figure 2.4: In vivo and ex vivo characterization of RNK material.

1 x 10^6 cells from RNK-1, -3, -7, and -16 were injected i.p. into young F344 rats and time to disease was measured. [A] Sanger sequencing of primary spleen mononuclear cells harvested from leukemic animals showed *Jak1* Y1034C mutation found only in RNK-16. [B] Those engrafted with RNK-16 had significantly shorter time to disease onset compared to the others. [C] Spleen cells were harvested from leukemic rats at euthanasia. Immunoblot analysis showed increased STAT1, -3, and -5 phosphorylation in RNK-16 relative to RNK-1, -3, and -7.

2.4 DISCUSSION

This study characterized a JAK1 Y1034C mutation found in a naturally occurring F344 rat NK-LGL leukemia model. RNK-16, characterized as highly cytotoxic [117], was established as an *in vitro* cell line [119] and model for aggressive NK-LGL leukemia [120]. Whole genome sequencing in the RNK-16 cell line revealed variants in eight oncogenes. Sanger sequencing of the RNK-16 cell line and *ex vivo* RNK-16 spleen material confirmed a single variant, JAK1 Y1034C, in all tested material. Lack of validation of other variants found in the RNK-16 cell line in the *ex vivo* RNK-16 spleen material indicates that mutations may have been acquired as a result of *in vitro* cell culture expansion [132].

Aberrant activation of JAK/STAT signaling is a hallmark of LGL leukemia. Increased activation of this pathway results from increased cytokine signaling [1,133] and somatic activating mutations in STAT3 [110,68,66] and STAT5B [81,110,134], further implicating the oncogenic role of this pathway in LGL leukemia. While JAK1 mutations have not been reported in LGL leukemia patients, mutations in JAK1 have been identified in several hematological malignancies [101–103,105,107,135]. The majority of mutations occur in the pseudokinase domain, and have been characterized to have oncogenic potential [136] and patients with such mutations have poor prognoses [135].

The activation loop within the C-terminal PTK domain includes two adjacent tyrosine phosphorylation sites. Mutation of the first tyrosine to an alanine abrogated kinase activation, indicating that the first tyrosine is necessary for JAK1 activation. An alanine substitution to the second tyrosine allowed kinase activation, showing that activation is not dependent upon the second tyrosine [137]. We detected a mutation at Y1034, which is the second tyrosine within the activation loop. While not necessary for kinase activation, mutations at this location may affect enzymatic activity [138], as well as the

specificity and strength of interactions with substrates, thereby leading to altered downstream signaling. Random mutagenesis experiments on human JAK1 have shown that the specific substitution of cysteine for the second tyrosine, analogous to the mutation that we detected in rat JAK1, drives clonal outgrowth and increases JAK/STAT signaling [136].

Here we demonstrated that *Jak1* Y1034C is a naturally occurring somatic mutation found in leukemic rats that was shown to elevate the phosphorylated levels of STAT1, STAT3 and STAT5. We observed the largest fold change of phosphorylated STAT5 by mutant relative to WT JAK1, suggesting STAT5 may be more readily phosphorylated by mutant JAK1 [137,139]. Mutation of JAK1 did not increase total JAK1 protein. While we were unable to assess the phosphorylation of JAK1 itself, presumably due to the overlap of mutation location and antibody epitope, increased phosphorylation of JAK1 was shown when the substitution of cysteine for the second tyrosine was performed in human JAK1 [137]. Additionally, future mass spectrometry-based analyses could be insightful in this regard.

In vivo studies involved the transplantation of primary RNK-1, -3, -7, and -16 material into young F344 rats. Previous characterization of these strains specified high cytotoxicity of RNK-16 compared to other strains, and our study enhanced their findings by examining time to disease onset, JAK1 mutation status, and phosphorylated STAT protein levels. We found that rats transplanted with RNK-16 have significantly more rapid disease development. The *Jak1* Y1034C mutation was detected only in ex vivo RNK-16 spleen material, which also exhibited increased protein levels of phosphorylated STAT1, STAT3 and STAT5. High cytotoxicity of RNK-16 compared to other RNK strains may be in part explained by the *Jak1* Y1034C mutation, which increases downstream STAT signaling and may drive more aggressive leukemogenesis. Interestingly, we observed increased phosphorylated STAT5 in ex vivo RNK-7 material, suggesting that other factors aside from a *Jak1* mutation may promote STAT5 phosphorylation. Differing genetic, epigenetic, and signaling alterations may explain

differences between the various RNK strains. Performing WGS on other RNK primary material may reveal other variants in addition to the *Jak1* Y1034C mutation that may contribute to the pathogenesis of rat NK-LGL leukemia.

JAK1 Y1034C was reported once in gastric carcinoma [140], but had not been functionally characterized. Importantly, transfection of JAK1 Y1034C into HEK293-FT cells increased downstream STAT phosphorylation compared to WT JAK1. Mutation of JAK1 did not increase total JAK1 protein. We were unable to assess phosphorylation of JAK1 itself presumably due to the overlap of mutation location and antibody epitope. Future mass spectrometry-based analyses could be insightful in this regard. Y1034C occurs in the activation loop of the C-terminal PTK domain and is adjacent to another phosphorylation site. Thus, the location of this mutation may affect enzymatic activity [138] as well as the specificity and strength of interactions with substrates, thereby leading to altered downstream signaling. In fact, we demonstrated that JAK1 Y1034C elevated the phosphorylated levels of STAT 1, 3 and 5 and caused the largest fold change of phosphorylated STAT5 over WT JAK1, emphasizing STAT5 as a key regulator of NK cell growth, survival and cytotoxicity [141]. Gain of function STAT5B mutations have been reported in LGL leukemia and are shown to drive oncogenic transformation in association with aggressive forms of NK cell lymphomas/leukemias [81,110,134].

In vivo studies involved transplantation of primary RNK-1, -3, -7 and -16 material into young F344 rats. Previous characterization of these strains specified high cytotoxicity of RNK-16 compared to other strains, and our study enhanced their findings by examining time to disease onset, JAK1 mutation status, and phosphorylated STAT protein levels. We found rats transplanted with RNK-16 have significantly more rapid disease development. The JAK1 Y1034C mutation was detected only in *ex vivo* RNK-16 spleen material, which also exhibited increased protein levels of phosphorylated STAT1, STAT3 and STAT5. High cytotoxicity of RNK-16 compared to other RNK strains may be in part explained by the JAK1 Y1034C mutation, which increased

downstream STAT signaling and may drive more aggressive leukemogenesis. While we did not fully sequence the other RNK primary material, there may be other variants in addition to the JAK1 Y1034C mutation that may contribute to the aggressive nature of RNK-16.

In summary, this work presents WGS of a spontaneously occurring NK-LGL leukemia model leading to novel characterization of a somatic activating JAK1 Y1034C mutation. The activating mutant may be a useful tool for biochemical studies of JAK/STAT signaling. This work reinforces the critical contributions of JAK/STAT pathway activation in hematologic malignancies, especially those of T- and NK-cell origin. Additionally, RNK-16 engraftment represents an *in vivo* model of a leukemia driven by mutationally activated JAK1 that may have utility for the evaluation and development of JAK1 inhibitors.

3 DISCOVERY AND CHARACTERIZATION OF NOVEL STAT3 MUTATIONS FOUND IN T-LGL LEUKEMIA PATIENTS

ABSTRACT

Dysregulation of the JAK/STAT pathway is a hallmark of LGL leukemia. Increased STAT1 and STAT3 activity is reported in T-cell LGL leukemia patients. Recently, somatic mutations in STAT3 were reported by our lab and other groups. High prevalence of STAT3 mutations are distinctive to LGL leukemia where roughly 40% of patients exhibit one or more STAT3 mutations. STAT3 is domains include N-terminal, coiled-coil, DNA binding, linker, and SH2 domain. The majority of reported STAT3 mutations are located in the SH2 domain, revealing hotspot mutations of Y640F and D661Y. Majority of these reported mutations were a result of exome sequencing targeted to the SH2 domain. We hypothesized that in addition to STAT3 mutations in the SH2 domain, we would identify mutations spanning the other domains.

In this study, we performed paired whole genome sequencing of 38 T-LGL leukemia patients and revealed several novel somatic mutations outside of the SH2 domain. These include previously unreported mutations within the coiled-coil and DNA binding domain. Within our cohort, we report incidence of STAT3 mutation of 58% (22 out of 38). Functional characterization of these novel mutations included studying its effects by STAT3 phosphorylation, DNA binding and a STAT3 reporter assay. The novel mutations were characterized in parallel with previously published activating STAT3 mutations, Y640F and D661Y. We confirmed Y640F and D661Y to be the most activating, and among the novel mutations, we characterized H410P in the DNA binding domain to be the most activating. These findings strengthen the evidence of the pathogenic role STAT3 plays in LGL leukemia and emphasizes the importance of sequencing the entire STAT3 gene.

3.1 INTRODUCTION

Large granular lymphocyte (LGL) leukemia is a lymphoproliferative disorder characterized by clonal expansion of activated cytotoxic T cells or natural killer (NK) cells [1,2]. In healthy individuals, LGL respond to antigen recognition by clonal proliferation and undergo cell death following antigen clearance. However, in LGL leukemia, these lymphocytes evade cell death, resulting in an accumulation of circulating LGLs. This expansion causes symptoms including neutropenia, splenomegaly, and anemia. While LGL leukemia typically runs an indolent course, most patients eventually require treatment for symptoms. LGL leukemia is strongly associated with several autoimmune disorders such as rheumatoid arthritis, and patients experience chronic infections and decreased quality of life. While the pathogenesis of LGL leukemia is unclear, several dysregulated survival pathways have been identified and well established as a pathogenic feature of LGL leukemia.

One of many pathways involved in the pathogenesis of LGL leukemia is the Janus Kinase /Signal Transducer of Activation and Transcription (JAK/STAT) pathway [1,97]. Aberration of this signaling cascade is implicated in many diseases, making it an attractive target for cancer therapy [142]. STAT3 is a latent transcription factor that regulates the transcription of both pro-survival and of its own negative regulator genes. It is a member of the STAT protein family, which includes STAT1, STAT2, STAT3, STAT4, STAT5a, STAT5b and STAT6. All STAT proteins share highly conserved domains including N-terminal, coiled-coil, linker, DNA-binding, Src-homology 2 (SH2), and a transcriptional domain. STATs reside in the cytoplasm and are recruited after cytokine or growth factor binding to its membrane bound receptor complex. Ligand binding causes activation of JAK proteins by phosphorylation, which is followed by the phosphorylation of the intracellular tail of the receptor complex. This creates a docking site to which STATs will bind and become phosphorylated, leading to dimerization. Dimerized STATs are able to translocate into the nucleus and bind to DNA, targeting gene transcription [143–145]. While STAT3 targets vary for different

cell types, STAT3 downstream targets include many proteins associated with inflammation, increased cell proliferation and anti-apoptosis.

In LGL leukemia, STAT3 is constitutively active and plays a key role in $CD8^+$ T cell proliferation and progression of disease. We validated the pathogenicity of a dysregulated STAT3 pathway by demonstrating the induction of apoptosis of leukemic cells after disruption of the STAT3 pathway via pharmacological inhibitors [45]. Koskela et al. identified a remarkable 40% prevalence of somatic STAT3 mutations in LGL leukemia [68]. Since then, STAT3 mutations have been reported in 27–72% of LGL leukemia patient cohorts [65,146,147]. Initial reports found all STAT3 mutations in the Src homology 2 (SH2) domain, important in STAT dimerization. Mutational hotspots include Y640 and D661, which account for over 70% of the mutations. Mutations in other regions including the DNA binding domain and coiled-coil domain have since been reported [69]. Most mutations have been reported to increase the activity of STAT3 in transcriptional reporter assays.

Multiple correlations have been observed in patients with STAT3 mutations. Patients with STAT3 mutations are associated with increased symptoms such as neutropenia and anemia, and are more likely to need therapy. Additionally, patients with STAT3 mutations are more likely to present with rheumatoid arthritis than those with nonmutated STAT3. The first prospective clinical trial demonstrated a complete response to treatment in all patients with Y640F mutations. In contrast, only half of the patients with other STAT3 mutations responded and one quarter without STAT3 mutation responded [15].

The goal of this project is to identify novel STAT3 mutations that further emphasize the pathogenicity and specificity of STAT3 mutations to LGL leukemia. We performed paired whole genome sequencing (WGS) of 38 T-LGL leukemia patients and found several novel mutations outside of the established mutational hotspot domain, SH2.

within the coiled-coil and DNA binding domain. Discovery of novel mutations led to functional characterization by inserting WT and mutant STAT3 into WT HEK cells and STAT3 KO HEK cells.

3.2 Materials and Methods

PATIENT CONSENT AND SAMPLE ENRICHMENT

All studies were conducted under IRB-approved protocols for the LGL Leukemia Registry at the University of Virginia. All patients met inclusion criteria for diagnosis of T-LGL leukemia and were chosen to fit our criteria of a minimum of 70% leukemic cells in each WGS sample.

WHOLE GENOME SEQUENCING

We completed whole genome sequencing (WGS) of matched peripheral blood mononuclear cells (PBMCs) and saliva from 38 T-LGL patients at a target of 40X normal/80X tumor coverage (Illumina). Prior to sequencing, PBMC DNA was extracted by magnetic bead isolation (Anaprep, BioChain Institute). Saliva DNA was collected with Oragene OG-500 collection kits (DNA Genotek, Canada) and precipitated according to manufacturer's directions. We used Mutect2 [148] and Strelka [149] to identify somatic mutations in this cohort using COSMIC v77 and dbSnp v138 as whitelist and blacklist, respectively.

STAT3 MUTAGENESIS

Empty, WT STAT3 and STAT3 mutant plasmids were purchased from GeneCopoeia. We designed expression constructs to utlizie the LV224 plasmid with a EF1a promoter as shown in Figure 3.1. Glycerol stocks were streaked onto ampicillin plates overnight. Colonies were picked and grown in 5mL ampicillin LB broth overnight. 2mL of 5mL culture was inoculated in 200mL ampicillin LB broth overnight for maxi-prep. Invitrogen PureLink HiPure Plasmid Maxiprep (Fisher, Cat#K210007) protocol was

followed and DNA quantification was assessed by dsDNA broad range on Qubit (Thermofisher, Cat#Q32850).

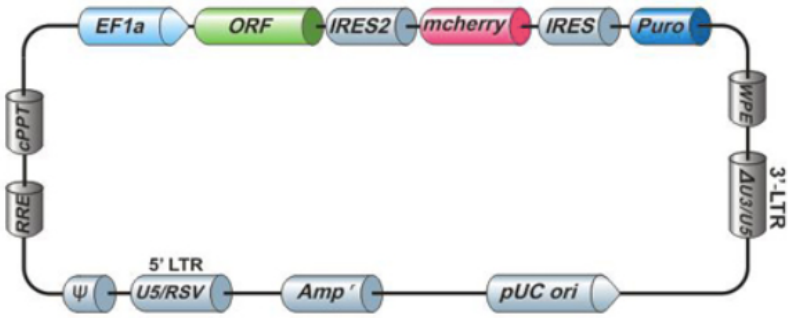

Figure 3.1: Map of vector used in STAT3 overexpression clones.

CELL LINES AND TRANSFECTION

WT HEK-293T cells were cultured in DMEM with 10% FBS. STAT3 KO HEK-293T (STAT3KO) were purchased from Genecopoeia in a 70% KO mixed cell vial. Single cell isolation was performed by plating 20 cells on a 10mm cell culture treated plate. Sterilized cloning rings were used to transfer single cell colonies to 96 well plate. 14 total colonies were transferred and western blot analysis of whole cell lysates determined which clone to transfect with STAT3 plasmids. All plasmids were transfected using Lipofectamine 3000 (Invitrogen (Carlsbad, CA, USA), Cat. L3000008) into WT HEK293T and clone 3 STAT3KO cells. 72 hours post transfection, media was changed to DMEM + 10% FBS + Puromycin for selection. Transfected cells were kept in selection media for maintenance.

WESTERN BLOTTING

Whole cell lysates were prepared in RIPA buffer (ThermoFisher (Carlsbad, CA, USA)) 72 h post-transfection; proteins were electrophoresed on a 4–12% acrylamide gel (ThermoFisher) and subsequently transferred to a Polyvinylidene fluoride (PVDF) membrane. Membranes were blocked and incubated with varying antibodies. Cell

signaling technology primary antibodies used in this study included Phospho-STAT3 (Y705, Cat #9131), Phospho-STAT3 (S727, Cat #9134), STAT3 (Cat #9139), Phospho-STAT1 (Y701, Cat #&649), STAT1 (CAT #9175), Phospho-STAT5 (Y694, Cat #9351), and STAT5 (Cat #9363). After incubation overnight at 4°C with a primary antibody, blots were incubated with a secondary antibody (anti-rabbit IgG–HRP (Horseradish Peroxidase) linked (Cat #7073) or anti-mouse IgG–HRP linked (Cat #7076)) for one hour, and washed before treating with Clarity enhanced chemiluminescence (ECT; Biorad) reagent. Membranes were imaged using a ChemiDoc MP instrument and analyzed using ImageLab (Biorad (Hercules, CA, USA)).

DNA BINDING ASSAY

Nuclear extracts from HEK-293T cells transfected with control, WT STAT3 and STAT3 mutant vectors were obtained using NE-PER Nuclear and Cytoplasmic Extraction Reagents (ThermoFisher, Cat# 78833). Plates were harvested when 70-80% confluent using ice cold PBS and followed steps as described in the protocol, including an extra wash step with CER I for complete removal of cytoplasmic extract. STAT3 transcription factor in 2ug nuclear protein samples were determined using the TransAM STAT3 Transcription Factor Assay Kit (Active Motif). The absorbance at 450 nm were acquired by using Cytation-5 Multi-Detection Microplate reader (Bio-TEK) following the manufacturer's protocols. Positive control, competitor dsDNA as well as no probe control for STAT3 were provided by Active Motif and used in each assay. Each sample was plated in triplicate and three biological replicates were performed.

REPORTER ASSAY

Three biological replicates were performed by transfecting Negative, positive and STAT3 reporter plasmids into stable mutant WT HEK cell lines using lipofectamine for 72 hours. At 72 hours, cells were harvested and plated in 96 well plate and luciferase was measured using Cytation-5 Multi-Detection Microplate reader (Bio-TEK) following protocols. Another three biological replicates were performed by transfecting negative, positive and STAT3 reporter plasmids in parallel with STAT3

overexpression vectors into WT HEK-293T cells with lipofectamine for 72 hours in 96 well plates. 72 hours after transfection, luciferase activity was measured.

STATISTICAL ANALYSIS

Significance between two treatment groups was determined by the two-tailed unpaired Student's *t*-test with $p<0.05$ considered statistically significant. Each experiment contained three or more technical replicates. Graphs depict mean and standard error of the mean (SEM) from a single experiment. Analyses were performed in GraphPad Prism.

3.3 RESULTS

WHOLE GENOME SEQUENCING REVEALED NOVEL STAT3 MUTATIONS

WGS of 38 T-LGL leukemia patients revealed 22 patients with STAT3 mutations. (**Figure 3.2**). Of those, 16 of those STAT3 mutations were found in the SH2 domain. The majority of mutations were found in the known hotspots, D661 and Y640. Five novel mutations, (L203V, K294E, D334A, H410P and Q448E) and a previously described mutation F174S were found to span the coiled-coil and DNA binding domains. Including all mutations, the percentage of STAT3 mutations increased to 56%.

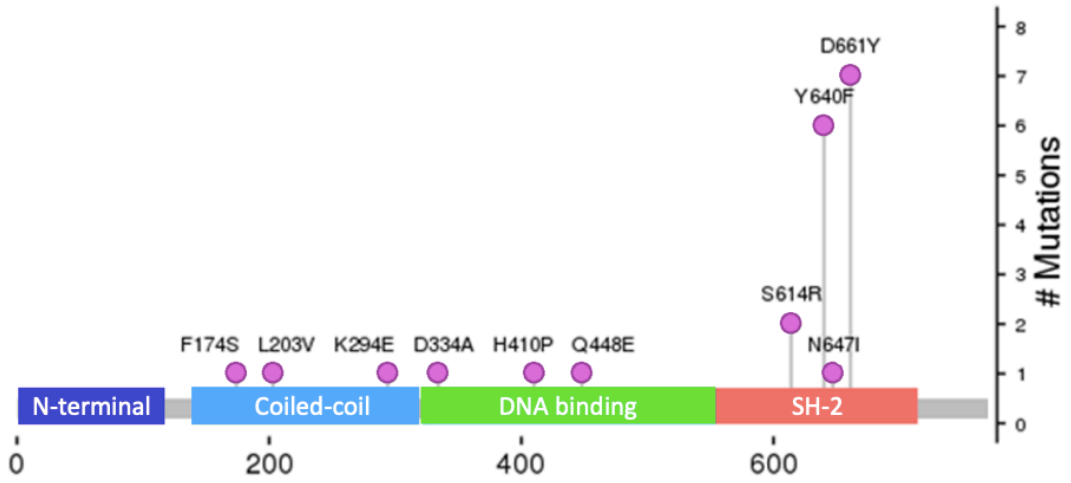

Figure 3.2: STAT3 mutations found in T-LGL leukemia cohort by WGS.

Lollipop plot showing all (22) STAT3 mutations found in 38 T-LGL leukemia patients. Mutations in the SH2 domain were the most prevalent, emphasizing known hotspot locations, Y640 and D661. Novel mutations outside of the SH2 domain were found among the coiled-coil and DNA binding domains.

SELECT NOVEL STAT3 MUTATIONS INCREASED STAT3 PHOSPHORYLATION IN WT HEK CELLS

To understand the functional implications of novel STAT3 mutations outside of the SH2 domain, we designed and purchased WT and mutant STAT3 overexpression clones. WT and mutant STAT3 overexpression constructs were transfected into WT HEK cells. Assessed by western blot, we observed increased STAT3 phosphorylation in WT HEK cells transfected with L203V, D334A, H410P and Q448E STAT3 constructs relative to WT HEK cells transfected with WT STAT3. (**Figure 3.3**) There was no difference between WT HEK cells transfected with WT STAT3 and those transfected with K294E STAT3. Out of the novel mutations, H410P showed the highest increase of STAT3 phosphorylation relative to WT STAT3 overexpression. Unexpected additional banding above the WT STAT3 was observed in all samples transfected with STAT3. Western blot probing revealed a mCherry:STAT3 fusion (**Figure 3.4**). Molecular weight of mCherry is 28.8kDa. In select STAT3 vector transfected WT HEK samples, mCherry bands were found above the 28kDa molecular marker as well as above the 98kDa molecular marker. With the molecular weight of STAT3 at 88kDa, a mCherry:STAT3 fusion would be expected to be between the 188kDa and 98kDa molecular marker.

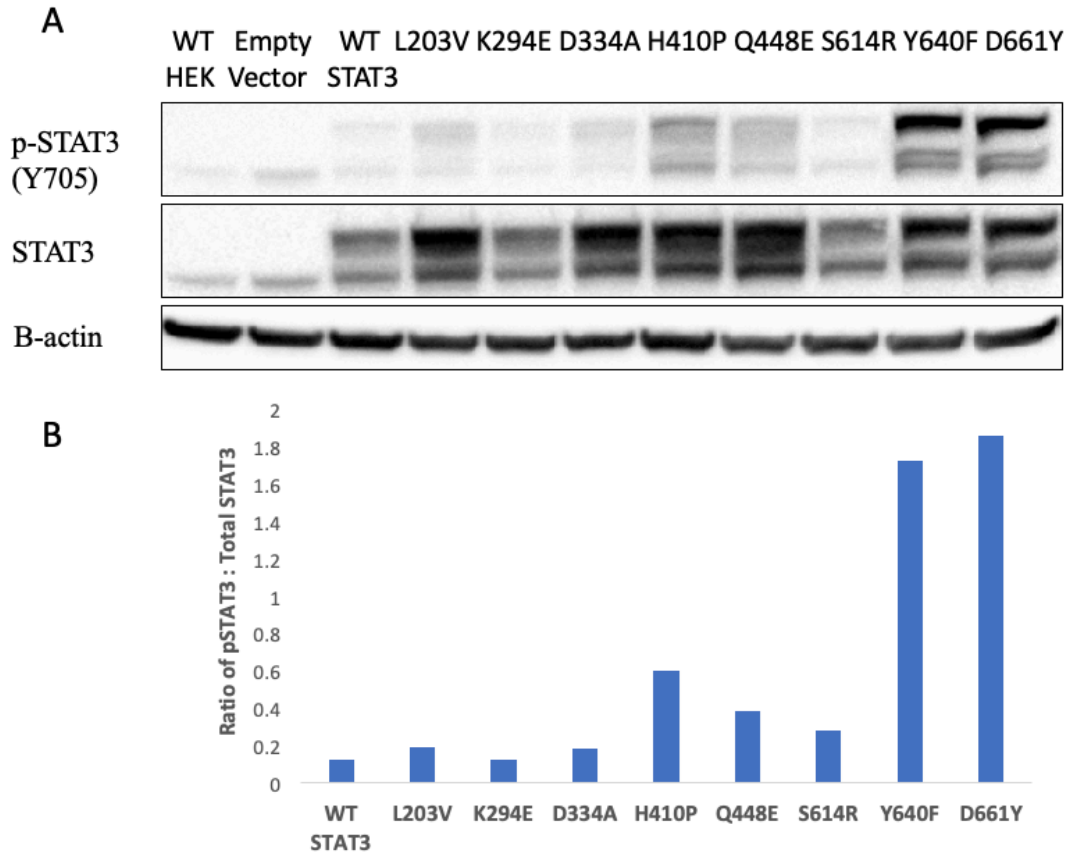

Figure 3.3: Comparison of STAT3 phosphorylation by western blot.

[A] Whole cell lysate of WT HEK cells transfected with STAT3 overexpression plasmids were run on a gel and probed for p-STAT3. Dramatic increase of p-STAT3 compared to STAT3 overexpression was observed in known activating mutants, Y640F and D661Y located in the SH2 domain. Out of the novel mutants, the largest increase in p-STAT3 was observed in H410P, followed by Q448E, both located in the DNA binding domain. Quantification of p-STAT3 over total STAT3 were graphed in [B].

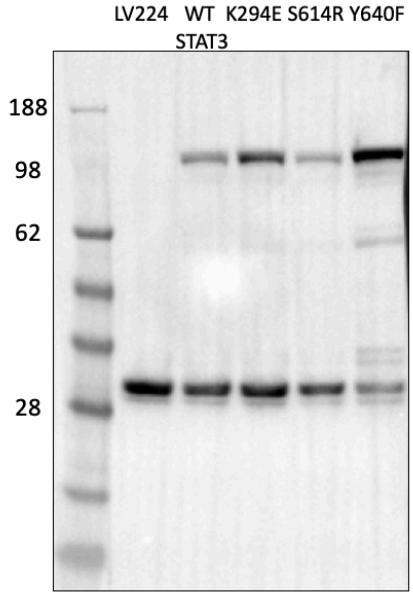

Figure 3.4: Additional banding of STAT3 due to mCherry:STAT3 fusion

Western blot of whole cell lysate from select plasmid transfected samples probed for mCherry show mCherry protein at the molecular weight above STAT3 indicating a read through of the IRES within the plasmid.

NOVEL STAT3 MUTATIONS INCREASED STAT3 DNA BINDING IN WT HEK CELLS

We then tested STAT3 activation by two separate assays. The first used a STAT3 ELISA-based assay with nuclear extracts from WT HEK cells transfected with WT and mutant STAT3 constructs. Nuclear extracts were added to wells coated in immobilized STAT3 consensus binding sites and absorbance was measured. All mutations increased DNA binding relative to the DNA binding of WT STAT3 overexpression. **(Figure 3.5**). The known activating mutations, D661Y and Y640F showed the highest fold change relative to WT STAT3 overexpression.

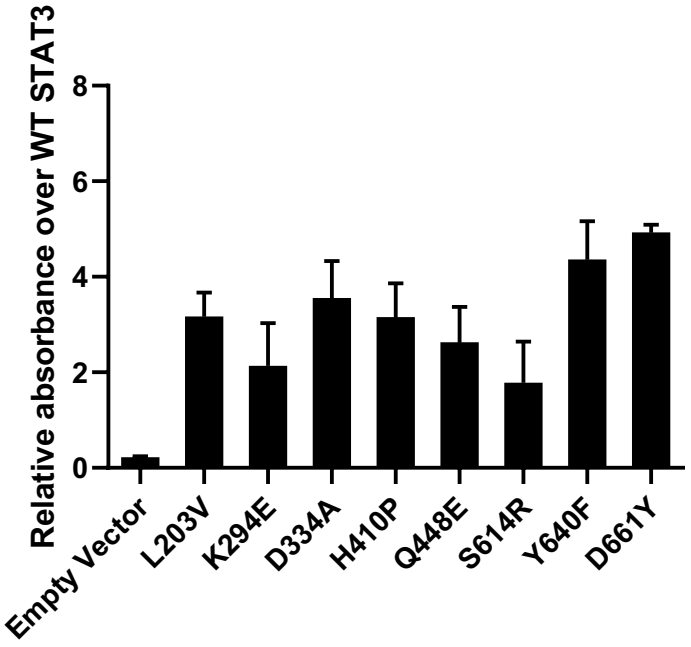

Figure 3.5: STAT3 mutations increased DNA binding.

Nuclear extracts of WT HEK-293T transfected with plasmids were added to a plate coated with immobilized STAT3 consensus binding sites. Absorbance was measured at 450nm and calculated relative to WT STAT3 overexpression. Each sample was plated in triplicate and three biological replicates were performed. Experiments performed by J.Y., K.H.D. and T.T.W.

H410P STAT3 SHOWED HIGHEST STAT3 ACTIVATION

To further characterize the functional implications of the novel STAT3 mutations, we transfected STAT3 reporter plasmids either in parallel with STAT3 overexpression plasmids or transfected into stable mutant HEK-293T cells. We observed H410P STAT3 in the DNA binding domain with the largest fold increase of STAT3 activity relative to WT STAT3 overexpression (**Figure 3.6**). Q448E and D661Y both had a robust increase in STAT3 activation while the other mutants showed minimal effects. Summary of STAT3 mutant characterization can be found in **Table 3.1**.

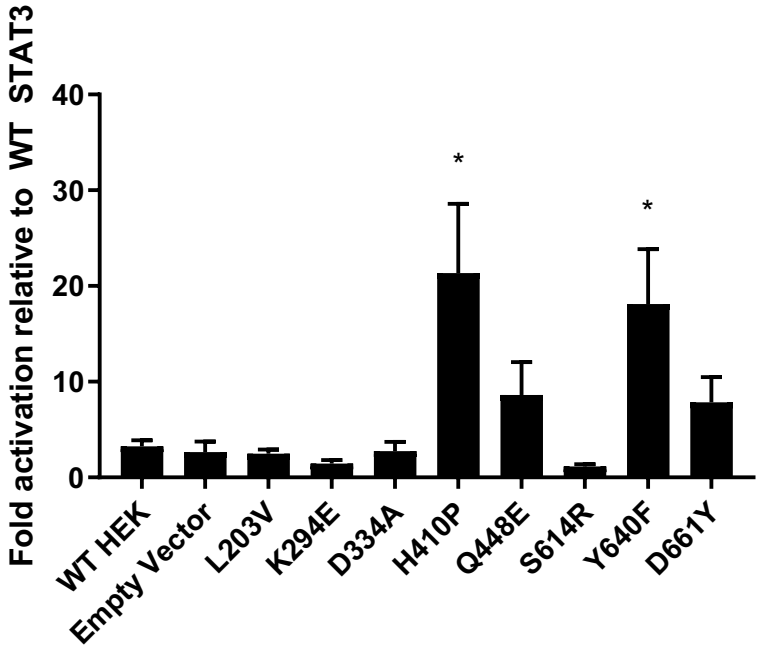

Figure 3.6: STAT3 reporter assay showed H410P STAT3 to exhibit the largest increase in STAT3 activation.

Stable STAT3 overexpression HEK cells were tranfected with a STAT3 response element luciferase reporter (n=3) or STAT3 response element luciferase reporter was transfected in parallel with STAT3 WT and mutant plasmids (n=3) and luciferase activity was measured after 72 hours. Results are reported as fold change relative to WT STAT3 overexpression and all samples were performed in triplicate. ($p < 0.05$)

Table 3.1: Summary of WT HEK STAT3 mutation characterization

Summary of all mutations characterized in this study including its location in the STAT3 gene, the resulting amino acid change, and quantification of the various functional assays. The quantification is annotated by color; those in red show the largest increase followed by orange for moderate increase relative to WT STAT3 overexpression.

	Mutation	Location	Amino Acid change	Fold change of STAT3 phosphorylation over WT STAT3	DNA binding	Reporter assay fold activation
Mutations found in WGS cohort	L203V	Coiled-coil	Leucine - Valine	1.6	3.34	2.48
	K294E	Coiled-coil	Lysine – Glutamic Acid	1.0	2.00	1.44
	D334A	DNA binding	Aspartic Acid – Alanine	1.5	3.53	2.74
	H410P	DNA binding	Histidine – Proline	4.9	3.41	21.35
	Q448E	DNA binding	Glutamine – Glutamic Acid	3.1	2.83	8.63
Previously characterized as activating mutations	S614R	SH2	Serine – Arginine	2.3	1.88	1.13
	Y640F	SH2	Tyrosine – Phenylalanine	14.1	4.56	18.13
	D661Y	SH2	Aspartic Acid - Tyrosine	15.2	4.85	7.84

STAT3 KO HEK-293T CELLS LACK STAT3 BUT SHOW INCREASED STAT1 AND STAT5

The above work featured the overexpression of STAT3 in WT HEK cells. To get a clearer picture of functional effects of STAT3 mutations, we purchased STAT3KO cells from GeneCopoeia. Cells were single cell cloned to obtain a clean STAT3 KO population and STAT3 levels were assessed shown in a representative western blot. **(Figure 3.7)** Select clones show lack of STAT3, but increased STAT1 and STAT5. Viability (not shown) was not affected, indicating STAT3 is not necessary for the survival of HEK cells and the ability of STAT1 and STAT5 to compensate for the lack of STAT3.

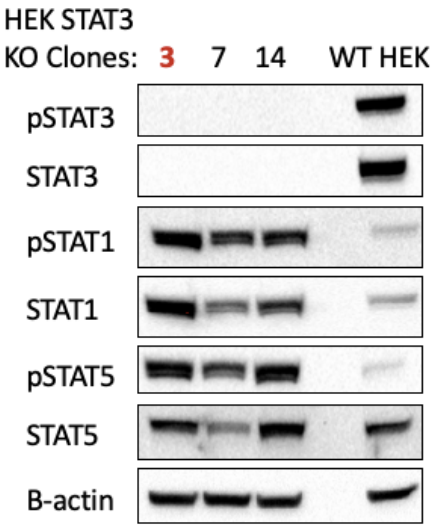

Figure 3.7: STAT3 KO HEK-293T show lack of phosphorylated and total STAT3.

Western blot analysis of whole cell lysate of three distinct single cell isolated STAT3KO cells show STAT1 and STAT5 rescue. Clone 3 (bolded in red) was later transfected with STAT3 mutant plasmids for further characterization.

STAT3 MUTATIONS SHOW SIMILAR STAT3 PHOSPHORYATION PATTERN IN STAT3 KO HEK-293T CELLS

STAT3 WT and mutant plasmids were transfected into clone 3 STAT3KO cells **(Figure 3.8)**. We observed similar STAT3 phosphorylation pattern as seen with WT HEK STAT3 mutant transfections. The known activation mutations, Y640F and D661Y showed the highest Y705 STAT3 phosphorylation. L203V, D334A, H410P and Q448E showed increased Y705 STAT3 phosphorylation compared to WT STAT3. Probing of phosphorylation at S727 showed an almost identical pattern to phosphorylation at Y705, with the exception of a strong lower band that has been observed in subsequent replicates (data not shown). This band was not observed in the western blots of WT HEK overexpression STAT3 vectors (data not shown). Expectedly, the STAT3:mCherry fusion was detected similar to Figure 3.4. Further functional characterizations of STAT3KO are currently ongoing.

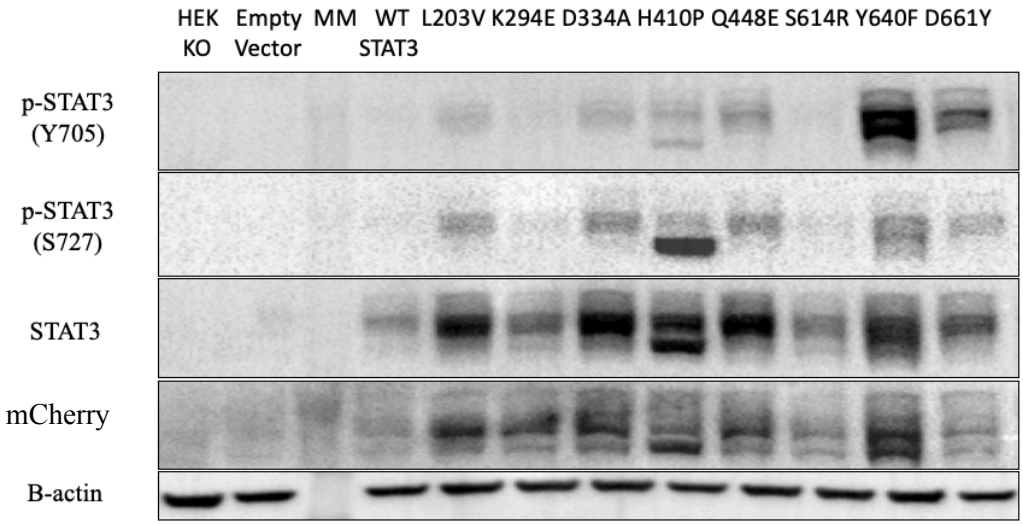

Figure 3.8: Western blot characterization of STAT3KO transfected with STAT3 WT and mutant plasmids show similar pattern compared to WT HEK transfection.

Whole cell lysate from STAT3KO transfected with STAT3 WT and mutant plasmids were probed for phosphorylated STAT3 (Y705 and S727), total STAT3, mCherry and β-actin. Samples prepared by T.T.W. and western blot run by K.H.D.

3.4 DISCUSSION

WGS of a large T-LGL leukemia patient cohort uncovered several novel mutations outside of the SH2 domain. (**Figure 3.2)** On average, roughly 40% of all T-LGL leukemia patients harbor a STAT3 mutation within the SH2 domain, but all LGL leukemia patients exhibit increased STAT3 signaling. We expected to find roughly 40% of patients to have a STAT3 mutation, and hypothesized that there were other STAT3 mutations. Six mutations outside of the SH2 domain were found, including five novel STAT3 mutations. Functional characterization of these novel mutations was studied through phosphorylation by western blot, DNA binding by an ELISA based assay, and activation via STAT3 reporter assay. Quantification of these assays are summarized in **Table 3.1**.

An unexpected and intriguing observation was extra bands on western blots when probing for phosphorylated or total STAT3. Despite the insertion of a several stop codons and an IRES between the STAT3 sequence and mCherry in the plasmid, we observed a mCherry:STAT3 fusion, indicating a read through. While the fusion of mCherry to STAT3 creates a larger protein, we have demonstrated its ability to be phosphorylated, translocated into the nucleus and initiated transcription. The limitation created is that the incidence of readthrough is unknown. This may be ameliorated with single cell cloning of transfected cells to reduce variation. It would be helpful to create clones that have no readthrough or consistent readthrough, and single cell cloning would isolate a single clone.

Characterizations of mutations were not all in agreement, resulting in variations in analysis of the response to the different assays. For example, the ELISA based DNA binding assay found all mutations to have increased DNA binding, including K294E and S614R that did not exhibit increases in STAT3 phosphorylation or STAT3 activation by reporter assay. One explanation is that the quantification of STAT3

phosphorylation by western blot is not very accurate as the amount of total STAT3 in the various groups were not similar. Total STAT3 in L203V, D334A, H410P, Q448E, Y640F and D661Y were significantly increased in comparison to K294E and S614R. More total STAT3 results in more STAT3 available for activation, which can affect the interpretation of how these mutations affect STAT3 activation. To distinguish the effects of the mutation itself rather than the effects of increased STAT3, it is necessary to normalize protein concentrations for western blots to STAT3 rather than total protein. Running a western blot where the samples are normalized to total STAT3 would allow for proper comparison between mutants and may reveal alternative results. Differences of total STAT3 may hide the extent of activation, as the mutations may activate all available STAT3 but is overshadowed as there is less STAT3 available.

The DNA binding assay is an *in vitro* assay using nuclear extracts also normalized using total nuclear protein. Western blots of nuclear extracts (not shown) also show disproportional amounts of total STAT3 that could modify interpretations of these mutations. Using the amount of extract normalized to total STAT3 may also cause variations in analysis. While the other assays have their merits, most studies characterizing novel mutations typically use reporter assays due to its sensitivity and ability to comprehensively quantify the activation of transcription factors. STAT3 activation is a complex process that involves many other variables and cofactors that may be affected by mutations. These include co-binding partners and STAT3 activators or repressors.

Important components of STAT3 signaling that are often overlooked in disease pathogenesis studies are the negative regulators. Negative regulators work in tandem with activators to maintain immune homeostasis. Previous studies documented the loss of STAT3 negative regulators in cancers [150,151] and more recent studies revealed their potential as tumor suppressors, using pharmacological targeting as promising therapeutic approaches in cancer [152,153]. There are three families of STAT3

negative regulators; suppressor of cytokine signaling (SOCS), protein inhibitor of activated STAT (PIAS) and protein tyrosine phosphatases.

The SOCS negative regulators cause inhibition by competitive binding. Of the 8 known members of the SOCS family, SOCS1 and SOCS3 are characterized as negative regulators of STAT3. SOCS1 and SOCS3 can inhibit the JAK/STAT pathway by acting as a substrate for JAKs, blocking their kinase activity [154]. qPCR of LGLL patient cells contain low SOCS1 RNA expression compared to CD8+ T cells from normal donors/controls [15]. This may lead to decreased SOCS1 protein levels and lessened control on STAT3. Furthermore, Teramo et al found that decreased SOCS3 protein and mRNA contributed to leukemic LGL survival. In addition, they observed SOCS3 restoration with a demethylating agent resulted in lowered STAT3 activation and apoptosis [88]. These data suggest further research into the characterization of other STAT3 negative regulators.

The PIAS family regulates diverse cytokine and growth factor signaling pathways through protein-protein interactions. PIAS3 specifically inhibits STAT3 by negatively regulating STAT3 transcriptional activity through a formation of a STAT3-PIAS3 complex [155]. This complex blocks STAT3 binding to DNA and its subsequent transcription regulation. Low PIAS3 levels were found in T cell lymphoma [150] as well as in squamous cell lung cancer, where its low expression level predicted poor overall survival [156]. Increasing concentration of PIAS3 in lung cancer cells decreased STAT3 phosphorylation [157] and cell proliferation [158], indicating the role of PIAS3 in the control of STAT3 activity and proliferation of transformed cells. The characterization of PIAS3 expression in LGLL has not been studied. If low levels of PIAS3 were to be found in T-LGLL patient cells, it would decrease the negative regulation of STAT3 activity and support the constitutive activity of STAT3. We may also find that STAT3 mutations affect the formation of the STAT3-PIAS3 complex, particularly whether mutations in certain domains of STAT3 affect binding of PIAS3 to STAT3, leading to a lack of STAT3 negative regulation.

As tyrosine phosphorylation is a critical step in JAK/STAT activation, it is important to maintain cell homeostasis through the removal of phosphorylation by phosphatases. The tyrosine phosphatases that inhibit STAT3 include src homology 2 (SH2)-containing phosphatase-1 (SHP1), SHP2, and protein tyrosine phosphatases (PTPRT, PTPRK, PTPN2). SHP1, SHP2 and PTPN2 inhibit STAT3 through the removal of phosphates on activated JAKs [159]. Studies show that loss of SHP1 in anaplastic large-cell lymphoma contributes to the pathogenesis of the disease by the loss of inhibition of JAK3/STAT3 pathway and decrease of JAK3 degradation [160]. In breast and colorectal cancer, sorafenib is shown to upregulate SHP1 activity, inducing a decrease of STAT3 activation in vitro and in vivo [152]. This demonstrates that a decrease in SHP1 is implicated in cancer and can be pharmacologically targeted. A somatic mutation in protein tyrosine phosphatase receptor T (PTPRT) was discovered in LGL leukemia [66]. PTPRT binds to and dephosphorylates STAT3 at Y705 and is shown to be a tumor suppressor in several cancers [85]. In head and neck squamous cell carcinoma, the PTPRT promoter is highly methylated which results in a downregulation of PTPRT mRNA [161]. Reducing the phosphatase activity of PTPRT allows STAT3 to stay phosphorylated and hence activated longer, contributing to the perpetuation of oncogenesis. STAT3 regulators need to be further studied not only in the context of LGL leukemia but also in the context of STAT3 mutations.

Our studies characterized H410P STAT3 as an activating mutation. H410 is located within the DNA binding domain and sits in the middle of a β-strand, as part of a β-sheet. According to the crystal structure, H410 engages in electrostatic interactions with the DNA and disruption of those interactions would interfere with DNA binding [162]. Our data shows H410P to be an activating mutation, resulting in increased STAT3 phosphorylation, DNA binding and activation compared to WT STAT3. Future studies are needed to further characterize this mutation. While this particular amino acid change has never been found, a mutation at this residue has been reported [69] and was also characterized by phosphorylation in HEK cells in agreement with our findings.

It is not known whether any amino acid substitution would result in increased activation, or if it is amino acid dependent. It would be of interest to study the effect of various amino acids at this residue on its interactions with DNA.

A non-canonical STAT3 signaling pathway includes STAT3 activity in the mitochondria. Localization of STAT3 to the mitochondria requires serine phosphorylation at 727. S727 phosphorylation is not fully understood and its role is still controversial. It has been reported to enhance transcriptional activation [163,164] and promote tumorigenesis [165] and in some cases, decrease tyrosine phosphorylation [166,167]. In the mitochondria, STAT3 has been shown to interact with components important in reactive oxygen species (ROS) regulation [168]. Using the STAT3KO model, we observed increased S727 STAT phosphorylation in all STAT3 mutations except K294E and S614R. Again, this may be altered when using total STAT3 as the control for protein concentrations in western blot analysis. Interestingly, we found a strong distinct S727 phosphorylation band only in STAT3KO transfected with H410P STAT3. This has been replicated and further exploration is needed to confirm our findings to understand if this band represents use this as a tool to study mitochondrial STAT3 regulation and its role in disease progression.

In conclusion, we report an increase from 40% to 56% STAT3 mutated patients in our cohort when including mutations outside of the SH2 domain. This result indicates the importance to sequence the entire STAT3 gene as the occurrence of STAT3 mutations in LGL leukemia is likely underreported. Whole genome sequencing revealed five novel STAT3 mutations outside of the SH2 domain that were characterized in this study by STAT3 phosphorylation using western blots, DNA binding by an *in vitro* ELISA based assay and a STAT3 reporter assay. These findings emphasize the significant role STAT3 plays in LGL leukemia. Further studies are needed to explore the consequences these mutations within the complicated realm of T cell biology.

4 TARGETING THE JAK/STAT PATHWAY BY IL-2 AND IL-15 BLOCKADE

This chapter is adapted from:
Wang TT, Yang J, Zhang Y, Zhang M, Dubois S, Conlon KC, Tagaya Y, Hamele CE, Dighe S, Olson TL, Feith DJ, Azimi, N, Waldmann TA, Loughran TP. IL-2 and IL-15 blockade by BNZ-1, an inhibitor of selective γ-chain cytokines, decreases leukemic T-cell viability. Leukemia. 2019 May;33(5):1243-55.

Conceptualization, N.A., T.P.L., T.T.W.; data curation, T.T.W., J.Y., Y.Z., S.D., M.Z., and S.D; formal analysis, T.T.W., J.Y. and Y.Z..; funding acquisition, T.A.W. and T.P.L.J.; investigation, T.T.W., J.Y., and Y.Z.; methodology, T.T.W. Y.Z.,; CTCL studies, Y.Z., M.Z., and T.A.W.; writing—original draft, T.T.W. and T.A.W.; writing—review and editing, T.T.W., J.Y., Y.Z., Y.T., T.L.O., D.J.F., N.A., T.A.W. and T.P.L.J.

ABSTRACT

Interleukin-15 (IL-15) and IL-2 drive T-cell malignancies including T-cell large granular lymphocyte (T-LGL) leukemia and HTLV-1 driven adult T-cell leukemia (ATL). Both cytokines share common γ-chain receptors and downstream signaling pathways. T-LGL leukemia is characterized by clonal expansion of cytotoxic T cells and is associated with abnormal JAK/STAT signaling. ATL is an aggressive CD4+ T cell neoplasm associated with HTLV-1. T-LGL leukemia and ATL share dependence on IL-2 and IL-15 for survival and both diseases lack effective therapies. BNZ-1 is a pegylated peptide designed to specifically bind the γc receptor to selectively block IL-2, IL-15 and IL-9 signaling. We hypothesized that treatment with BNZ-1 would reduce cytokine mediated proliferation and viability. Our results demonstrated that *in vitro* treatment of a T-LGL leukemia cell line and *ex vivo* treatment of T-LGL leukemia patient cells with BNZ-1 inhibited cytokine mediated viability. Furthermore, BNZ-1 blocked downstream signaling and increased apoptosis. These results were mirrored in an ATL cell line and in *ex vivo* ATL patient cells. Lastly, BNZ-1 drastically reduced leukemic burden in an IL-15-driven human ATL mouse xenograft model. Thus, BNZ-1 shows great promise as a novel therapy for T-LGL leukemia, ATL and other IL-2 or IL-15 driven hematopoietic malignancies.

4.1 INTRODUCTION

Cytokines that share the common gamma-chain (γc) receptor are essential for development and maturation of lymphocytes as well as immune function and activation. Specifically, IL-2 and IL-15 promote survival and proliferation of T-cells and downstream effects that include induction of the JAK/STAT pathway [54]. IL-2 is produced almost exclusively by T cells and signals through the heterotrimeric IL-2 receptor complex, including IL2Rα (CD25), IL2/IL15Rβ (CD122) and the γc receptor (CD132) [169]. IL-15 is produced mainly by dendritic cells and monocytes, and signals through IL-15Rα together with shared CD122 and γc receptor subunits. The two unique receptor α chains are differentially distributed on cells and are required for high affinity binding [54]. Combinations of γc cytokines are involved in the pathogenesis of a diverse array of human diseases. [54,170–172] Implications of IL-2 and IL-15 in several T-cell malignancies have been well established [170,173–181]. In this study, we focus on effects of dysregulated IL-2 and IL-15 signaling in large granular lymphocyte leukemia (LGLL) and HTLV-1 driven adult T cell leukemia (ATL).

LGLL is defined by a clonal expansion of large granular lymphocytes in blood. LGL make up 10-15% of peripheral blood mononuclear cells (PBMC), are activated upon antigen recognition, expand quickly, and then undergo apoptosis upon antigen clearance. However, in LGLL, these cells resist apoptosis and clonally expanded leukemic LGL can account for up to 90% of PBMC [182]. This LGLL population can be separated into natural killer (NK) cells (typically CD3-CD56+CD16+) [182] or T-cells (typically CD3+CD8+CD56-CD57+CD28-TCR-αβ+) [183]. There is not a cure for LGLL and current treatments include low doses of broad immunosuppressants, including methotrexate, cyclophosphamide and/or cyclosporine, thus indicating a need to develop more specific therapeutic options [14].

LGLL is associated with dysregulation of several signaling pathways, including MAPK, PI3K-Akt, sphingolipid metabolism, NF-κB and JAK/STATs [97]. Additionally, gain-of-function mutations in *STAT3* [65,68,69] and/or *STAT5b* [78] are found in up to 40% of patients, emphasizing the role of JAK/STATs in the disease. Moreover, independent of STAT3 mutation status, all patients exhibit constitutively activated STAT3 and STAT1 [45,68]. STAT activating mutations have been shown to provide a growth advantage [67] but they are not sufficient for leukemic cell proliferation, rather they enhance upstream signals from cytokine activation of the JAK/STAT pathway and result in a persistence of activated STATs [110]. The pathogenesis of a dysregulated JAK/STAT pathway combined with the high prevalence of activating mutations suggests a pathway-directed therapeutic opportunity. IL-15 in particular has been implicated in the pathogenesis of LGLL. Significantly elevated levels of IL-15 mRNA and IL-15Rα are found in patient PBMCs [56,57]. Using a systems biology approach, IL-15 was identified as one of two master regulators of the disease [53], making IL-15 an attractive target for therapies.

HTLV-1 derived ATL is an aggressive disorder involving Tregs (typically CD2+CD3+CD4+CD25+CD7-) [180,184] that also exhibits aberrant cytokine signaling. Many of the immune abnormalities in early ATL have been linked to HTLV-1 Tax that directly and through activation of NF-κB induces the expression of IL-2 and IL-15 and their specific receptors (IL-2Rα and IL-15Rα) as well as IL-9, leading to excessive signaling through proinflammatory autocrine and paracrine loops [184–186].. This leads to activation of JAK1/3 and STAT5 signaling pathways [187]. It was previously demonstrated that IL-2/IL-2Rα, IL-9 and IL-15/IL-15Rα are overexpressed in ATL PBMCs and cooperate to yield *ex vivo* spontaneous proliferation of PBMCs [188], which is an important tool to evaluate potential interventional strategies and specific therapeutic agents. When *ex vivo* leukemic cells are incubated with antibodies to IL-2Rα, IL-15 and IL-9, proliferation is profoundly inhibited (over 80%), thereby demonstrating the cytokine dependency of ATL cell proliferation and survival.

Due to the vital role that IL-2 and IL-15 play in LGLL and ATL, there is strong rationale for therapy directed at their signaling pathways. Both diseases have attempted therapies targeting one specific cytokine through monoclonal antibodies. In T-LGLL, a Phase I trial of a humanized monoclonal antibody to the IL2/IL15Rβ (CD122) receptor (Hu-Mikβ1) failed to exhibit clinical efficacy [93]. Hu-Mikβ1 blocked *trans*-presentation of IL-15, the main mechanism of IL-15 presentation [189]. However, in the presence of elevated IL-15Rα in LGLL patients, IL-15 can efficiently signal through *cis* presentation. In ATL, a clinical trial of humanized anti-Tac (daclizumab, anti-IL-2Rα) [190] was limited by the fact that the antibody inhibited only IL-2 and had no effect on IL-9 or IL-15 mediated proliferation. An alternative approach using a JAK inhibitor demonstrated unacceptable toxicity when dose and dosing strategies sufficient to block the signaling pathway were utilized [191]. To address this challenge, the BNZ-1 PEGylated peptide that targets IL-2, IL-15 and to a lesser extent IL-9 was developed [170]. Since the functional redundancy among γc cytokines is largely due to the sharing of the γc subunit, we rationally chose to target this binding interface with the goal of inhibiting multiple γc cytokines.

BNZ-1, formerly known as BNZ 132-1-40 [170], is a helical peptide designed to bind directly to the γc molecule and is PEGylated to increase its half-life. It can selectively block IL-2, IL-15, and IL-9 binding while leaving other γc and non-γc cytokine signaling unaffected [170]. Previously, BNZ-1 effectively inhibited *ex vivo* HTLV-1 associated myelopathy/ tropical spastic paraparesis PBMC proliferation [192] and *in vivo* proliferation of murine CD8+ T cell leukemia in an IL-15 transgenic mouse model [170]. In addition, BNZ-1 exhibited no adverse effects on other immune cells and maintained selectivity for T_{regs}, CD8+ T and NK cells. Furthermore, a recent phase 1 clinical trial proved BNZ-1 to be well tolerated in healthy subjects [193]. These positive results prompted us to determine the efficacy and mechanism of BNZ-1 in LGLL and ATL.

In this study, we show the therapeutic potential and mechanism of BNZ-1 in LGLL and HTLV-derived ATL. We hypothesized that attenuation of both IL-2 and IL-15 signaling pathways would result in decreased viability, proliferation, and ultimately death of cancer cells. Here, we not only show the successful treatment using BNZ-1 *in vitro* and *ex vivo* in T-LGLL and ATL cell line models and patient PBMCs, but also demonstrate the efficacy of BNZ-1 by reducing leukemic burden in an *in vivo* HTLV-1 derived ATL mouse model.

4.2 Materials and Methods

CELL LINES

TL-1 is an IL-2-dependent patient-derived T-LGLL cell line [41]. TL-1 was immortalized with the retroviral HTLV-2 tax gene [41] and is maintained in RPMI 1640 with 10% FBS (Seradigm) supplemented with IL-2 (200 U/mL, Miltenyi Biotec). NKL is an IL-2 dependent cell line derived from a CD3-CD16+CD56+ NK-LGL patient and maintained in RPMI with 10% FBS and supplemented with IL-2 (100 U/mL) [194]. 32D is an IL-3-dependent murine myeloid precursor cell line that expresses IL-2Rα and γc but not IL-2Rβ [195]. 32Dβ cell line was established by transfection with an extra-chromosomal DNA expression vector pREP9 (Invitrogen) encoding human IL-2Rβ. The 32Dβ cells were maintained in IL-2 (40 U/mL) to retain IL-2Rβ expression in the transfected cell line [195]. ED40515(+) is a human IL-2/IL-15-dependent ATL cell line which was kindly provided by Michiyuki Maeda [196] (Kyoto University, Japan). ED40515(+)/luciferase cell line was produced by infection of wild-type ED40515(+) ATL cells with lentivirus expressing luciferase. ED40515(+) cells were maintained in RPMI 1640 with 10% FBS, 100 U/mL penicillin and 100 μg/mL streptomycin, 100 U/mL recombinant human IL-2 in an atmosphere containing 5% CO_2. ED40515(+)/luciferase cells were maintained in the same culture medium as used for ED40515(+) cells with an exception that the medium contained G418 (0.1 mg/mL).

CELL VIABILITY ASSAY

Cell viability was assessed by the CellTiter-Glo Assay (Promega). TL-1, NKL and primary T-LGLL patient PBMC's were seeded at 2,500 viable LGL cells per well of 384 well plates in triplicate and cytokine deprived overnight. BNZ-1 pretreatment for 20 minutes was followed by addition of varying doses of IL-2 or IL-15 and luminescence was measured at 24, 48 and 72 hours. CellTiter-Glo reagent was added to wells at 1:1 ratio and incubated in the dark at room temperature for 20 minutes prior to reading. Plates were read using a Cytation3 plate reader (Biotek) and normalized to blank reading of RPMI-10% FBS and substrate. Bars represent relative light units (RLU; mean ± standard deviation).

WESTERN BLOT ANALYSIS

5 x 10^6 cells were plated for overnight cytokine deprivation and pretreated with BNZ-1 (20 minutes) prior to addition of IL-2 or IL-15. After 30 minutes of cytokine treatment, cells were washed with PBS and then lysed with RIPA buffer (ThermoFisher) plus protease inhibitor cocktail (Sigma-Aldrich) and phosphatase inhibitor cocktails (Sigma-Aldrich). BCA assays were performed to determine protein concentration (Pierce). Proteins were electrophoresed on a 4-12% acrylamide gel (ThermoFisher), transferred to PVDF membranes (BioRad) and immunostained with varying antibodies. Cell Signaling Technology primary antibodies used in this study include: Phospho-STAT3 (Y705; Cat #9131); STAT3 (Cat #9139); Phospho-STAT1 (Y701; Cat #7649); STAT1 (Cat #9175); Phospho-STAT5 (Y694; Cat #9351); STAT5 (Cat #9363); Phospho-Akt (S473; Cat #4060); Akt (Cat #9272); Phospho-p44/42 MAPK (Erk1/2;T202/Y204; Cat #4370); and p44/42 MAPK (Erk1/2; Cat #9102). After incubation overnight at 4˚C with primary antibody, blots were incubated with secondary antibody (anti-rabbit IgG-HRP linked (Cat# 7074) or anti-mouse IgG-HRP linked (Cat#7076)) for one hour and washed before treating with Clarity enhanced

chemiluminescence (ECL; Biorad) reagent. Blots were imaged using a ChemiDoc MP instrument and analyzed using Image Lab (Biorad).

CELL PROLIFERATION ASSAY

The 32Dβ cells maintained in medium containing IL-2 (40 U/mL) were washed with PBS for 3 times. Aliquots ($1x10^4$) of the 32Dβ cells were seeded in 96-well plates with medium containing IL-2 (100 U/mL), or IL-15 (5 ng/mL), or murine IL-3 (500 ng/mL) together with serial dilutions of BNZ-1 (Bioniz Therapeutics Inc) and incubated for 48 hours. Aliquots ($1x10^4$) of ED40515(+) cells were cultured in medium containing IL-15 (2.5 ng/mL) and serial dilutions of BNZ-1 for 72 hours. The PBMCs isolated by Ficoll-Hypaque density centrifugation from patients with IL-2, IL-9, IL-15 autocrine smoldering ATL at 1 X 10^6/mL in 96 microtiter plates in RPMI 1640 media supplemented with 10% FBS at 37°C in 5% CO_2 were cultured *ex vivo* for 6 days with and without BNZ-1 or with 10 μg/mL of antibody added at initiation of the cultures. A single antibody directed against the cytokine IL-2, IL-9 or IL-15 was used or with their combination. Cells were pulsed during the last 6 hours with 1 μCi (0.037 MBq) of ^{3}H-thymidine (Perkin Elmer) then harvested and counted in a MicroBeta2 microplate counter. The experiments were performed in duplicate or triplicate and the data are expressed as mean or mean ± SD. Both IL-2 and IL-15 were provided by the Biopharmaceutical Department of the National Cancer Institute.

APOPTOSIS DETECTION

Apoptosis was assessed by flow cytometry analysis of propidium iodide (PI) and APC-annexin V stained cells. TL-1 cells were IL-2 starved overnight and seeded at 500 000 cells per well. Cryopreserved patient PBMCs were thawed and incubated in RPMI 1640 plus 10% FBS overnight. Cell viability was assayed by trypan blue exclusion assay and was over 90%. BNZ-1 was added 20 minutes prior to addition of IL-2 (2.5

U/mL), IL-15 (2.5 U/mL), or IL-2 (2.5 U/mL) and IL-15 (2.5 U/mL). At 72 hours, cells were incubated with PI (BD Biosciences, Cat #556463) and/or APC-annexin V antibody (BC Biosciences, Cat #550474) stains for 15 minutes and then washed in PBS immediately prior to FAC analysis. All conditions, including appropriate single stains, fluorescence minus one and compensation controls were performed in triplicate. At least 20 000 cells were analyzed on BD Biosciences LSRFortessa and results were analyzed using FCS Express 9 (De Novo Software).

EX VIVO CULTURES OF PBMCS

T-LGLL patients, studied under the University of Virginia IRB #17070 "Pathogenesis of Large Granular Lymphocyte Leukemia", met the clinical criteria of T-LGL leukemia with increased numbers of CD3+, CD8+/CD57+ T lymphocytes or CD3−, CD16+/CD56+ NK cells in the peripheral blood [14]. T-LGLL patient blood samples were obtained and informed consents signed for sample collection according to the Declaration of Helsinki using a protocol approved by the Institutional Review Board of the University of Virginia. Blood was subjected to Ficoll-Hypaque (Sigma Aldrich) gradient centrifugation for PBMC isolation and cells were cultured *ex vivo* in RPMI 1640 medium with 10% FBS. Patient samples used to assess apoptosis by flow cytometry were previously frozen, and cell viability was determined by trypan blue exclusion assay prior to the start of treatment. Relevant patient data can be found in **Table 4.1**. Peripheral blood specimens were screened for somatic activating mutations in *STAT3* by Sanger sequencing as previously described [197]. Blood was subjected to Ficoll-Hypaque (Sigma Aldrich) gradient centrifugation for PBMC isolation and cells were cultured *ex vivo* in RPMI 1640 medium with 10% FBS. They were then plated for either cell viability assay, western blotting or flow cytometry analysis.

Table 4.1: Summary of all patients used in LGLL studies.

T-LGLL patients were acquired from the LGL Leukemia Registry. LGL percentages were obtained from clinical flow cytometry report that most closely matched the date of sample collection. STAT3 mutations were determined by Sanger sequencing as described in the Material and Methods. The sample from patient 2090 included a silent AUC to AUA mutation at codon 653 that did not change the amino acid.

Patient ID	Subtype	Age	Sex	% LGL	STAT3
1370	T-LGL	78	F	82	D661V
1613	T-LGL	63	M	86	WT
1875	T-LGL	64	F	90	D661Y
1906	T-LGL	58	M	53	WT
1954	T-LGL	47	M	38	WT
1985	T-LGL	58	M	47	Y640F
2051	T-LGL	72	F	84	D661Y
2090	T-LGL	57	F	92	I653I, K658N, I659L

ATL patient blood samples were obtained from patients under the care of the Clinical Trials Team, Lymphoid Malignancies Branch, National Cancer Institute (NCI), National Institutes of Health (NIH). This study protocol was approved by the Institutional Review Board of the NCI. Informed consent was obtained in writing in accordance with the Declaration of Helsinki. Mononuclear cells (PBMC) were isolated from anticoagulated blood by density centrifugation and then cultured *ex vivo* in RPMI 1640 medium containing 10% FBS with or without different therapeutic reagents for 6 days. The cells were pulsed during the last 6 hours with 1 μCi of ^{3}H-thymidine. Then, the cells were harvested with a cell harvester and counted in a MicroBeta2 microplate counter. Assays were performed in triplicate and the data are expressed as mean ± SD. The anti-IL-2Rα antibody (daclizumab) was purchased from Roche. Anti-human IL-15 antibody (clone # 34593) was purchased from R&D systems and anti-human IL-9 antibody (clone # MH9A3) from Biolegend.

MURINE ATL MODEL

The tumor model of cytokine-dependent ATL, ED40515(+)/luciferase, was established in 4-6 week old human IL-15 transgenic NSG (NOD/SCID/gamma) female mice (Taconic). Expression of IL-15 by the IL-15 transgenic mice was established and provided the inclusion/exclusion criteria. No animals were excluded in this study. The cytokine-dependent ATL model was established by i.v. injection of $1x10^7$ ED40515(+)/luciferase cells into human IL-15 transgenic NSG mice (Taconic). Treatment was initiated seven days later when serum sIL-2Rα levels were >500 pg/mL. The ED40515(+)/luciferase tumor-bearing NSG mice were block randomized into three groups with six mice per group, with comparable average sIL-2Rα levels among the groups. Tumor-bearing mice received BNZ-1 at a dose of 40 mg/kg i.v., twice a week for 4 weeks or ruxolitinib at a dose of 50 mg/kg/day by subcutaneous osmotic pumps for 4 weeks. An additional group of the mice that received i.v. injection of PBS alone served as a control. Throughout the experiment, the tumor growth was monitored by serum sIL-2Rα concentrations and by bioluminescence images. No blinding was done. Sample size was determined as six per group as we would need at least five subjects in each group to have a 90% probability of showing a statistically significant difference (if using $p< 0.05$) or at least six subjects in each group to have a 80% probability of showing a statistically significant difference (if using $p< 0.01$) based on reference websites from Taconic. All animal experiments were approved by the National Cancer Institute Animal Care and Use Committee (NCI ACUC) and were performed in accordance with NCI ACUC guidelines.

DETECTION OF SERUM CONCENTRATION OF THE SOLUBLE IL-2RA (SIL-2RA)

The blood samples were taken from the tumor-bearing mice. Measurement of the serum concentrations of the sIL-2Rα, a surrogate tumor marker of the IL-2Rα expressing ATL cells, was performed using an enzyme-linked immunosorbent assay (ELISA) purchased

from R&D Systems (soluble Tac, catalogue no. DR2A00, Minneapolis, MN). The ELISAs were performed as indicated in the manufacturer's instruction manual.

STATISTICAL ANALYSIS

Statistical analyses for all experimental systems utilized unpaired Student's *t* test.

4.3 RESULTS

BNZ-1 EXHIBITED SELECTIVE TARGETING OF CYTOKINE-INDUCED PROLIFERATION

BNZ-1 mediated effects were exclusively related to IL-2 and IL-15 blockade [170]. We have verified the reported results by using 32Dβ cells that express IL-2Rβ and respond to IL-2 [195]. Both IL-2 and IL-15 stimulated 32Dβ cell proliferation in a dose-dependent manner (**Figure 4.1A**). The proliferation of the cells was completely inhibited by BNZ-1 while the off-target non-γc-mediated proliferation induced by IL-3 was not inhibited (**Figure 4.1B**). These studies support the view that BNZ-1 is not generally toxic and has specificity for inhibition of IL-2 and IL-15 mediated proliferation.

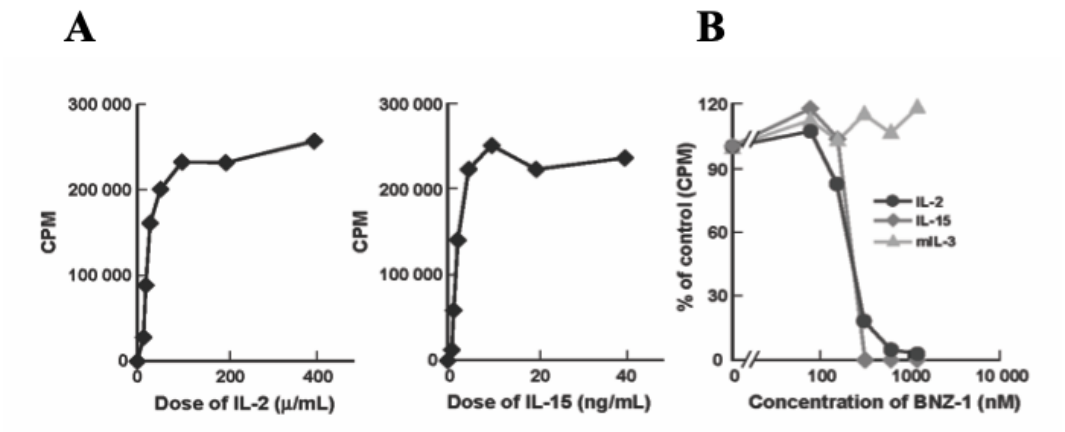

Figure 4.1: BNZ-1 exhibited selective targeting of proliferation in 32Dβ cell line.

[A] Dose response curve of 32Dβ cells to IL-2 and IL-15 demonstrates the responsiveness to IL-2 and IL-15 upon expression of IL-2Rβ. Aliquots of 32Dβ cells were seeded in 96-well culture plates and incubated with serial dilutions of IL-2 and IL-15 for 48 hours. The cells were pulsed during the last 6 hours with ^{3}H-thymidine. The proliferation of the cells reached plateau at the dose of 100 U/mL for IL-2 and 10 ng/mL for IL-15. [**B**] BNZ-1 inhibited the proliferation of 32Dβ cells mediated by IL-2 and IL-15, but not by IL-3. Aliquots of 32Dβ cells were seeded in 96-well culture plates in the medium with 100 U/mL of IL-2 or with 10 ng/mL of IL-15 or with 500 ng/mL of IL-3. Then the cells were incubated with serial dilutions of BNZ-1 for 48 hours. The cells were pulsed during the last 6 hours with ^{3}H-thymidine. IL-2 at 100 U/mL = 0.8 nM and IL-15 at 10 ng/mL = 0.8 nM. Performed in Waldmann lab at the NCI.

BNZ-1 REDUCED CYTOKINE MEDIATED VIABILITY AND DOWNSTREAM PATHWAY ACTIVATION IN A T-LGL LEUKEMIA CELL LINE

Initial experiments of BNZ-1 efficacy in LGLL were performed on TL-1, an IL-2 dependent T-LGLL patient-derived cell line [41]. Prior to evaluating effects of BNZ-1, we treated cytokine deprived TL-1 cells with varying concentrations of IL-2 and IL-15 to characterize cytokine mediated survival and expansion. Cell viability decreased in the absence of cytokine supplementation and cell numbers increased upon cytokine addition in a dose-dependent manner, indicating the dependence of survival and proliferation on cytokine treatment (**Figure 4.2**).

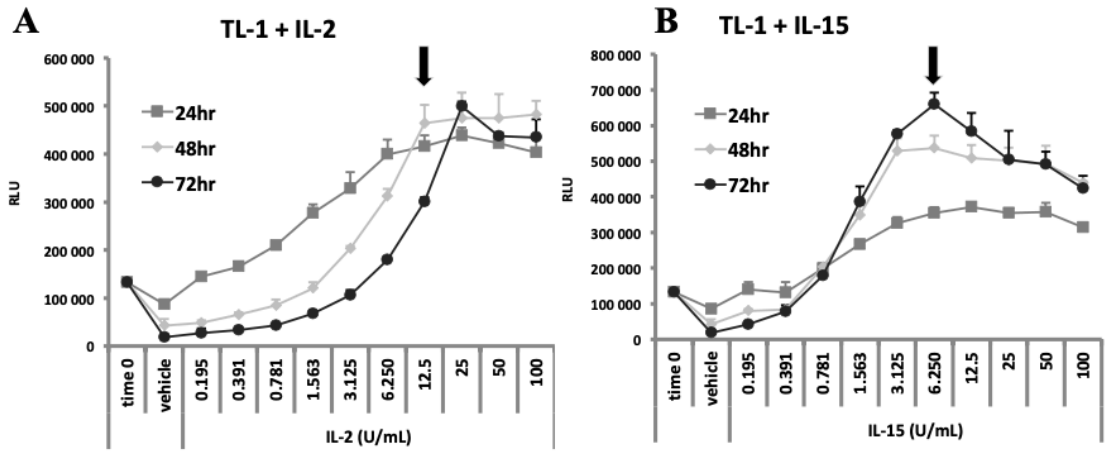

Figure 4.2: IL-2 and IL-15 dose response curves in a T-LGLL cell line.

TL-1 cells were cytokine starved for 12 hours then treated with varying IL-2 [A] or IL-15 [B] levels to determine effective cytokine doses. Red arrows indicate the minimum cytokine concentration that resulted in maximal expansion of cells as measured by CellTiter Glo assays done at 24, 48 and 72h after cytokine addition. IL-2 at 12.5 U/mL = 0.19 nM. IL-15 at 6.25 U/mL = 0.19 nM. N = 3. * $P < 0.05$; ** $P < 0.005$; *** $P < 0.0005$.

To test the effect of BNZ-1 on IL-2 and IL-15 induced cell expansion *in vitro*, a pretreatment of BNZ-1 (5 μM) was added to TL-1 cells prior to cytokine addition and relative cell numbers were measured at 24, 48 and 72 hours. At all time points, cytokine-only treatment increased viable cells and cytokine stimulation was inhibited by BNZ-1 pretreatment (representative data shown for 48 hours, **Figure 4.3A,B**). IL-15 mediated cell expansion was affected to a greater extent than IL-2. Treatment with BNZ-1 alone showed no toxicity in the absence of cytokine, and BNZ-1 was less effective at blocking expansion at higher cytokine doses. The cytokine doses most capable of mediating survival and expansion while maintaining BNZ-1 effectiveness were 12.5 U/mL (190 pM) for IL-2 and 6.25 U/mL (190 pM) for IL-15, which exhibited BNZ-1-mediated reductions of 30% and 92%, respectively. Our next experiment was to determine the BNZ-1 dose response in TL-1 cells treated with varying doses of BNZ-1 prior to IL-2 (12.5 U/mL) or IL-15 (6.25 U/mL) addition. For IL-2 treatment, addition of BNZ-1 at 10 μM resulted in a 50% reduction of cell expansion. For IL-15, BNZ-1 at 1 μM reduced viable cell numbers by more than half and BNZ-1 blocked essentially all IL-15 induced cell survival at 5 and 10 μM (**Figure 4.3C,D**). These data show BNZ-1 can significantly inhibit IL-2 and IL-15 induced expansion in a T-LGLL cell line.

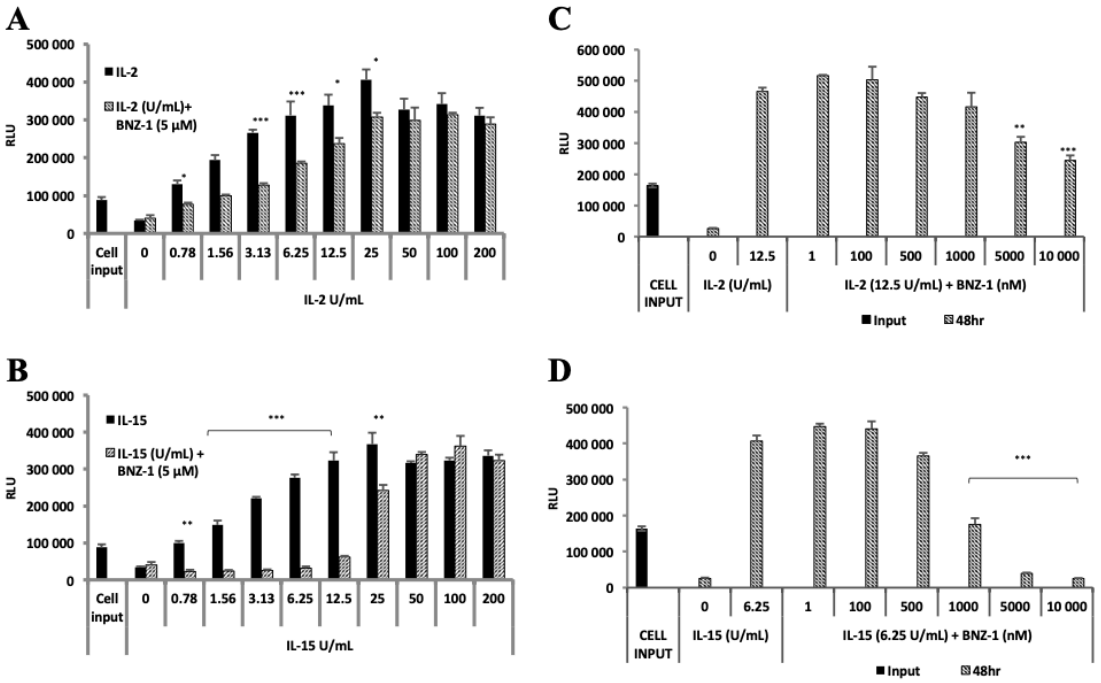

Figure 4.3: BNZ-1 decreased IL-2 and IL-15 mediated viability in a T-LGLL cell line.

TL-1 cells were cytokine starved for 12 hours then pretreated with BNZ-1 (5 µM) for 20 minutes followed by varying IL-2 [A] and IL-15 [B] to determine effective cytokine doses. IL-2 at 12.5 U/mL and IL-15 at 6.25 U/mL gave a robust increase in TL-1 viability, and BNZ-1 caused significant reduction of cell expansion induced by both cytokines. Cells were then treated with increasing concentrations of BNZ-1 in the presence of these doses of IL-2 [C] and IL-15 [D]. Cell viability induced by IL-2 was halved by 10 µM of BNZ-1 and IL-15-induced cell survival was attenuated by 1 µM of BNZ-1, and fully blocked at 5 and 10 µM. IL-2 at 12.5 U/mL = 0.19 nM. IL-15 at 6.25 U/mL = 0.19 nM. Bars represent relative light units (RLU; mean ± standard deviation) of CellTiter Glo assays done at 48h. N = 3; * $P < 0.05$; ** $P < 0.005$; *** $P < 0.0005$.

BNZ-1 BLOCKED SIGNALING PATHWAYS DOWNSTREAM OF IL-2 AND IL-15

BNZ-1 (10 μM) reduced the phosphorylation of downstream IL-2 signaling pathways at 30 minutes post-treatment including STAT3, STAT1, STAT5, Akt and ERK in a cytokine concentration dependent manner in TL-1 cells (**Figure 4.4A**). BNZ-1 reduced the IL-2 mediated activation of STAT3, STAT1 and STAT5 close to or below activation levels of untreated, cytokine-deprived cells. BNZ-1 incompletely blocked Akt and ERK activation by IL-2. Conversely, BNZ-1 drastically reduced IL-15 mediated phosphorylation of STAT3, STAT1, STAT5, Akt and ERK (**Figure 4.4C**). Additional time points of one, three, and six hours post cytokine addition were tested and results indicated that downstream activation remains blocked at these later time points (**Figure 4.5A,B).** Therefore, BNZ-1 effectively blocks IL-2 and IL-15 induction of signaling pathways important to leukemic cell survival and proliferation.

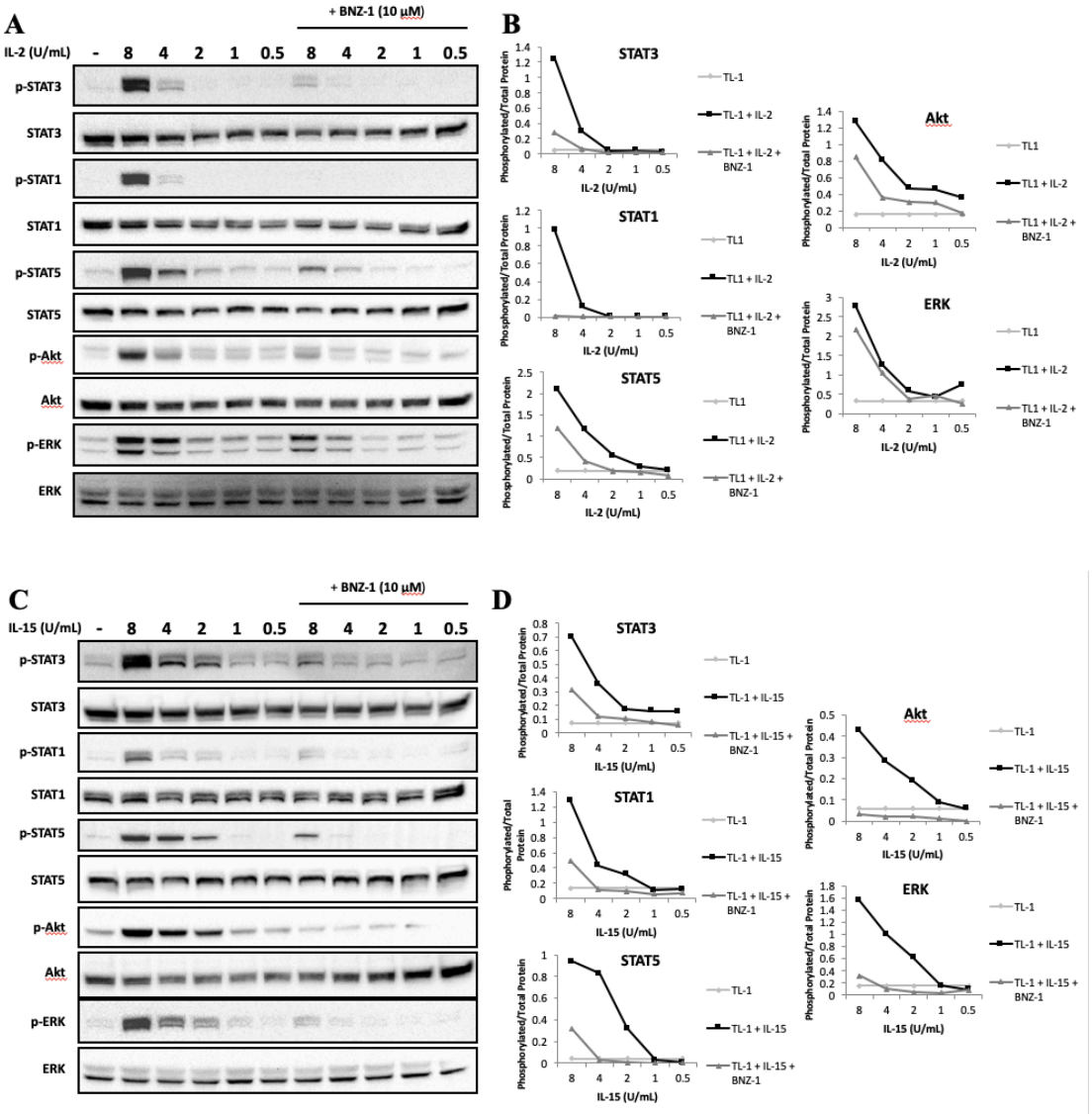

Figure 4.4: BNZ-1 inhibited IL-2 or IL-15 mediated phosphorylation events in a T-LGLL cell line.

TL-1 cells were pretreated with or without BNZ-1 in the presence of varying IL-2 or IL-15 doses. Western blot analyses demonstrated blockage of IL-2 [A] or IL-15 [C] mediated protein phosphorylation with BNZ-1 treatment (10 μM). Graphs of phosphorylated protein over total protein for IL-2 [B] or IL-15 [D] as quantified by ImageLab software. IL-2 at 8 U/mL = 0.12 nM. IL-15 at 8 U/mL = 0.24 nM.

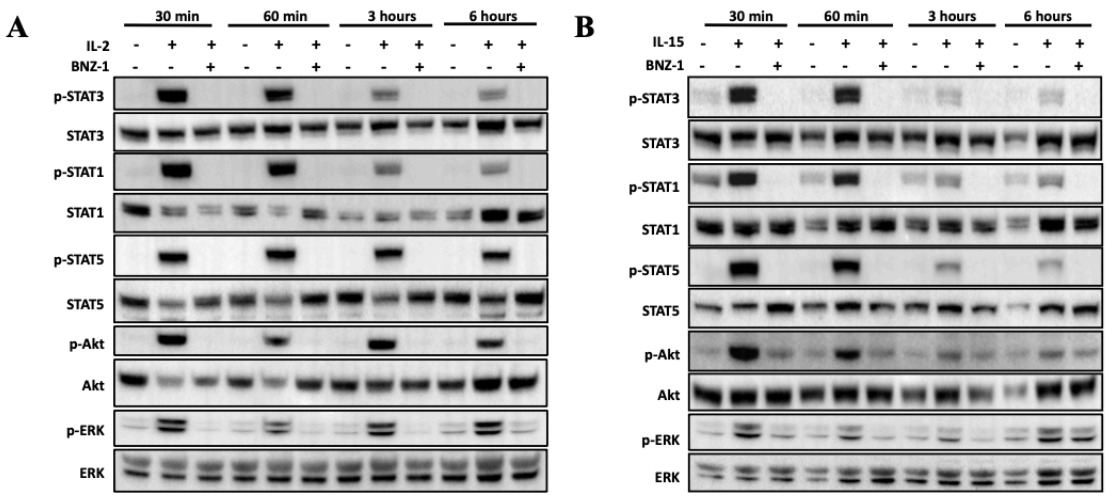

Figure 4.5: Time course of BNZ-1 inhibition of IL-2 or IL-15 mediated phosphorylation events in a T-LGLL cell line.

TL-1 cells were pretreated with or without BNZ-1 in the presence IL-2 (8 U/mL) or IL-15 (8 U/mL). Cells were harvested at either 30 minutes, 60 minutes, 3 hours or 6 hours after treatment. Western blot analyses demonstrated blockage of IL-2 [A] or IL-15 [B] mediated protein phosphorylation with BNZ-1 treatment (10 μM).

BNZ-1 INCREASED ANNEXIN V POSITIVE CELLS IN TL-1

To determine whether BNZ-1 treatment would induce apoptosis, cytokine stimulated TL-1 cells with and without BNZ-1 treatment were analyzed for apoptosis by flow cytometry (**Figure 4.6A**). BNZ-1 increased the number of cells that were positive for the apoptosis marker annexin V in all cytokine stimulated groups at 72 hours, with similar results at 48 hours (data not shown). Quantification of double negative (live) cells (**Figure 4.6B**) demonstrated an expansion of cells upon cytokine addition, especially IL-15, and loss of live cells with BNZ-1 treatment. Conversely, quantification of annexin V positive cells (**Figure 4.6C**) showed reduced early and late apoptotic cells with cytokine treatment and increased apoptotic cells upon BNZ-1 addition. Taken together, BNZ-1 reduced viability and enhanced apoptosis in the presence of IL-2, IL-15 or both cytokines.

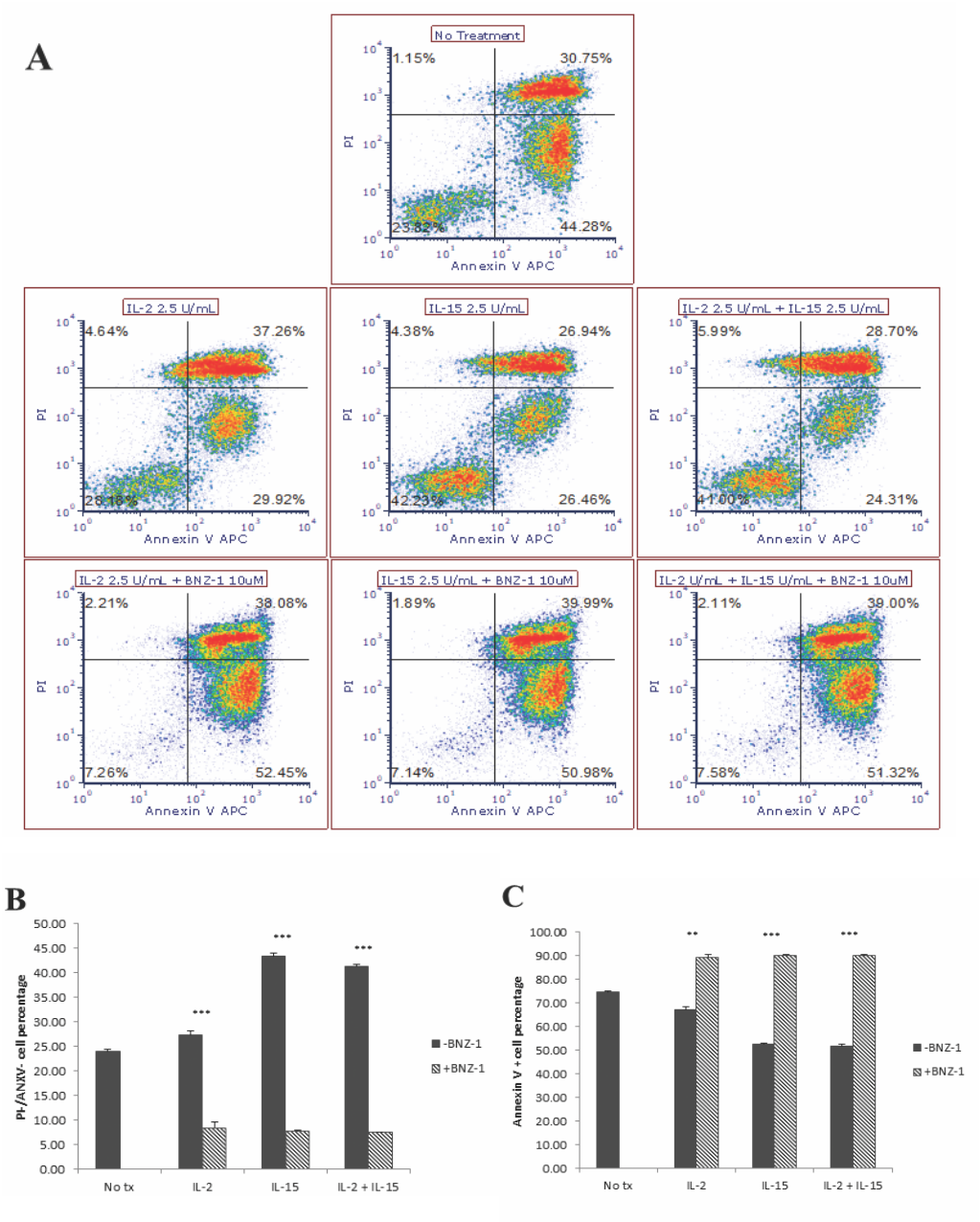

Figure 4.6: BNZ-1 increased annexin V positive cells in a T-LGLL cell line.

TL-1 cells were treated with or without BNZ-1 (10 µM) in the presence of IL-2 (2.5 U/mL), IL-15 (2.5 U/mL), or IL-2 and IL-15 (2.5 U/mL each). At 72 hours, cells were incubated with APC-annexin V and PI and analyzed by flow cytometry. **[A]** In each panel the lower left quadrant shows double negative (live) cells, lower right quadrant shows APC-annexin V positive cells (early apoptotic) and the upper right quadrant shows double positive cells (late apoptotic). **[B]** Quantification of double negative (live) cells and **[C]** APC-annexin V positive (apoptotic) cells in the indicated treatment groups.

BNZ-1 REDUCED CYTOKINE-MEDIATED SURVIVAL IN PRIMARY T-LGLL PBMCS

With the success of BNZ-1 treatment in the T-LGLL cell line, it was important to translate these findings to patient PBMCs that are known to require cytokine supplementation to survive *ex vivo*. T-LGLL patient PBMCs of known STAT3 mutational status were pretreated for 20 minutes with BNZ-1 prior to addition of IL-2 (**Figure 4.7A)**, IL-15 (**Figure 4.7B**), or IL-2 and IL-15 (**Figure 4.7C**) and percent viability relative to input control was determined at 72 hours. Treatment with cytokine alone stimulated cell survival and expansion in all samples. BNZ-1 (10 μM) impaired cytokine induced survival in all samples. BNZ-1 treatment did not cause any additional loss of viability relative to controls without cytokine supplementation (data not shown). Therefore, BNZ-1 inhibits cytokine-stimulated *ex vivo* survival and expansion of primary T-LGLL samples, regardless of STAT3 mutational status.

BNZ-1 REDUCED IL-15 MEDIATED STAT PHOSPHORYLATION IN PRIMARY T-LGLL PBMCS

To determine whether BNZ-1 blocked downstream phosphorylation in patient samples as observed in TL-1 cells (**Figure 4.4**), we tested PBMCs derived from two patients with wild-type STAT3 and two patients with mutant STAT3. Samples were treated with IL-15 after BNZ-1 pretreatment to study the effects on STAT phosphorylation *ex vivo.* There was a robust and clear decrease in IL-15 induced phosphorylation of STAT1, STAT3 and STAT5 with BNZ-1 pretreatment (5 μM and 10 μM) in all samples, regardless of STAT3 mutational status (**Figure 4.7D**).

BNZ-1 INDUCED APOPTOSIS IN PRIMARY T-LGLL PBMCS.

Lastly, we examined whether BNZ-1 was capable of inducing apoptosis in T-LGLL patient PBMC. Previously frozen T-LGLL patient PBMCs were stimulated with IL-2

(**Figure 4.7E**), IL-15 (**Figure 4.7F**), or IL-2 and IL-15 (**Figure 4.7G**) in the presence or absence of BNZ-1 treatment. After 72 hours, samples were stained with PI and annexin V to assess apoptosis induction. We demonstrated that cytokine treatment reduced the amount of apoptotic cells compared to those not given cytokine. In contrast, co-treatment with BNZ-1 increased apoptotic cells in all five patient samples. In the presence of BNZ-1, the percent of apoptotic cells rose to a level equal to or exceeding the level observed in the no treatment group.

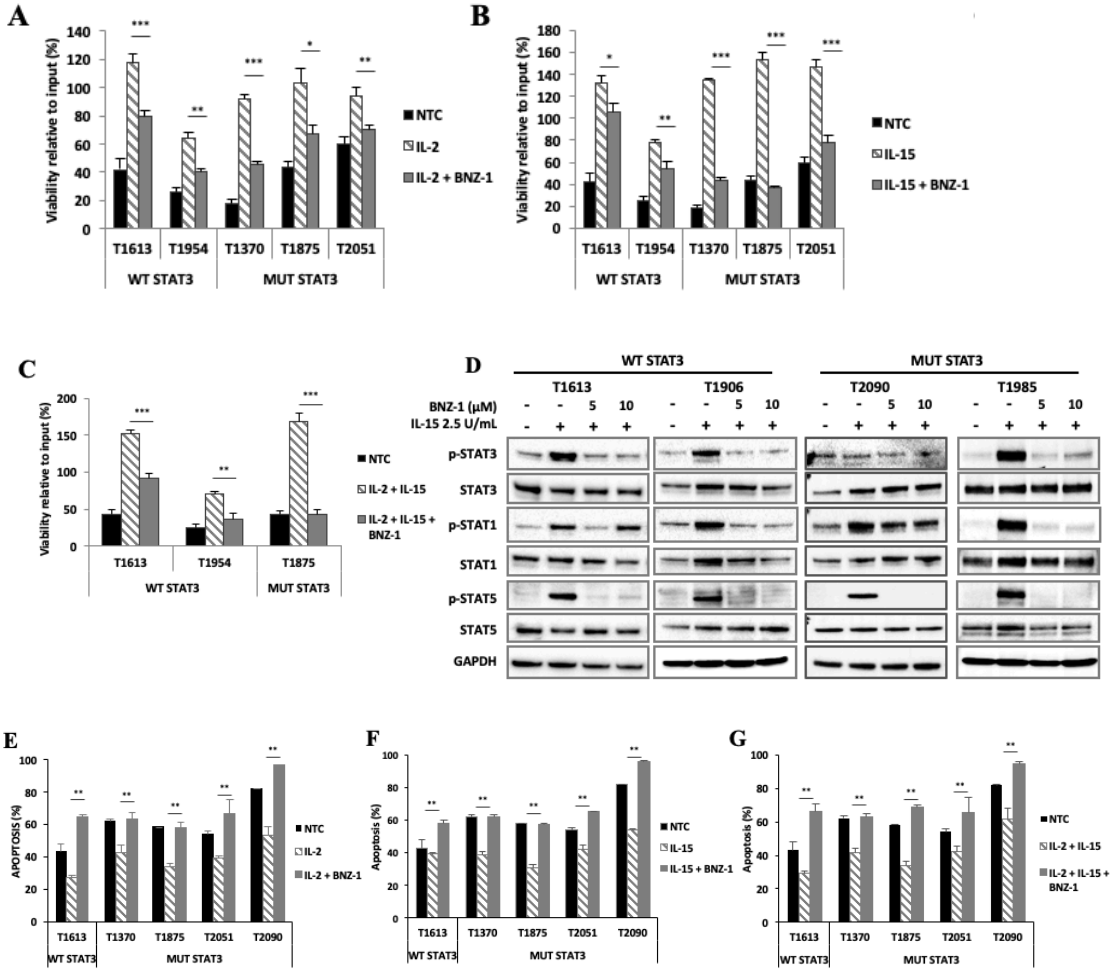

Figure 4.7: BNZ-1 reduced cytokine mediated viability, blocked IL-15 mediated phosphorylation, and induced apoptosis in T-LGLL patient PBMCs.

PBMC from T-LGL leukemia patients with and without *STAT3* mutations were not treated (NTC) or pretreated with BNZ-1 (10 μM) for 20 min followed by IL-2 [A], IL-15 [B] or IL-2 and IL-15 [C] for an additional 24 hrs. Cell viability was measured using CellTiter Glo in triplicate. Results are shown as mean ± SD relative to the input control (100%). BNZ-1 reduced cytokine mediated viability in T-LGLL patient PBMC with and without *STAT3* mutations at 72 hours. T1613 was treated at 2.5 U/mL of IL-2 and IL-15. T1954 and T1875 were treated at 6.25 U/mL of IL-2 and 3.13 U/mL of IL-15. T1370 and T2051 were treated with 10 U/mL of IL-2 and IL-15. [D] PBMC from T-LGL leukemia patients with and without *STAT3* mutations were pretreated with BNZ-1 (5 or 10 μM) for 20 min followed by IL-15 (2.5 U/mL) for an additional 24 hr. Total protein was harvested and STAT protein phosphorylation was determined by western blot assay. T-LGL leukemia patient PBMCs with and without STAT3 mutations were stimulated with IL-2 [E], IL-15 [F] or IL-2 and IL-15 [G] in the presence or absence of BNZ-1. At 72 hours, cells were stained with APC-Annexin V and PI and analyzed by flow cytometry. Percent apoptosis normalized to NTC. WT, wild-type; MUT, mutant; * $P < 0.05$ **; $P < 0.005$ ***; $P < 0.0005$.

BNZ-1 INHIBITED CYTOKINE STIMULATED SURVIVAL AND SIGNALING IN AN NK-LGL LEUKEMIA CELL LINE.

We also tested the effects of BNZ-1 on a NK-LGLL leukemia cell line (NKL). We determined the cytokine concentrations that most efficiently increased cell expansion and maximized potency of BNZ-1 for both IL-2 and IL-15 (**Figure 4.8A, B**). BNZ-1 (5 μM) inhibited IL-15 induced NKL cell viability by approximately 58% whereas BNZ-1 (10 μM) reduced IL-2 dependent cell viability by roughly 20%. Treatment of NKL cells with BNZ-1 dramatically reduced IL-15 induced phosphorylation of STAT3, STAT1 and ERK. There was a less drastic decrease of STAT5 phosphorylation (**Figure 4.8C**). Taken together, BNZ-1 showed promise in NK-LGLL model systems.

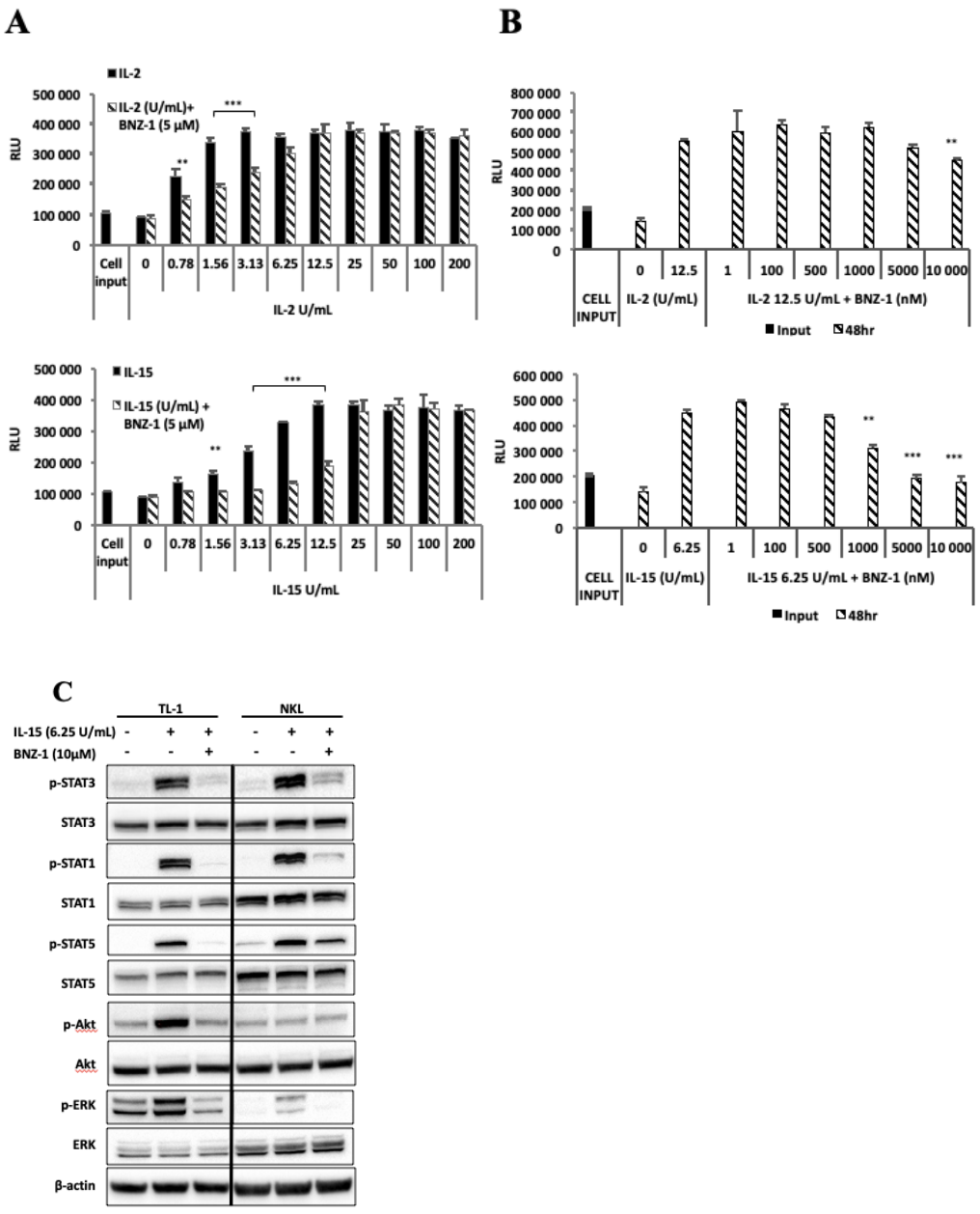

Figure 4.8: BNZ-1 reduced NK-LGLL cytokine-mediated cell viability and phosphorylation.

[A] NKL cells were pretreated with BNZ-1 and cell viability was assessed at 72 hours after addition of IL-2 or IL-15. **[B]** BNZ-1 dose determination in NKL cell line. BNZ-1 reduced IL-2 mediated cell viability at 10 µM. BNZ-1 more effectively reduced IL-15 mediated cell viability. Cell viability was assessed by CellTiter Glo and viability was graphed relative to no treatment control. Bars represent relative light units (RLU; mean ± standard deviation) of CellTiter Glo assays. N = 3. * $P < 0.05$; ** $P < 0.005$; *** $P < 0.0005$. **[C]** Comparison of inhibition of IL-15 (6.25 U/mL) mediated phosphorylation events in TL-1 and NKL cell lines. IL-2 at 12.5 U/mL = 0.19 nM. IL-15 at 6.25 U/mL = 0.19 nM.

BNZ-1 INHIBITED PROLIFERATION IN A CYTOKINE DEPENDENT ATL CELL LINE AND *EX VIVO* PBMCS FROM PATIENTS WITH SMOLDERING/CHRONIC ATL.

Next the efficacy of BNZ-1 was determined in a second T-cell disease model, ATL. Human cytokine-dependent ATL cell lines represent a model of smoldering/chronic ATL, which are clinical disease states that manifest constitutive cytokine production, JAK/STAT activation and spontaneous *ex vivo* proliferation of ATL cells. The ATL cell line used in the present study requires a supply of extrinsic human IL-2 or IL-15 for their survival *in vitro* and *in vivo*. We demonstrated that BNZ-1 inhibited IL-2 or IL-15 or IL-2 plus IL-15 mediated proliferation of the cytokine-dependent ATL cell line ED40515(+) (**Figure 4.9A)**. We then tested the effects of BNZ-1 on 6-day *ex vivo* spontaneous proliferation of PBMCs from patients with smoldering/chronic ATL. The *ex vivo* spontaneous proliferation of PBMCs from 3 patients with smoldering/chronic ATL, as assessed by thymidine uptake, was inhibited by an average of 72 percent by the addition of the anti-IL-2Rα monoclonal antibody, daclizumab (**Figure 4.9B)** and by a comparable amount by the combination of daclizumab, anti-IL-15 and anti-IL-9. BNZ-1 (1 μM) inhibited the proliferation of the PBMCs from 3 patients with ATL by an average of 51 percent, whereas BNZ-1 at 10 μM inhibited this *ex vivo* proliferation by an average of 73 percent **(Figure 4.9B).** PBMCs of patients with smoldering ATL were stained with a CD3, a CD4, a CD25 antibody, PI and annexin V **(Figure 4.9C).** Increasing doses of BNZ-1 significantly decreased percentages and total numbers of $CD3^+CD4^+CD25^+$ ATL cells, whereas percentages and numbers of normal $CD3^+CD4^+CD25^-$ T cells were not affected **(Figure 4.9D)**. However, no $CD3^+CD4^+CD25^+$ ATL cells were detected positive for annexin V.

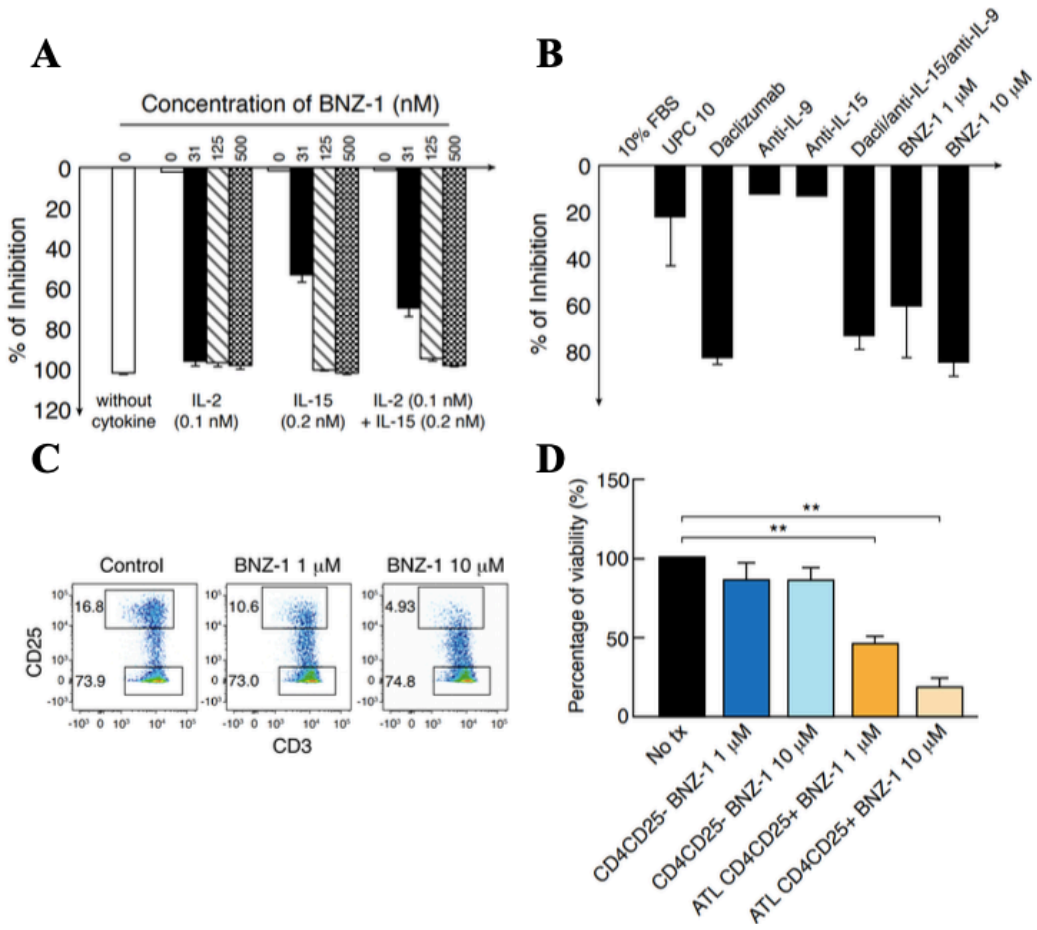

Figure 4.9: BNZ-1 inhibited proliferation of an ATL cell line and of smoldering/chronic ATL PBMCs.

[A] Effect of BNZ-1 on the proliferation of cytokine-dependent ATL cell line ED40515(+). Aliquots of ED40515(+) cells were seeded in 96 well-culture plates in medium with 12.5 u/mL of IL-2 or 2.5 ng/mL of IL-15 or IL-2 (12.5 u/mL) plus IL-15 (2.5 ng/mL). Then the cells were incubated with serial dilutions of BNZ-1 for 72 hours. The cells were pulsed during the last 6 hours with 1μCi ^{3}H-thymidine. BNZ-1 effectively inhibited the proliferation of ED40515(+) cells mediated by IL-2 alone or IL-15 alone or IL-2 plus IL-15. **[B]** BNZ-1 inhibited the 6-day *ex vivo* spontaneous proliferation of PBMCs from patients with smoldering ATL. The PBMCs isolated by Ficoll-Hypaque density centrifugation from patients with IL-2, IL-9, IL-15 autocrine smoldering ATL at 1 X 10^{6}/mL in 96 microtiter plates in RPMI 1640 media supplemented with 10% FBS at 37°C in 5% CO_2 were cultured *ex vivo* for 6 days with and without BNZ-1 or with 10 μg/mL of antibody added at initiation of the cultures. When a single antibody directed against the cytokine IL-2, IL-9 or IL-15 was used or with their combination (5 μg/mL each). ^{3}H-thymidine was added during the last 6 hours of the cultures. Cells were then harvested and analyzed for ^{3}H-thymidine incorporation. The value was calculated as: % inhibition = (cpm of proliferation without BNZ-1 – cpm of proliferation with BNZ-1)/(cpm of proliferation without BNZ-1) X 100. **[C]** PBMCs of patients with smoldering ATL with IL-2, IL-9, IL-15 autocrine mediated proliferation have been plated at 10^{6} cells/mL, in the presence or absence of BNZ-1 (1 and 10 μM). At day 3, cells have been stained with a CD3, a CD4, a CD25 antibody, PI and annexin V. Percentages and total numbers of $CD3^{+}CD4^{+}CD25^{+}$ ATL cells significantly decreased in the presence of increasing doses of BNZ, whereas **[D]** percentages and numbers of normal $CD3^{+}CD4^{+}CD25^{-}$ T cells were not affected. Performed in Waldmann lab at the NCI.

BNZ-1 SHOWED THERAPEUTIC EFFICACY IN AN IL-2/IL-15 DEPENDENT *IN VIVO* MODEL OF HUMAN ATL.

The majority of the studies of BNZ-1 have evaluated its action on cell lines and *ex vivo* cells. Nata et al. reported that BNZ-1 effectively inhibited the *in vivo* proliferation of CD8+ T cells in an IL-15 transgenic mouse model. Here we utilized the cytokine-dependent ED40515(+) xenograft tumor model to provide *in vivo* validation that BNZ-1 exhibits the acceptable pharmacokinetic and safety profile to be effective in the treatment of an IL-2/IL-15 dependent tumor. The model of IL-2/IL-15 dependent ATL was generated by i.v. injection of $1x10^7$ ED40515(+)/luciferase-expressing cells into female IL-15 transgenic NSG mice. ATL cells express human IL-2Rα and release it into the biological fluids including the serum. One week after injection of the tumor cells, when the average soluble human IL-2Rα was approximately 700 pg/mL (**Table 4.2**), the animals were randomized to treatment groups and therapy was started. Ruxolitinib (50 mg/kg/day) was administered by pump s.c. for four weeks. BNZ-1 (40 mg/kg) was administered i.v. two times per week for four weeks. Tumor burden over time was assessed by bioluminescence imaging (**Figure 4.10A,B**). Leukemic burden was greatly reduced by BNZ-1 when compared to PBS-treated control mice, which was similar to that observed with the JAK1/2 inhibitor, ruxolitinib. To further assess whole animal tumor burden and evaluate antitumor efficacy, serum IL-2Rα levels were quantitated. BNZ-1 therapy was associated with greatly reduced IL-2Rα levels at four and seven weeks of treatment, which is indicative of reduced quantities of prevailing tumor tissue (**Figure 4.10C**).

Table 4.2: Level of CD25 in animals one week after injection of tumor cells.

Levels of human CD25 (IL-2Rα) were measured one week after injection of $1x10^7$ ED40515(+)/luciferase-expressing cells. Animals were randomized into separate groups prior to start of therapy. Average sIL-2Rα was comparable in all groups, which ensured similar leukemic burden at the onset of treatment. Performed in Waldmann lab at the NCI.

GROUP	Mouse #	hCD25 ELISA	AVERAGE	STDEV
control	#29	558	710	132
control	#30	640		
control	#31	885		
control	#32	800		
control	#33	666		
BNZ-1	#09	605	730	83
BNZ-1	#24	747		
BNZ-1	#25	695		
BNZ-1	#26	811		
BNZ-1	#27	789		
BNZ-1	#28	783		
Ruxolitinib	#04	585	711	85
Ruxolitinib	#07	718		
Ruxolitinib	#08	793		
Ruxolitinib	#36	781		
Ruxolitinib	#37	677		
Ruxolitinib	#38	683		

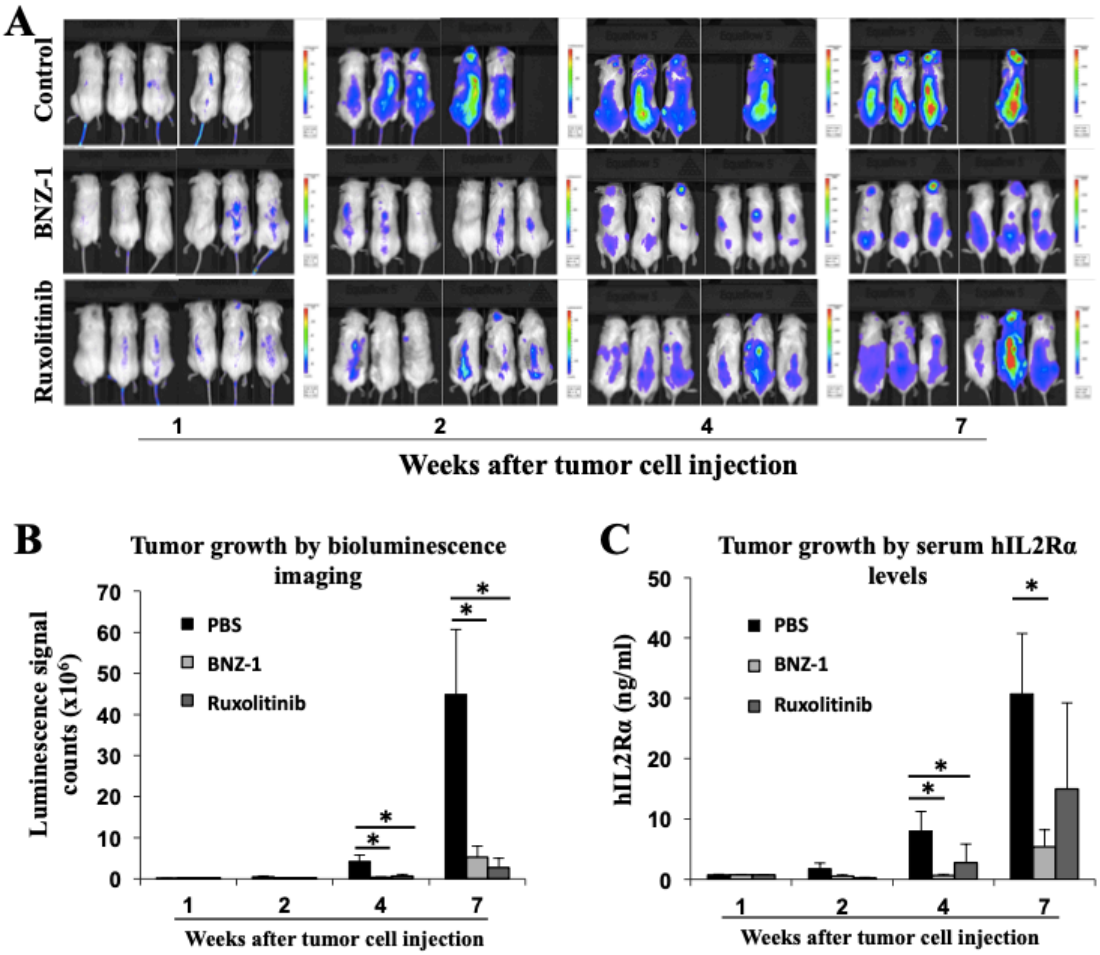

Figure 4.10: BNZ-1 inhibited cytokine-dependent ATL growth *in vivo*.

Human IL-15 transgenic NSG mice were injected i.v. with 1x107 ED40515(+)/luciferase cells. One week later, the tumor-bearing mice were divided into 3 groups (n=5-6) with comparable average levels of serum sIL-2Rα and therapy was started. BNZ-1 was given i.v. at a dose of 40 mg/kg twice weekly for 4 weeks and ruxolitinib was continuously administered by a subcutaneous mini-osmotic pump at a dose of 50 mg/kg/day for 4 weeks. **[A]** Bioluminescence imaging of IL-2/IL-15-dependent ED40515(+)/luciferase ATL-bearing mice confirmed efficacies of BNZ-1 and ruxolitinib. **[B]** Average total luminescent signals of the tumor-bearing mice. The animals treated with both BNZ-1 and ruxolitinib had significantly lower luminescent signals when compared with those in the PBS control group (*$P < 0.05$). **[C]** The mean concentrations of tumor surrogate marker, human sIL-2Rα, levels in the IL-2/IL-15-dependent ED40515(+)/luciferase ATL-bearing mice before and after treatment. The animals treated with BNZ-1 had significantly decreased values of sIL-2Rα when compared with those in the PBS control group (*$P < 0.05$). Treatment of the tumor-bearing mice with ruxolitinib showed similar therapeutic efficacy as BNZ-1 did. Results of two independent assessments of tumor burden and human sIL-2Rα levels yield similar data, emphasizing the efficacy of BNZ-1 in a human ATL xenograft mouse model. Performed in Waldmann lab at the NCI.

4.4 DISCUSSION

IL-2 and IL-15 are key cytokine drivers in multiple T-cell malignancies including LGLL [57], ATL [184], cutaneous T-cell lymphoma (CTCL) [174,179], gamma-delta T-cell lymphoma (γδTCL) [110] and anaplastic large cell lymphoma (ALCL) [176]. Studies of BNZ-1 in LGLL and ATL allowed us to test the hypothesis that cytokine receptor blockade may exhibit widespread therapeutic benefit in these malignancies. The pathogenesis of both LGLL and ATL depends on the dysregulation of IL-2 and IL-15 signaling, making these cytokines and their signaling pathways attractive therapeutic targets [56,97,171,177,197]. In this study, we demonstrated the efficacy of an IL-2, IL-15 and IL-9 inhibitor peptide, BNZ-1, in T-LGLL and HTLV-1 derived ATL. Treatment of T-LGLL and ATL cell lines with BNZ-1 reduced IL-2 and IL-15 mediated cell viability and proliferation. In addition, the loss of STAT 1/3/5, ERK and Akt activation provided a mechanism for the impaired cytokine mediated expansion in T-LGL leukemic cells. Not only did BNZ-1 cause the loss of activation in these critical signaling pathways, we showed that BNZ-1 induced apoptosis in cytokine supplemented T-LGLL cell line and patient PBMCs. We also showed its ability to block the expansion of cytokine dependent and independent *ex vivo* PBMCs in both T-LGLL and ATL. Lastly, BNZ-1 therapy drastically reduced leukemic burden in an *in vivo* IL-15 transgenic ATL mouse model. Together, this study proved BNZ-1 to be an effective form of therapy in both T-LGL leukemia and HTLV-1 derived ATL model systems.

To prove the selectivity of BNZ-1 for IL-2 and IL-15, BNZ-1 was evaluated in the 32Dβ cell line. 32Dβ cells are IL-3 dependent and were modified to express all three subunits of the IL-2 receptor complex, including the common γ-chain. Both cytokines utilize the γc receptor, the designated target of BNZ-1. In contrast, IL-3 does not utilize the common γc. BNZ-1 inhibited IL-2 and IL-15 mediated proliferation in 32Dβ but not that of IL-3. The critical importance of this lack of inhibition of IL-3 mediated proliferation is two-fold. First, it shows that BNZ-1 is not universally toxic to cells.

Second, these studies provide evidence of specificity of BNZ-1 for IL-2 and IL-15, which are the putative targets of this agent.

Increased γc receptor signaling results in increased activation of downstream targets including STAT1/3/5, ERK and Akt, which are strongly implicated in the pathogenesis of T-LGLL [45,182,183]. The loss of STATs, Akt and ERK phosphorylation in leukemic cells upon BNZ-1 treatment indicates the superior ability of BNZ-1 to successfully block multiple signaling pathways activated by cytokine stimulation when compared to conventional JAK inhibitors that only inhibit the JAK/STAT pathway.

To fully examine the efficacy of BNZ-1 in T-LGLL, we utilized parallel studies in both cell lines and patient PBMCs to estimate its putative success in a future clinical trial. We demonstrated that BNZ-1 reduced cytokine mediated viability, blocked downstream pathway activation and induced apoptosis in cell lines and in T-LGLL patient samples. Patient PBMC samples contain varying amount of leukemic LGL, and patient samples used in this study ranged from 38% to 92% LGL in their PBMCs. Regardless of tumor purity, BNZ-1 succeeded at reducing leukemic cell viability, blocking downstream activation and inducing apoptosis, thereby strengthening the evidence of BNZ-1 efficacy.

STAT3 somatic mutations are found in up to 40% of all LGLL patients and constitutive activation of STAT3 is found in all patients, emphasizing the pathogenetic role of this aberrant pathway in T-LGLL [45,65,68]. Knowing the importance of STAT3 mutation in T-LGLL, we were curious whether a STAT3 mutation would affect the inhibitory effects of BNZ-1. Regardless of STAT3 mutation status, BNZ-1 reduced the ability of both IL-2 and IL-15 to support *ex vivo* survival and expansion of leukemic cells, blocked downstream protein activation after cytokine treatment and induced apoptosis. This supports the current understanding that mutant cells still require cytokine signaling at the receptor level and that an activating mutation alone does not induce constitutive

phosphorylation of STAT1 or STAT3 [65,69]. Therefore, BNZ-1 has the capability to be a positive therapy in all T-LGLL patients and would not be limited based on STAT3 mutational status.

In this study, we also demonstrated the efficacy of BNZ-1 on *ex vivo* primary human ATL leukemic cell spontaneous proliferation, thereby providing the required evidence that BNZ-1 is effective with non-manipulated human cells. We evaluated the BNZ-1 strategy to reduce the excessive immune activation that occurs in HTLV-1 associated ATL by simultaneously inhibiting the effects of multiple pro-inflammatory autocrine and paracrine cytokine loops involved in the pathogenesis of early disease [184]. BNZ-1 was demonstrated to be a potent inhibitor of *ex vivo* spontaneous proliferation of PBMCs from ATL patients and exhibited comparable or superior activity when compared to ruxolitinib. It is of interest that the addition of BNZ-1 to T-cell LGLL PBMCs led to apoptosis of the leukemic cells whereas leukemic cell apoptosis was not observed in ATL PMBCs but rather a reduced persistence of the leukemic cells. This observation may be due to loss of apoptotic cells before evaluation at this 72 hour time point or may reflect the fact that in ATL, HTLV-1 encoded Tax transactivates the anti-apoptotic protein Bcl-X(L) [198,199].

The PEGylated BNZ-1 peptide was developed to improve the pharmacokinetic properties, increase bioavailability and reduce immunogenicity for clinical studies [170,192]. It was critical to determine the efficacy of this agent in *in vivo* models in addition to the mouse model for CD8+ T cell leukemia based on IL-15 transgenic T cells [170,200], to consider its pharmacokinetics and safety profile in living mice, and to be assured that the BNZ-1 was effective *in vivo*. In an *in vivo* mouse model of ED40515(+) ATL leukemia, BNZ-1 exhibited efficacy at least comparable and likely superior to that mediated by the JAK1/2 inhibitor ruxolitinib. It is noteworthy that the superior efficacy of BNZ-1 was achieved with twice weekly dosing as opposed to continuous delivery of ruxolitinib by osmotic pump. This is consistent with our earlier observation that BNZ-1 was superior to tofacitinib, a pan-JAK inhibitor, in protecting

host animals from leukemic death in our mouse CD8+ leukemia model [170]. Thus, BNZ-1 displayed appropriate pharmacokinetics, safety and efficacy to provide effective treatment in an *in vivo* model of cytokine-dependent ATL.

Taken together, these preclinical studies indicate that BNZ-1 may be a valuable candidate to treat T-LGLL and the smoldering and chronic forms of ATL, both of which lack safe and curative treatments. In this study BNZ-1 inhibited the proliferation of cytokine dependent ATL and T-LGLL cell lines and patient PBMC's and induced apoptosis in a T-LGLL cell line and patient PBMC's. Additionally, it proved effective in reducing leukemic burden in an *in vivo* model of cytokine-dependent ATL. Early results from a completed single and multiple ascending dose clinical trials in healthy volunteers (NCT03046459 and NCT03239379) demonstrated that BNZ-1 was well tolerated with no major side effects [193]. Pharmacodynamic biomarkers showed high specificity to IL-2 and IL-15 (manuscript in preparation). These preclinical and early clinical successes indicate that BNZ-1 represents a promising therapeutic option for multiple disorders with dysregulated γc cytokines and abnormal activation of JAK/STAT pathways.

5 FUTURE DIRECTIONS

This body of work focuses on delving deeper into the JAK/STAT pathway in LGL leukemia. This pathway has been characterized by increased activation of STAT3 in all patients, and mutations in STAT3, STAT5b and in other genes associated with this pathway have been well documented in several patient cohorts. Demonstration of pervasive activation of this pathway in the presence or absence of mutations indicate a need for explanation of augmented STAT3 activation. We aimed to further the understanding of STAT3 activation using genomic methods and discovered other mutations within STAT3 and the JAK/STAT pathway that may explain aberrant STAT3 signaling in LGL leukemia.

5.1 FUTURE DIRECTIONS CHAPTER 2

We found a novel JAK1 mutation in RNK-16 cell line, which is a cell line adapted from a F344 rat model of aggressive NK-LGL leukemia. Compared to the F344 control, the RNK-16 cell line we found thousands of variants. Through querying the COSMIC database, we narrowed the variants to eight oncogenes. We were able to validate all variants in the RNK-16 cell line, but when testing *ex vivo* primary RNK-16 material, only the JAK1 variant was validated, meaning this JAK1 mutation was present from the initiation of the disease rather than a somatic mutation acquired as a result of cell culture. Furthermore, RNK-16 was characterized as one of the more highly aggressive strains of RNK and out of the four strains tested, only RNK-16 *ex vivo* material harbored the JAK1 mutation.

While our results do not prove this mutation results in a more aggressive disease course, evidence of increased STAT signaling compared to other RNK strains help to correlate the status of JAK1 mutation and aggressiveness of the disease. Further experimentation is needed to support the hypothesis that this mutation causes an aggressive disease. We have proven this mutation to increase downstream STAT signaling and would hypothesize that the increased STAT signaling causes increased aggressive disease course. This can be measured by time to disease onset and by cytotoxicity assays of

leukemic material. One avenue to pursue would be to manipulate RNK-16 primary *ex vivo* material for transplantation into young F344 rats. Transplanting F344 rats with RNK-16 with WT JAK1 and Y1034C JAK1 to measure time to disease onset and cytotoxicity assay results would distinguish any disease phenotypic changes between the groups. If our hypothesis is confirmed and time to disease onset is lower and cytotoxicity of leukemic material is increased in those rats transplanted with Y1034C JAK1 RNK-16, then it suggests Y1034C JAK1 causes a more aggressive disease course through increased STAT signaling. This would then raise the question of how increased STAT phosphorylation leads to a more aggressive disease. Differential gene expression by RNA-seq of leukemic material would reveal genes and pathways affected by Y1034C JAK1 and increased STAT signaling. We had only observed increased STAT signaling but there may be other intracellular signaling pathways affected by a mutated JAK1.

It may be possible that Y1034C JAK1 itself does not affect disease phenotype. In this case, it suggests the amalgamation of variants in RNK-16 instigate the aggressive nature of this strain. It would be compelling to study the differences between the RNK strains by whole genome sequencing along with RNA-seq. Understanding the differential gene expressions of RNK strains in combination with a full catalogue of variants between the *ex vivo* RNK material may help to more fully distinguish features of each RNK strain and identify genes important in disease progression.

Although this finding in a spontaneous NK-LGL leukemia rat model is fascinating, to date, we and others have not observed any JAK1 mutation in T-cell or NK-LGL leukemia patients. Because this mutation is found in a model for the rare, aggressive NK-LGL leukemia, it may be that JAK1 mutations would be found in that specific subtype and less common in the indolent, or chronic subtypes that are more frequently observed. Because of the rarity of this aggressive form of NK-LGL leukemia, patient samples are difficult to obtain. This model gives us the opportunity to use transplantation of RNK material into F344 rats as a viable *in vivo* model to test putative

therapeutic treatments. There is potential use of this model to study therapeutics for this malignant disease and help to improve the prognosis of patients with aggressive NK-LGL leukemia.

5.2 FUTURE DIRECTIONS CHAPTER 3

The discovery of STAT3 mutations in LGL leukemia resulted in the addition of routine clinical STAT3 mutation testing. However, these clinical sequencing panels are restricted to the SH2 domain of STAT3, rather than the entire gene. In this project, we used whole genome sequencing to fully sequence the STAT3 gene, aiming to reveal mutations outside of the SH2 domain that may contribute to augmented STAT3 signaling. We found five novel STAT3 mutations in a T-LGL leukemia patient cohort. Not all of the mutations increased STAT3 activation. Limitations of this study include the unexpected creation of a mCherry:STAT3 fusion protein. Furthermore, the occurrence of the read-through is not consistent. Even in a STAT3 null HEK model, we continue to observe multiple banding of STAT3. While experiments indicate this fusion does not prevent STAT3 from its responsibilities in intracellular signaling, we cannot say for certain that it has no effect on its phosphorylation, dimerization or DNA binding. Ideally, we would procure a mutant plasmid that does not generate any unexpected outcomes.

Initial future directions for this project include studying the effects of mutations in a more relevant leukemic model, such as the Jurkat cell line, or ideally, human primary CD8+ cells. Using a more appropriate model is imperative because the context in which STAT3 is being studied is critical for a comprehensive understanding of mutant STAT3 consequences in LGL leukemia. Out of the novel mutations we studied, one mutation in particular, H410P STAT3 showed the most dramatic effect by STAT3 phosphorylation and STAT3 activation measured by a STAT3 reporter assay. Further mechanistic studies are required to understand how H410P and other mutations affect DNA binding. STAT3 has several intracellular interactions that affect its

transcriptional activity including DAXX, Y14, ZIPK, KAP1 [201], ARL3 [202] and others. These interactions are reported to affect modulate transcription, either by activation or suppression. Little is known how these mutations may affect these interactions. Furthermore, we found H410P in a STAT3KO model increased phosphorylation at S727. Phosphorylation at this residue is required for STAT3 mitochondrial localization. Evidence shows ATP production is regulated by STAT3 in the mitochondria through respiration and oxidative phosphorylation [168]. STAT3 in the mitochondria interacts with GRIM-19, an essential protein in the mitochondrial complex 1 [203]. Current understanding of mitochondrial STAT3 in promoting cellular transformation is lacking. We would propose performing co-immunoprecipitation of to pull down WT and mutant STAT3 in cytosolic, nuclear and mitochondrial fractions to study binding partners and how associations with binding partners may be affected by mutant STAT3. In particular, we would be interested in changes in association with GRIM-19 in H410P STAT3 cells compared to WT STAT3. We can probe these fractions for p-S727 and key mitochondrial proteins to understand whether mutant STAT3 affects mitochondrial complexes. Further characterization of this mutation in the non-canonical pathways may reveal roles mitochondrial STAT3 have in not only lymphocyte biology but also role in cancer progression.

In addition to affecting signaling complexes, we would expect aberrant STAT3 signaling to impact gene expression, which can be studied by RNA sequencing in WT and mutant STAT3 in leukemic or T-cell contexts. RNA sequencing would profile global differential gene expression and identify gene expression changes. To understand how mutant STAT3 differentially regulates gene transcription, we may conduct STAT3 chromatin immunoprecipitation followed by sequencing to reveal STAT3 binding sites that may be altered due to mutant STAT3. It would be ideal to map global binding sites of STAT3 in a normal cell context, compared to STAT3 WT and mutant STAT3 LGL leukemia. We would expect to observe transcriptional changes resulting from mutations and their effect on STAT3 dependent gene expression.

The creation of mutant STAT3 cell lines allows our lab to test therapies directed at STAT3. Targeting STAT3 is an attractive option for several disorders and cancers. Numerous approaches have been used to block STAT3 signaling as treatment, however, very few have progressed into clinical trials. Currently, we are testing novel putative STAT3 targeted therapies for their efficacy in LGL leukemia as well as studying responses to these drugs using STAT3 mutant cell lines. It is important to observe changes in efficacy of STAT3 drugs in the context of WT and mutant STAT3. Trials using JAK inhibitors have reported a lack of response in patients with a JAK2 mutation, and we would expect so find similar results with use of STAT3 inhibitors against mutant STAT3. Depending upon the strategy of STAT3 inhibition, we would expect certain mutants to respond distinctly. For example, inhibitors targeting dimerization may not be as efficacious against Y640F STAT3 in the SH2 dimerization domain. Targeting STAT3 is well supported by an overwhelming amount of preclinical and clinical data in hematological cancers and efforts are continuing to develop an effective STAT3 inhibitor that will have clinical impact for patients.

5.3 Future Directions chapter 4

Lastly, discovering new targets and testing new therapeutic targets is a core aim of our lab. While a predominantly indolent disease, there is no cure for LGL leukemia. Untreated LGL leukemia leads to the development of neutropenia, anemia, infections and potentially dependence on transfusions. In Chapter 4, we tested the efficacy of a peptide targeting IL-15. While targeting IL-15 had been previously unsuccessful [204], we show using a peptide blocking the common gamma receptor was efficacious in preclinical studies. BNZ-1 was capable of significantly inhibiting downstream signaling and increased LGL leukemia cell apoptosis. These positive results, in combination with successful phase 1 results progressed BNZ-1 to a phase 1/2 clinical trial for T-LGL leukemia and CTCL indications.

20 T-LGL leukemia patients were enrolled in the study and efficacy was measured by changes in blood counts. Out of the 20 patients, four patients had a partial response. A total of four patients were enrolled for transfusion dependent anemia and three of those patients became transfusion independent. A total of 11 patients were enrolled for neutropenia and one of those patients had resolution of neutropenia. Flow cytometry analysis of patient samples showed all responders with increased apoptosis of CD3+CD8+CD5+ T cells within 24 hours of their first dose while leaving their CD4+ T cells unaffected. (Unpublished data) This shows that while BNZ-1 is capable of inducing apoptosis of leukemic LGL, but in the majority of patients, that was not sufficient to observe any clinical response. However, BNZ-1 did show evidence of clinical response, particularly in patients with transfusion dependent anemia.

More correlative studies are needed to understand the mechanisms of BNZ-1 in patients. Specifically, further studies are necessary to elucidate the lack of clinical response. It may be that for some, dosages need to be increased, or there may be a relationship between STAT3 mutations and clinical response to BNZ-1. While we did not observe differences in response to BNZ-1 in patient samples with or without STAT3 mutation, it is possible STAT3 mutations may affect clinical responses. Initial studies include Sanger sequencing for all patients of STAT3 exon 21 and 20. This may show STAT3 mutation to predict response to BNZ-1, similar to the results of the first clinical trial for LGL leukemia where STAT3 mutations predicted response to Methotrexate [15].

The results of this clinical trial have shown that this form of blockade increases leukemic apoptosis for all patients, but it does not translate to clinical responses. Apoptosis was tested 24 hours after initial dose, but responses at other time points have not been tested. It would be imperative to know how long BNZ-1 is efficacious in reducing leukemic burden. Weekly dosing may not be enough, or potentially increasing the concentration of BNZ-1 may result in more patients with clinical responses.

Additionally, while increase of apoptosis was observed, it is not clear what proportion of disease was remaining. Further characterization of patient samples is needed to understand the lack of clinical response. This can be studied by quantifying changes to leukemic cells and observe changes to TCR clones where we may observe the disappearance or reduction in clone size.

There are numerous aberrant pathways that contribute to LGL leukemia suggesting IL-15 blockade may not be adequate. Combinatorial treatments blocking parallel pathways such as PDGF, the second node in the LGL leukemia survival network [53] may be a more efficacious treatment option. Unfortunately for the patients who had a positive response to BNZ-1, as of Jan 8, 2020, a Spanish pharma company, Almirall, has plans to purchase BNZ-1 to further clinical studies for CTCL and alopecia indications. While BNZ-1 may never be approved for patients with LGL leukemia, there is hope that blockade of IL-15 signaling in LGL leukemia may help more patients in the future.

5.4 Conclusion

The high prevalence of STAT3 mutations are specific to LGL leukemia [65,147]. Even in the absence of STAT3 mutation, all LGL leukemia patients exhibit constitutively active STAT signaling [45]. Activated STAT signaling is largely unexplained in the ~50% of LGL leukemia patients without STAT3 or STAT3 related mutations. Possible explanations include the fact that sequencing has not been exhaustive. The majority of patient samples are routinely sequenced for STAT3 mutations in the SH2 domain, but the discovery of mutations outside of the SH2 domain suggests a more thorough sequencing of the entire STAT3 gene. In Chapter 3, we used whole genome sequencing to interrogate the entire STAT3 gene and observed several mutations outside of the SH2 domain.

Next, the largest current limitation in understanding the molecular changes in LGL leukemia is the lack of information regarding changes that occur in the genome outside of regions that code for proteins [205]. This requires whole genome sequencing combined with identification of regulatory regions in the LGL and normal cellular counterpart. Mutations in important DNA elements such as enhancers and promoters have yet to be thoroughly investigated and reported. Analysis of our whole genome sequencing data from Chapter 3 may reveal mutations that are in non coding regions that potentially cause aberrant expression patterns. Once these regions are known, overlap with WGS comparisons of tumor and normal will provide candidate mutations in regulatory regions that may be additional drivers of this disease. Epigenetic changes that may lead to the same result have similarly not been thoroughly examined and described. Combining whole genome sequencing data with our other genomic studies including ATAC-seq (Appendix), RNA-seq and ChIP-seq efforts will create a global transcriptional, epigenetic and gene expression landscape aiming to understand the pathogenesis of LGL leukemia. These studies will establish differential landscapes between healthy and leukemic material as well as between WT STAT3 and mutant STAT3.

A thorough cataloging of all of the mutations that occur in LGL leukemia is necessary to determine the dynamics of clonal evolution and drift in LGL leukemia pathogenesis and progression. Though current technology allows us to determine relative clone size through NGS of TCR sequences, we do not currently have a complete understanding of what causes clones to persist and fluctuate or how they contribute to the clinical symptoms associated with LGL leukemia. Ideally a comprehensive mutation panel, beyond *STAT3* and other genes described here, can be performed on multiple clones from oligoclonal disease in order to determine the full mutational burden. It will be critical to our understanding of LGL leukemia etiology to determine if clonal expansion precedes or is alternatively an end result of a mutational event. Exhaustive proof that mutations always lag behind expansion would support a continuous antigen response

as the persistent driver of these expansions, with subsequent individual mutations leading to the emergence of the largest clones. In contrast, evidence for mutations that precede clonal expansion would warrant further investigation of the role of dysregulated cellular circuitry.

We do not currently have complete linkage between molecular events and the symptoms of LGL leukemia, with cumulative studies focusing on STAT3 mutations. It will be necessary to identify other mechanisms that may cooperate with or obviate the need for STAT3 mutation in the transition from an indolent clonal expansion to one that causes significant pathology. It is likely that many patients do not notice symptoms or seek a diagnosis of LGL leukemia until the emergence of an expanded and problematic clone, which is likely to have a clear signature. In those asymptomatic patients where LGLL is more or less an incidental finding, it is important to identify the subsequent changes that cause symptoms. If this change is found to often be the expansion of an entirely new clone with a unique molecular profile it will be important to determine at what timepoint this clone appeared. Evidence of a clone with a known mutation at presentation, even if not dominant, may indicate the need for earlier treatment or closer clinical monitoring.

6 APPENDIX: CHARACTERIZING THE CHROMATIN ACCESSIBILITY IN T_{EMRA} AND T-LGL LEUKEMIA PATIENTS

ABSTRACT

Large granular lymphocytes (LGL) represent a morphologically distinct subset of normal circulating blood cells. They are about 2-3 times larger than red blood cells and have abundant cytoplasm with characteristic azurophilic granules [1]. Classically, this LGL subset is further divided into 85% CD3- natural killer (NK) cells and 15% CD3+ T cells and thought to be involved in normal immune response to viruses or cancer cells. It is understood that these cells undergo activated induced cell death (AICD) following the clearance of antigen. In contrast, LGL leukemia is characterized by a sustained clonal proliferation of circulating LGL cells. The majority of patients exhibit T type clones (T-LGL leukemia) and a minority have NK type clones (NK-LGL leukemia). A central goal of the Loughran lab is to elucidate the etiology and pathogenesis of LGL leukemia. The current model postulates multiple contributing factors including a viral transformation, chronic antigen-driven stimulus and somatic oncogenic mutation.

Terminally differentiated effector memory CD45RA+ T (Temra) cells are a subset of CD8+ effector memory T cells. These cells have been exposed to antigen and we have shown by cell surface markers using flow cytometry that the normal equivalent of LGL leukemic cells are Temra. In this chapter, we hypothesize that differences in chromatin accessibility determine the variable gene expression profiles between patients and Temra cells. We present the novel characterization of chromatin accessibility in Temra cells with parallel investigation of differences between Temra and leukemic LGL. We report thousands of differentially accessible genomic regions that are either highly accessible in patients or highly inaccessible in patients compared to Temra chromatin accessibility.

6.1 INTRODUCTION

T cell large granular lymphocyte (T-LGL) leukemia is a chronic disorder that typically results from clonal expansion of CD3+CD8+ cytotoxic T-lymphocytes [1–4]. LGL leukemia cells are constitutively activated cytotoxic cells characterized by profoundly dysregulated apoptosis, resulting in leukemic LGL survival [97,206]. We have shown that LGL leukemia cells exhibit CD3+CD8+CD45RA+CD62L-CCR7- and these cell surface markers are shared with effector memory RA+ T cells (Temra) [16]. Temra cells are a subset of CD8+ effector memory T cells that have responded to antigen, are terminally differentiated and persist long-term [207,208]. Effector memory T cells can be divided into two subsets; CD45RO Tem and CD45RA Temra. These similarities present a unique opportunity to study both a rare subset of normal T cell biology and its comparisons to LGL leukemia.

Dysregulation of several survival pathways are well documented in LGL leukemia. Increased STAT3 activation has been extensively reported and further studied in Chapter 3. While roughly 50% of patients harbor a STAT3 mutation, it does not fully explain the increased STAT signaling observed in all LGL leukemia patients or fully inform LGL leukemia pathogenesis. We have correlated STAT3 mutations with more severe symptoms, higher prevalence of comorbidity with autoimmune disease and variation in gene expression [15]. We hypothesize active or repressed regulatory DNA elements contribute to dysregulated survival pathways such as STAT3. The discovery of other regulatory pathways may inform which are important to the LGL leukemia. In this study, we aim to explore genomic regulation in both Temra and T-LGL leukemia.

Accessibility of DNA to binding of transcription or epigenetic factors reveals the broad regulatory landscape. Accessibility for Transposase-Accessible Chromatin with high-throughput sequencing (ATAC-seq) will allow us to understand the chromatin landscape, by defining open or closed region of chromatin [209,210]. When DNA is bound in histones, the chromatin is considered closed as the DNA is bound tightly and prevents the binding of transcription or epigenetic factors. Therefore, there is no active transcription occurring when chromatin is tightly bound. Accessible, or open

chromatin, is associated with active chromatin, as the DNA is unwound and accessible to binding by transcription factors such as STAT3, or by epigenetic factors that can affect transcription. ATAC-seq utilizes a Tn5 transposase that will fragment and tag accessible DNA with sequencing adapters that will create a sequencing library and be analyzed by sequencing [211].

While ATAC-seq informs the state of chromatin, our goal is to use parallel sequencing methods such as RNA-seq and Chromatin Immunoprecipitation followed by sequencing (ChIP-seq) to create a complete regulatory map of T-LGL leukemia. Integrating RNA-seq allows us to correlate promoter accessibility with gene expression, and ChIP-seq of epigenetic factors such as histone marks annotates the roles of the differentially accessible genomic regions. In this chapter, we hypothesize that differences in chromatin accessibility determines the variable gene expression profiles between patients and Temra cells.

6.2 MATERIALS AND METHODS

SAMPLE ISOLATION

Ten patient samples (**Table 6.1)** were selected from the whole genome sequencing cohort from **Chapter 3**. Patient vials were taken from liquid nitrogen and placed in RPMI supplemented with 10% FBS for two hours. Cells were enriched for CD8+ using CD8+ T cell Isolation Kit (Miltenyi Biotec, Cat#130096495) on an autoMACS Pro Separator following the manufacturer's protocol. T_{emra} cells from normal buffy coats (ZenBio) were isolated using the human CD8+ CD45RA+ Effector T cell Isolation Kit (Miltenyi Biotec, Cat#130094485) on an autoMACS Pro Separator according to manufacturer's protocols. 50,000 cells were counted as input for ATAC-seq.

Table 6.1: Characteristics of samples used in this study

Samples	F/M	STAT3	Cell type	Cell status
Normal 1m	M		Temra	fresh
Normal 2m	M		Temra	fresh
Normal 3m	M		Temra	fresh
Normal 4f	F		Temra	fresh
1758	F	WT	CD8	frozen
1770	M	WT	CD8	frozen
1893	F	Y640F	CD8	frozen
1934	M	Y640F	CD8	frozen
2396	M	WT	CD8	frozen
1947	F	WT	CD8	frozen
1602	M	WT	CD8	frozen
1762	M	K294E	CD8	frozen
1875	F	D661Y	CD8	frozen
1359	F	D661Y	CD8	frozen

ATAC-SEQ

Transposing frozen samples and removing mitochondrial DNA required the use of the Omni-ATAC method. 50000 cells were resuspended in ice-cold lysis buffer (10 mM Tris-HCl pH 7.4, 10 mM NaCl, 3 mM $MgCl_2$, 0.1% NP40, 0.1% Tween-20, 0.01% Digitonin). Varying amounts of transposase (Illumina, Cat# 20034197) were tested in the transposase reaction mix and we found 2.5 µL to be optimal for our samples. Purified transposed DNA was shipped to Penn State University for library preparation and sequencing on the NextSeq500 according to ENCODE standards at 1 x 50 bp using a high output kit.

DATA PROCESSING

Reads were mapped to the human hg19 and hg38 reference genome using Bowtie2. Conversion of SAM file into BAM file using Samtools [124] filtering for mapped reads only. Reads mapped to mitochondria were removed and BAM format was converted to BED format using Bedtools [212]. We identified nucleosome free regions (bp<100) where transcription factors are binding. Single end peak calling of nucleosome free regions using MACS2 [213] identified open genome regions. Annotating peaks to genes using chipseeker library identified genes closest to open regions and their function.

DIFFERENTIAL ATAC-SEQ DATA PROCESSING

Counts of fragments in nucleosome free regions were used to construct a DESeq2 [214] object to test for differences between patients and normals as well as STAT3 WT patients compared to STAT3 mutant patients. Only peaks that were found in at least two samples were used in the analysis. Differential analysis using DESeq2 output a BED file as input into Genomic Regions Enrichment of Annotations Tool (GREAT) [215].

6.3 RESULTS

VISUALIZATION OF PEAKS ON GENOME BROWSER

Peaks mapped to hg38 were visualized on the genome browser. Genes of interest PDGFβ (**Figure 6.1A**) and STAT3 (**Figure 6.1B**) show variation in accessible peaks as highlighted in red. Through network modeling, PDGF was identified as one of two master regulators in LGL leukemia [53] and STAT3 activation has been well documented in this disease [45,68]. The top four tracks are normal isolated Temra samples followed by patient samples.

A **B**

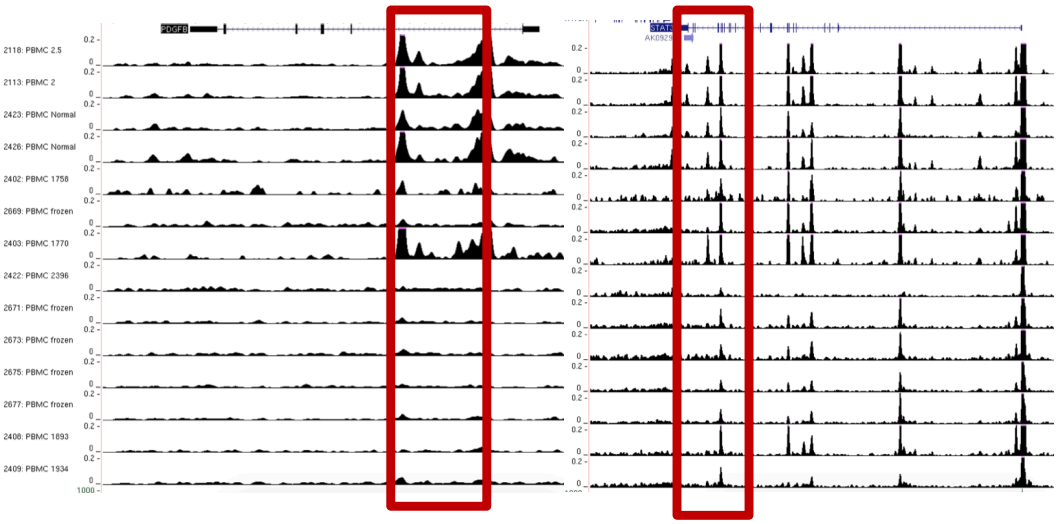

Figure 6.1: Visualization of peaks on hg38 genome.

Representative sequencing tracks of the **[A]** PDGFβ and **[B]** STAT3 loci show variations of accessible peaks.

PEAK STATISTICS

Reads of each sample were mapped to hg38 and checking the distribution of mapped reads (**Figure 4.3A**) confirm lack of mitochondrial DNA contamination. These reads were then used to call peaks using MACS2 in nucleosome free regions for annotation of these regions. Using chipseeker library and the plotAnnopie function, a summary of the annotations of peaks in the same patient sample identified the majority of peaks locate within 1kb of promoters (**Figure 4.3B**).

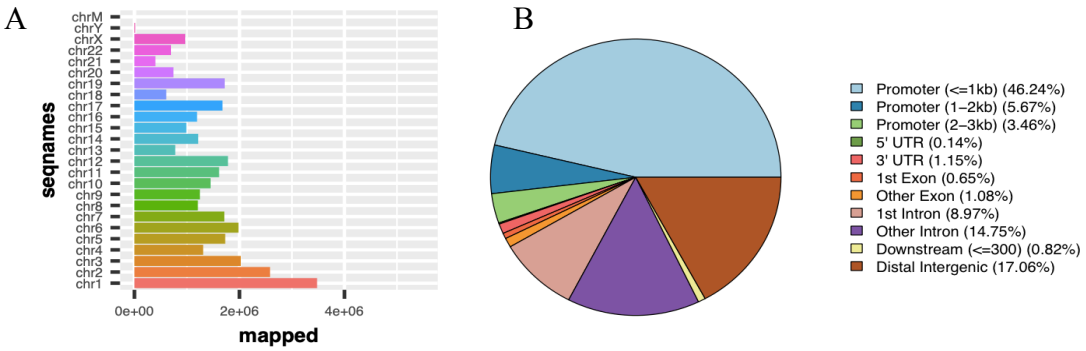

Figure 6.2: Distribution of mapped reads and annotation distribution

[A] Distribution of mapped reads of one representative patient sample. **[B]** In the same patient sample, proportion of peaks annotated to different genomic regions using Annopie function of MACS2.

OCCUPANCY ANALYSIS

Next, we used DESeq2 to call differentially open peaks between normals and patients and between patients with and without STAT3 mutation. DESeq2 uses count data to make differential calls (**Figure 6.3**) so that a higher count is a more accessible, or open peak and a lower count is a more closed or less accessible region. We show a representative genomic region where the patients show a high count, meaning this genomic region is more accessible in patients compared to normals. We also performed principle component analysis (PCA) of peak overlaps between all samples (**Figure 6.4A**). The PCA clearly defined the four normals from the patient samples. When trying to differentiate patients with or without STAT3 mutations, all patients clustered close together and there was not a distinct grouping based on mutation status (**Figure 6.4B**). To visualize overlap of peaks between all samples, an upset plot was used (**Figure 6.4C**) showing 14,563 genomic region overlaps between all samples which is expected as Temra and leukemic LGL share many similarities. We then show that normals share much overlap of peaks, which will be later analyzed. There are few peak overlaps between only patients, and even some peaks, although not many, shared only between patients with Y640F STAT3 mutation, P2408 and P2409.

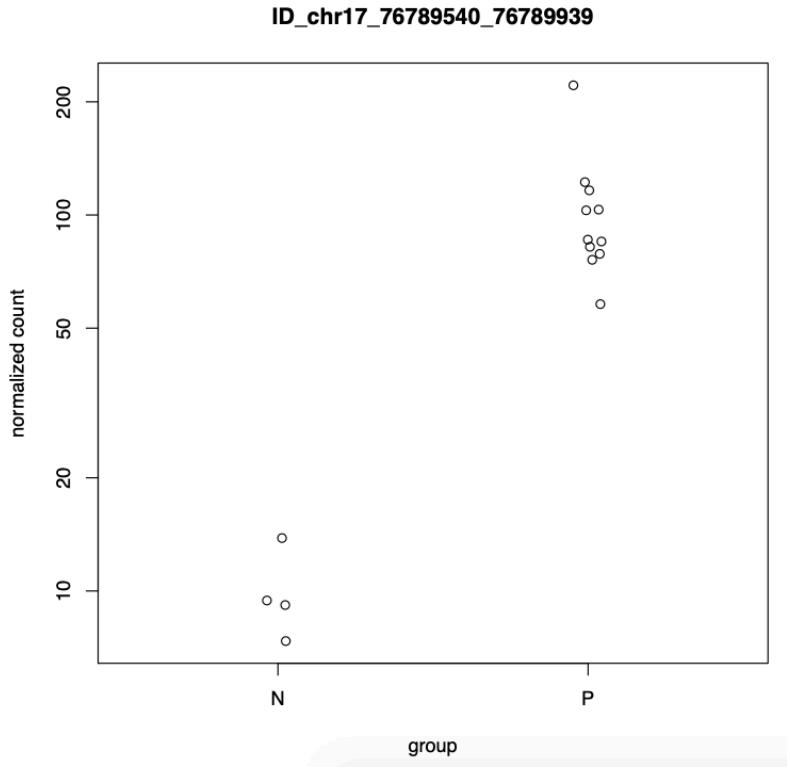

Figure 6.3: Differential counts at a representative genomic region.

Representative genomic region visualizing differential counts where high counts mean chromatin is more open and low counts mean chromatin is more closed.

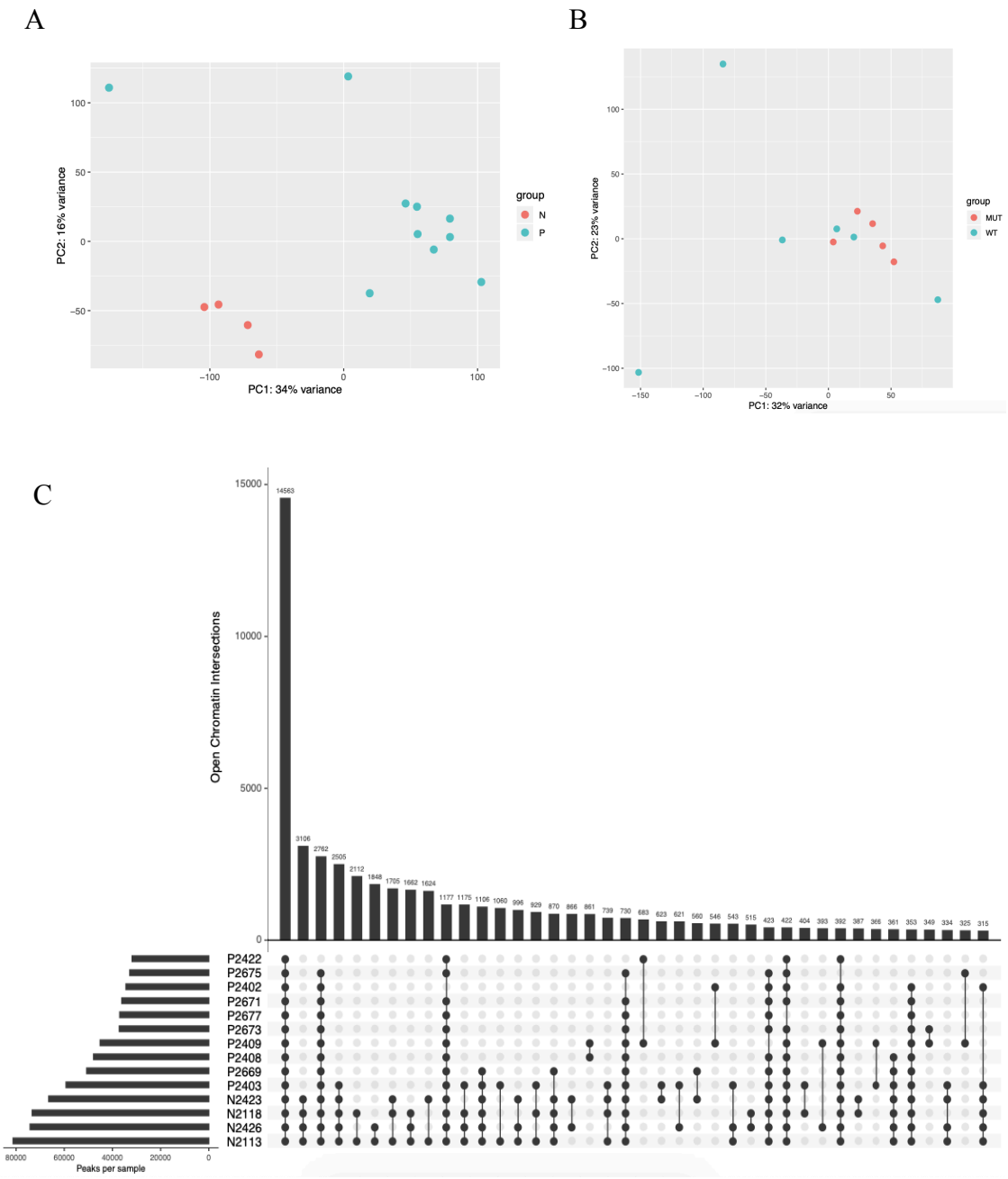

Figure 6.4: Differential analysis between patients and normals.

PCA of all ATAC-seq samples **[A]** separating patients (blue) and normals (red). PCA showing patient samples **[B]** distinguished by STAT3 WT and STAT mutant. Overlap of open chromatin between all samples shown in **[C]** with patient samples listed as P#### and normals listed as N####. Overlap peaks filtered to show only those found in at least two samples or more.

GO ONTOLOGY

Differential analysis using DESeq2 outputs a BED file that is then input into GREAT to analyze and annotate the genomic region inputs. These BED files are split into two; one annotating genomic regions that are more open in patients compared to normals (**Figure 6.5)** and another annotating genomic regions that are closed in patients compared to normals (**Figure 6.6**). There were 1217 genomic regions open in patient samples (**Figure 6.5A**) and while the majority of these regions were associated with two genes, there were a few genomic regions associated with zero genes. The majority of genomic regions were 50-500kb away from a transcription start site (TSS) (**Figure 6.4B**), indicating these regions may predominantly function through distal regulatory elements such as enhancers or repressors. Biological pathway annotations show multiple processes involved in activation of lymphocyte regulation, which is in agreement with our current model for LGL leukemia pathogenesis that leukemic LGL are activated by an unknown chronic antigen **(Figure 1.2)**.

In comparison to genomic regions open in patients compared to normals, we found 3065 regions closed in patients compared to normals **(Figure 6.6A)** and over 2/3 of these regions were associated with two or more genes. Similar to genes in (**Figure 6.5B**), these regions closed in patients were mostly found 50 to 500kb up or downstream from a TSS (**Figure 6.6B**). Interestingly, annotation of biological process revealed positive regulation of myeloid cell apoptotic processes (**Figure 6.6C**). As these were genomic regions found to be closed in patients compared to normals, this may point to the loss of positive regulation of apoptosis in patients. Positive regulation of B-cell activation and B-cell receptor signaling pathways were annotated to genomic regions closed in T-LGL leukemia patients compared to normal Temra samples. Coexistence of B-cell abnormalities have been documented in roughly 27% of T-LGL leukemia patients. [216]

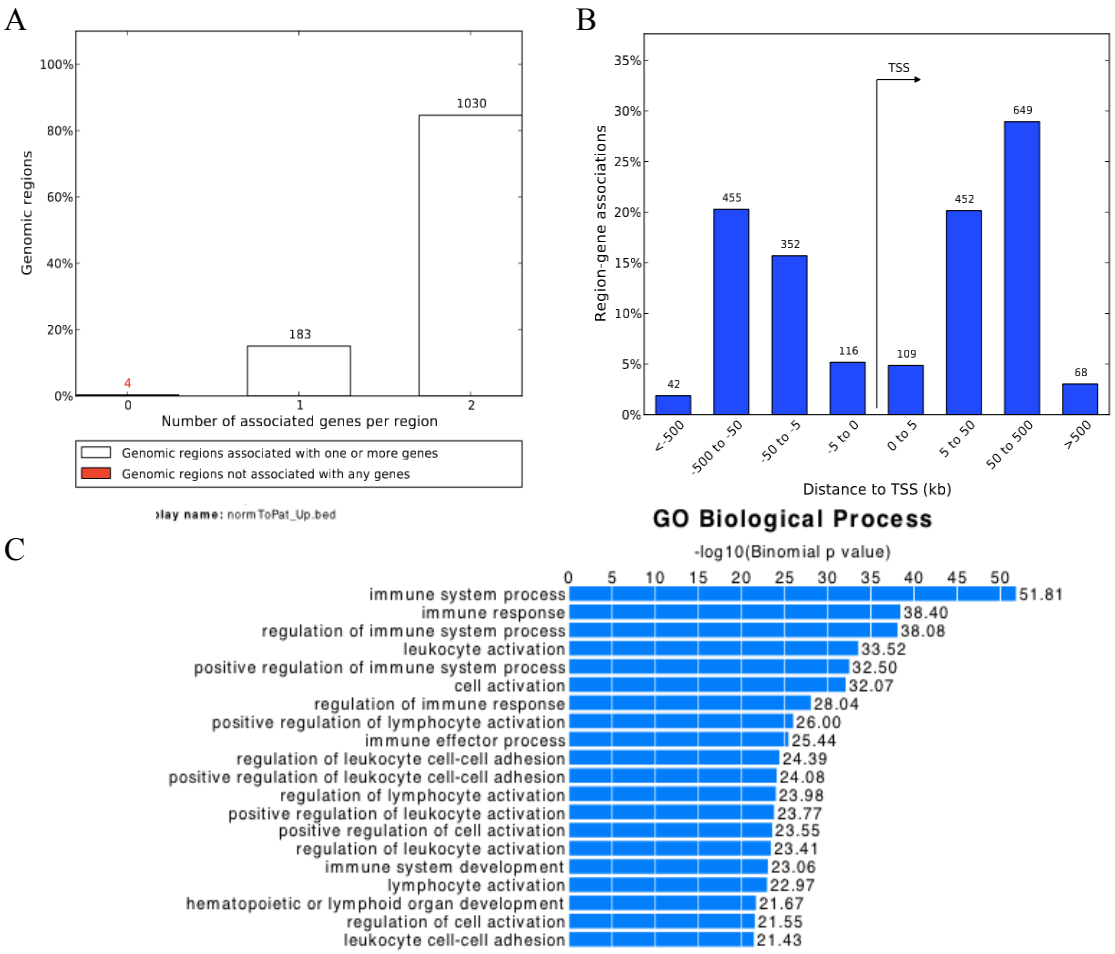

Figure 6.5: GREAT analysis of peaks open in patients compared to normals

1217 genomic regions were found to be open in patients compared to normals. **[A]** Over 1000 of those regions were associated with two or more genes. **[B]** Distance up and downstream of the TSS. **[C]** Gene ontology annotates the biological processes of genomic regions.

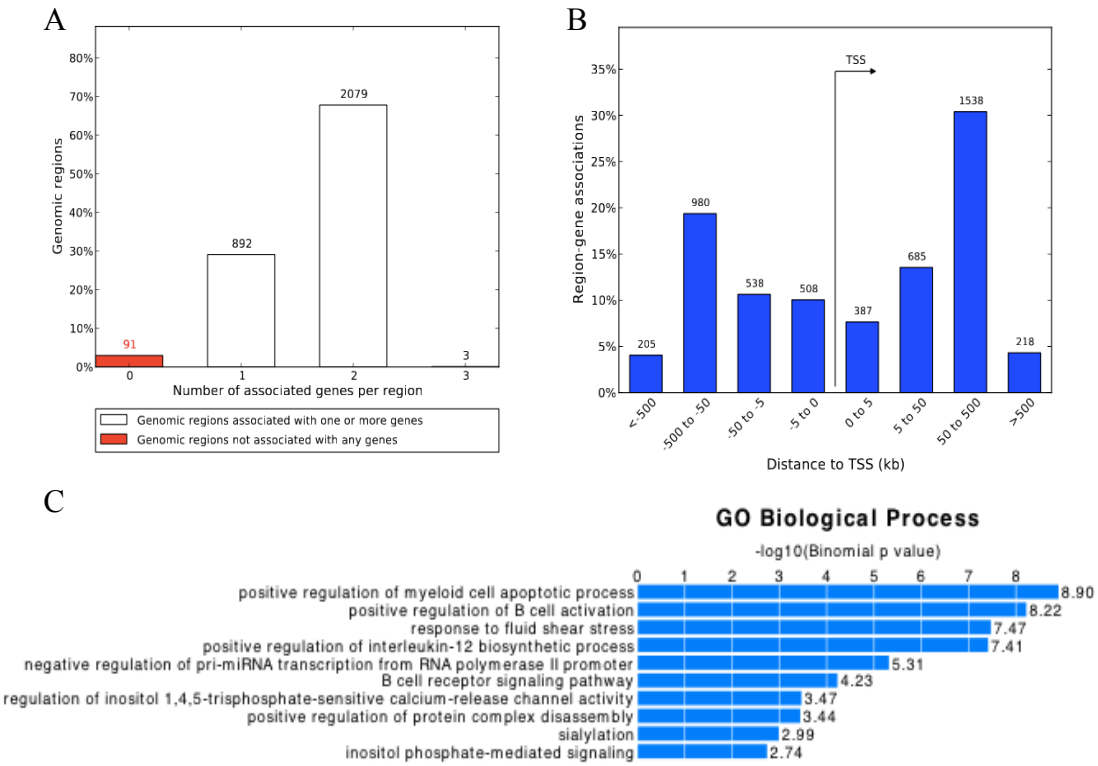

Figure 6.6: GREAT analysis of peaks closed in only patients

3065 genomic regions were found to be closed in patients compared to normals. Number of regions associated with zero, one, two or three genes **[A]** and distance up and downstream of the TSS are graphed in **[B]**. **[C]** Gene ontology annotates the biological processes of genomic regions.

6.4 DISCUSSION

This project profiles chromatin accessibility of normal Temra, T-LGL leukemia patient CD8+ cells with and without STAT3 mutations. Temras are a rare subset that has not been well studied and this data furthers the knowledge of normal Temra biology and leukemic T-LGL in parallel. ATAC-seq was utilized to map chromatin states by revealing areas of the genome that are accessible to Tn5 transposase. The accessibility of DNA to the transposase indicates the state of the dynamic chromatin structure that regulates gene transcription. Our analysis included Temra cells isolated from four normal donors. These terminally differentiated CD8+ T cells are not well characterized and this study is the first to report on the chromatin accessibility of Temra cells. In addition to the normal samples, we investigated chromatin states in ten T-LGL leukemia patient samples enriched for CD8+.

Peak visualization on the genome browser allows us to query genes of interest and determine whether there are any peak differences between samples. As seen in Error! R eference source not found., it is difficult to make inferences due to the variability between samples. It is clear that variability between samples may be due to using fresh samples versus frozen samples. We have done a few patient samples from clinic that were processed the same day that have produced clean peaks with minimal background. Unfortunately, waiting for the right patient to come to clinic is not feasible when trying to process multiple samples. Even with the addition of a dead cell removal kit in frozen samples, we did not visualize any improvement on the genome browser.

Results from the initial analysis of these samples show there are genomic region variations between T-LGL leukemic CD8+ patient samples and healthy donor Temra cells, which have been shown to be the normal counterpart. We found thousands of peaks that were differentially accessible, either open or closed, between patients and normals. PCA showed distinct clustering of normal samples and patient samples, but

patients with or without STAT3 mutations clustered together. The separation of normals and patients is encouraging, however, patient samples are frozen and enriched for CD8+ whereas normal samples are processed without being frozen and isolated for Temra. Ideally, we would be able to process patients and normals in identical methods. We have attempted to isolate patient samples for Temra, however, the output is small for the input needed for ChIP.

Through DEseq2 analysis, we annotated these differential genomic regions and found those that were more open were involved in the regulation of immune system and lymphocyte activation. This is in agreement with our current model of pathogenesis (Chapter 1) where LGL leukemia arises from an initial activation step that leads to clonal expansion. Genomic regions closed in patients compared to normals were most highly associated with biological processes involved in the positive regulation of apoptosis in myeloid cells. This was also an expected result as evading cell death is a key hallmark of leukemic LGL cells.

This study is ongoing and modifications to analysis pipeline are still being made. For example, we can find or develop a tool that is able to normalize the differences in sequencing depth and signal-to-noise ratio between samples. Because of these differences, some biological differences between samples may be hidden or overstated. This may explain the lack of differentiation between STAT3 WT and STAT3 mutated patient samples. Additionally, we aim to annotate these regions with gene names or more specific signaling pathways to discover regulatory pathways specific to LGL leukemia.

Nuclease accessibility, histone modifications and transcription factor binding all play important roles in gene regulation. These epigenetic features of chromatin can be studied using advanced sequencing technologies and the integration of these data sets can determine the chromatin landscape on a genome-wide scale. Advances in analysis

tools have allowed us to compare epigenetic profiles across different cell types to infer functional elements in genomes that control biological functions in either a healthy or disease context. Integration of RNA-seq already generated in our lab will correlate genome accessibility with differential gene expression. Furthermore, ongoing ChIP-seq of histone marks will distinguish between active areas of transcription or gene repression. Ultimately, the goal of this project is build a broad map of the regulatory landscape in LGL leukemia and to define genes or pathways differentially expressed that may lead to putative therapeutic targets.

REFERENCES

1. Lamy T, Moignet A, Loughran TP. LGL leukemia: from pathogenesis to treatment. Blood. 2017;129:1082–94.

2. Loughran TP. Clonal diseases of large granular lymphocytes. Blood. 1993;82:1–14.

3. Melenhorst JJ, Sorbara L, Kirby M, Hensel NF, Barrett AJ. Large granular lymphocyte leukaemia is characterized by a clonal T-cell receptor rearrangement in both memory and effector CD8(+) lymphocyte populations. Br J Haematol. 2001;112:189–94.

4. Sanikommu SR, Clemente MJ, Chomczynski P, Afable MG, Jerez A, Thota S, Patel B, Hirsch C, Nazha A, Desamito J, Lichtin A, Pohlman B, Sekeres MA, Radivoyevitch T, Maciejewski JP. Clinical features and treatment outcomes in large granular lymphocytic leukemia (LGLL). Leukemia & Lymphoma. 2018;59:416–22.

5. Shah MV, Hook CC, Call TG, Go RS. A population-based study of large granular lymphocyte leukemia. Blood Cancer J. 2016;6:e455.

6. Loughran Jr THOMAS P, KADIN ME, STARKEBAUM G, ABKOWITZ JL, CLARK EA, DISTECHE C, LUM LG, SLICHTER SJ. Leukemia of Large Granular Lymphocytes: Association with Clonal Chromosomal Abnormalities and Autoimmune Neutropenia, Thrombocytopenia, and Hemolytic Anemia. Ann Intern Med. 1985;102:169–75.

7. Campo E, Swerdlow SH, Harris NL, Pileri S, Stein H, Jaffe ES. The 2008 WHO classification of lymphoid neoplasms and beyond: evolving concepts and practical applications. Blood. 2011;117:5019–32.

8. Swerdlow SH, Campo E, Pileri SA, Harris NL, Stein H, Siebert R, Advani R, Ghielmini M, Salles GA, Zelenetz AD, Jaffe ES. The 2016 revision of the World Health Organization classification of lymphoid neoplasms. Blood. 2016;127:2375–90.

9. Semenzato G, Zambello R, Starkebaum G, Oshimi K, Loughran TP. The lymphoproliferative disease of granular lymphocytes: updated criteria for diagnosis. Blood. 1997;89:256–60.

10. De Kouchkovsky I, Abdul-Hay M. Acute myeloid leukemia: a comprehensive review and 2016 update. Blood Cancer J. 2016;6:e441.

11. Döhner H, Estey E, Grimwade D, Amadori S, Appelbaum FR, Büchner T, Dombret H, Ebert BL, Fenaux P, Larson RA, Levine RL, Lo-Coco F, Naoe T, Niederwieser D, Ossenkoppele GJ, Sanz M, Sierra J, Tallman MS, Tien H-F, Wei AH, Löwenberg B, Bloomfield CD. Diagnosis and management of AML in adults: 2017 ELN recommendations from an international expert panel. Blood. 2017;129:424–47.

12. Langerak AW, Groenen PJTA, Brüggemann M, Beldjord K, Bellan C, Bonello L, Boone E, Carter GI, Catherwood M, Davi F, Delfau-Larue M-H, Diss T, Evans P a. S, Gameiro P, Garcia Sanz R, Gonzalez D, Grand D, Håkansson A, Hummel M, Liu H,

Lombardia L, Macintyre EA, Milner BJ, Montes-Moreno S, Schuuring E, Spaargaren M, Hodges E, van Dongen JJM. EuroClonality/BIOMED-2 guidelines for interpretation and reporting of Ig/TCR clonality testing in suspected lymphoproliferations. Leukemia. 2012;26:2159–71.

13. van Krieken JHJM, Langerak AW, Macintyre EA, Kneba M, Hodges E, Sanz RG, Morgan GJ, Parreira A, Molina TJ, Cabeçadas J, Gaulard P, Jasani B, Garcia JF, Ott M, Hannsmann ML, Berger F, Hummel M, Davi F, Brüggemann M, Lavender FL, Schuuring E, Evans P a. S, White H, Salles G, Groenen PJTA, Gameiro P, Pott C, Dongen JJM van. Improved reliability of lymphoma diagnostics via PCR-based clonality testing: — Report of the BIOMED-2 Concerted Action BHM4-CT98-3936. Leukemia. Nature Publishing Group; 2007;21:201–6.

14. Lamy T, Loughran TP. How I treat LGL leukemia. Blood. 2011;117:2764–74.

15. Loughran TP, Zickl L, Olson TL, Wang V, Zhang D, Rajala HLM, Hasanali Z, Bennett JM, Lazarus HM, Litzow MR, Evens AM, Mustjoki S, Tallman MS. Immunosuppressive therapy of LGL leukemia: prospective multicenter phase II study by the Eastern Cooperative Oncology Group (E5998). Leukemia. 2015;29:886–94.

16. Yang J, Epling-Burnette PK, Painter JS, Zou J, Bai F, Wei S, Loughran TP. Antigen activation and impaired Fas-induced death-inducing signaling complex formation in T-large-granular lymphocyte leukemia. Blood. 2008;111:1610–6.

17. Moignet A, Lamy T. Latest Advances in the Diagnosis and Treatment of Large Granular Lymphocytic Leukemia. American Society of Clinical Oncology Educational Book. American Society of Clinical Oncology; 2018;616–25.

18. O'Keefe CL, Plasilova M, Wlodarski M, Risitano AM, Rodriguez AR, Howe E, Young NS, Hsi E, Maciejewski JP. Molecular analysis of TCR clonotypes in LGL: a clonal model for polyclonal responses. J Immunol. 2004;172:1960–9.

19. Wlodarski MW, O'Keefe C, Howe EC, Risitano AM, Rodriguez A, Warshawsky I, Loughran TP, Maciejewski JP. Pathologic clonal cytotoxic T-cell responses: nonrandom nature of the T-cell-receptor restriction in large granular lymphocyte leukemia. Blood. 2005;106:2769–80.

20. Garrido P, Ruiz-Cabello F, Bárcena P, Sandberg Y, Cantón J, Lima M, Balanzategui A, González M, López-Nevot MA, Langerak AW, García-Montero AC, Almeida J, Orfao A. Monoclonal TCR-Vβ13.1+/CD4+/NKa+/CD8−/+dim T-LGL lymphocytosis: evidence for an antigen-driven chronic T-cell stimulation origin. Blood. 2007;109:4890–8.

21. Sandberg Y, Kallemeijn MJ, Dik WA, Tielemans D, Wolvers-Tettero ILM, van Gastel-Mol EJ, Szczepanski T, Pol Y, Darzentas N, van Dongen JJM, Langerak AW. Lack of common TCRA and TCRB clonotypes in CD8+/TCRαβ+ T-cell large granular

lymphocyte leukemia: a review on the role of antigenic selection in the immunopathogenesis of CD8+ T-LGL. Blood Cancer Journal. 2014;4:e172.

22. Clemente MJ, Przychodzen B, Jerez A, Dienes BE, Afable MG, Husseinzadeh H, Rajala HLM, Wlodarski MW, Mustjoki S, Maciejewski JP. Deep sequencing of the T-cell receptor repertoire in CD8+ T-large granular lymphocyte leukemia identifies signature landscapes. Blood. 2013;122:4077–85.

23. Rodríguez-Caballero A, García-Montero AC, Bárcena P, Almeida J, Ruiz-Cabello F, Tabernero MD, Garrido P, Muñoz-Criado S, Sandberg Y, Langerak AW, González M, Balanzategui A, Orfao A. Expanded cells in monoclonal TCR-alphabeta+/CD4+/NKa+/CD8-/+dim T-LGL lymphocytosis recognize hCMV antigens. Blood. 2008;112:4609–16.

24. Nyland SB, Krissinger DJ, Clemente MJ, Irby RB, Baab KT, Jarbadan NR, Sokol L, Schaefer E, Liao J, Cuthbertson D, Epling-Burnette P, Paquette R, List AF, Maciejewski JP, Loughran TP. Seroreactivity to LGL leukemia-specific epitopes in aplastic anemia, myelodysplastic syndrome and paroxysmal nocturnal hemoglobinuria: results of a bone marrow failure consortium study. Leuk Res. 2012;36:581–7.

25. Sandberg Y, Almeida J, Gonzalez M, Lima M, Bárcena P, Szczepañski T, van Gastel-Mol EJ, Wind H, Balanzategui A, van Dongen JJM, Miguel JFS, Orfao A, Langerak AW. TCRγδ+ large granular lymphocyte leukemias reflect the spectrum of normal antigen-selected TCRγδ+ T-cells. Leukemia. 2006;20:505–13.

26. Zambello R, Falco M, Della Chiesa M, Trentin L, Carollo D, Castriconi R, Cannas G, Carlomagno S, Cabrelle A, Lamy T, Agostini C, Moretta A, Semenzato G, Vitale M. Expression and function of KIR and natural cytotoxicity receptors in NK-type lymphoproliferative diseases of granular lymphocytes. Blood. 2003;102:1797–805.

27. Epling-Burnette PK, Painter JS, Chaurasia P, Bai F, Wei S, Djeu JY, Loughran TP. Dysregulated NK receptor expression in patients with lymphoproliferative disease of granular lymphocytes. Blood. 2004;103:3431–9.

28. Scquizzato E, Teramo A, Miorin M, Facco M, Piazza F, Noventa F, Trentin L, Agostini C, Zambello R, Semenzato G. Genotypic evaluation of killer immunoglobulin-like receptors in NK-type lymphoproliferative disease of granular lymphocytes. Leukemia. Nature Publishing Group; 2007;21:1060–9.

29. Gattazzo C, Teramo A, Miorin M, Scquizzato E, Cabrelle A, Balsamo M, Agostini C, Vendrame E, Facco M, Albergoni MP, Trentin L, Vitale M, Semenzato G, Zambello R. Lack of expression of inhibitory KIR3DL1 receptor in patients with natural killer cell-type lymphoproliferative disease of granular lymphocytes. Haematologica. 2010;95:1722–9.

30. Gattazzo C, Teramo A, Passeri F, De March E, Carraro S, Trimarco V, Frezzato F, Berno T, Barilà G, Martini V, Piazza F, Trentin L, Facco M, Semenzato G, Zambello

R. Detection of monoclonal T populations in patients with KIR-restricted chronic lymphoproliferative disorder of NK cells. Haematologica. 2014;99:1826–33.

31. Battiwalla M, Melenhorst JJ, Sauntharajah Y, Nakamura R, Molldrem JJ, Young N, Barrett AJ. HLA-DR4 predicts haematological response to cyclosporine in T-large granular lymphocyte lymphoproliferative disorders. British journal of haematology. 2003;

32. Jerez A, Clemente MJ, Makishima H, Rajala H, Gómez-Seguí I, Olson T, McGraw K, Przychodzen B, Kulasekararaj A, Afable M, Husseinzadeh HD, Hosono N, LeBlanc F, Lagström S, Zhang D, Ellonen P, Tichelli A, Nissen C, Lichtin AE, Wodnar-Filipowicz A, Mufti GJ, List AF, Mustjoki S, Loughran TP, Maciejewski JP. STAT3 mutations indicate the presence of subclinical T-cell clones in a subset of aplastic anemia and myelodysplastic syndrome patients. Blood. 2013;122:2453–9.

33. Kawa-Ha K, Ishihara S, Ninomiya T, Yumura-Yagi K, Hara J, Murayama F, Tawa A, Hirai K. CD3-negative lymphoproliferative disease of granular lymphocytes containing Epstein-Barr viral DNA. J Clin Invest. 1989;84:51–5.

34. Suzuki R, Suzumiya J, Nakamura S, Aoki S, Notoya A, Ozaki S, Gondo H, Hino N, Mori H, Sugimori H, Kawa K, Oshimi K. Aggressive natural killer-cell leukemia revisited: large granular lymphocyte leukemia of cytotoxic NK cells. Leukemia. 2004;18:763–70.

35. Loughran TP, Zambello R, Ashley R, Guderian J, Pellenz M, Semenzato G, Starkebaum G. Failure to detect Epstein-Barr virus DNA in peripheral blood mononuclear cells of most patients with large granular lymphocyte leukemia. Blood. 1993;81:2723–7.

36. Loughran TP, Coyle T, Sherman MP, Starkebaum G, Ehrlich GD, Ruscetti FW, Poiesz BJ. Detection of human T-cell leukemia/lymphoma virus, type II, in a patient with large granular lymphocyte leukemia. Blood. 1992;80:1116–9.

37. Starkebaum G, Loughran TP, Kalyanaraman VS, Kadin ME, Kidd PG, Singer JW, Ruscetti FW. Serum reactivity to human T-cell leukaemia/lymphoma virus type I proteins in patients with large granular lymphocytic leukaemia. Lancet. 1987;1:596–9.

38. Sokol L, Agrawal D, Loughran TP. Characterization of HTLV envelope seroreactivity in large granular lymphocyte leukemia. Leuk Res. 2005;29:381–7.

39. Loughran TP, Hadlock KG, Yang Q, Perzova R, Zambello R, Semenzato G, Foung SK, Poiesz BJ. Seroreactivity to an envelope protein of human T-cell leukemia/lymphoma virus in patients with CD3- (natural killer) lymphoproliferative disease of granular lymphocytes. Blood. 1997;90:1977–81.

40. Grossman WJ, Kimata JT, Wong FH, Zutter M, Ley TJ, Ratner L. Development of leukemia in mice transgenic for the tax gene of human T-cell leukemia virus type I. Proc Natl Acad Sci U S A. 1995;92:1057–61.

41. Ren T, Yang J, Broeg K, Liu X, Loughran Jr. TP, Cheng H. Developing an in vitro model of T cell type of large granular lymphocyte leukemia. Leukemia Research. 2013;37:1737–43.

42. Nyland SB, Feith DJ, Poss M, Olson TL, Krissinger DJ, Poiesz BJ, Ruscetti FW, Loughran TP. Retroviral sero-reactivity in LGL leukaemia patients and family members. British Journal of Haematology. 2020;188:522–7.

43. Lamy T, Liu JH, Landowski TH, Dalton WS, Loughran TP. Dysregulation of CD95/CD95 Ligand-Apoptotic Pathway in CD3+ Large Granular Lymphocyte Leukemia. Blood. 1998;92:4771–7.

44. Perzova R, Loughran TP. Constitutive expression of Fas ligand in large granular lymphocyte leukaemia. Br J Haematol. 1997;97:123–6.

45. Epling-Burnette PK, Liu JH, Catlett-Falcone R, Turkson J, Oshiro M, Kothapalli R, Li Y, Wang J-M, Yang-Yen H-F, Karras J, Jove R, Loughran TP. Inhibition of STAT3 signaling leads to apoptosis of leukemic large granular lymphocytes and decreased Mcl-1 expression. J Clin Invest. 2001;107:351–62.

46. Liu JH, Wei S, Lamy T, Li Y, Epling-Burnette PK, Djeu JY, Loughran TP. Blockade of Fas-dependent apoptosis by soluble Fas in LGL leukemia. Blood. 2002;100:1449–53.

47. Epling-Burnette PK, Bai F, Wei S, Chaurasia P, Painter JS, Olashaw N, Hamilton A, Sebti S, Djeu JY, Loughran TP. ERK couples chronic survival of NK cells to constitutively activated Ras in lymphoproliferative disease of granular lymphocytes (LDGL). Oncogene. 2004;23:9220–9.

48. Schade AE, Powers JJ, Wlodarski MW, Maciejewski JP. Phosphatidylinositol-3-phosphate kinase pathway activation protects leukemic large granular lymphocytes from undergoing homeostatic apoptosis. Blood. 2006;107:4834–40.

49. Schade AE, Wlodarski MW, Maciejewski JP. Pathophysiology defined by altered signal transduction pathways: the role of JAK-STAT and PI3K signaling in leukemic large granular lymphocytes. Cell Cycle. 2006;5:2571–4.

50. Kothapalli R, Nyland SB, Kusmartseva I, Bailey RD, McKeown TM, Loughran TP. Constitutive production of proinflammatory cytokines RANTES, MIP-1beta and IL-18 characterizes LGL leukemia. Int J Oncol. 2005;26:529–35.

51. Shah MV, Zhang R, Irby R, Kothapalli R, Liu X, Arrington T, Frank B, Lee NH, Loughran TP. Molecular profiling of LGL leukemia reveals role of sphingolipid signaling in survival of cytotoxic lymphocytes. Blood. 2008;112:770–81.

52. Kothapalli R, Kusmartseva I, Loughran TP. Characterization of a human sphingosine-1-phosphate receptor gene (S1P5) and its differential expression in LGL leukemia. Biochim Biophys Acta. 2002;1579:117–23.

53. Zhang R, Shah MV, Yang J, Nyland SB, Liu X, Yun JK, Albert R, Loughran TP. Network model of survival signaling in large granular lymphocyte leukemia. Proc Natl Acad Sci U S A. 2008;105:16308–13.

54. Waldmann TA. The biology of interleukin-2 and interleukin-15: implications for cancer therapy and vaccine design. Nat Rev Immunol. 2006;6:595–601.

55. Hodge DL, Yang J, Buschman MD, Schaughency PM, Dang H, Bere W, Yang Y, Savan R, Subleski JJ, Yin X-M, Loughran TP, Young HA. Interleukin-15 enhances proteasomal degradation of bid in normal lymphocytes: implications for large granular lymphocyte leukemias. Cancer Res. 2009;69:3986–94.

56. Zambello R, Facco M, Trentin L, Sancetta R, Tassinari C, Perin A, Milani A, Pizzolo G, Rodeghiero F, Agostini C, Meazza R, Ferrini S, Semenzato G. Interleukin-15 Triggers the Proliferation and Cytotoxicity of Granular Lymphocytes in Patients With Lymphoproliferative Disease of Granular Lymphocytes. Blood. 1997;89:201–11.

57. Chen J, Petrus M, Bamford R, Shih JH, Morris JC, Janik JE, Waldmann TA. Increased serum soluble IL-15Rα levels in T-cell large granular lymphocyte leukemia. Blood. 2012;119:137–43.

58. Kristensen T, Larsen M, Rewes A, Frederiksen H, Thomassen M, Møller MB. Clinical relevance of sensitive and quantitative STAT3 mutation analysis using next-generation sequencing in T-cell large granular lymphocytic leukemia. J Mol Diagn. 2014;16:382–92.

59. Ley TJ, Mardis ER, Ding L, Fulton B, McLellan MD, Chen K, Dooling D, Dunford-Shore BH, McGrath S, Hickenbotham M, Cook L, Abbott R, Larson DE, Koboldt DC, Pohl C, Smith S, Hawkins A, Abbott S, Locke D, Hillier LW, Miner T, Fulton L, Magrini V, Wylie T, Glasscock J, Conyers J, Sander N, Shi X, Osborne JR, Minx P, Gordon D, Chinwalla A, Zhao Y, Ries RE, Payton JE, Westervelt P, Tomasson MH, Watson M, Baty J, Ivanovich J, Heath S, Shannon WD, Nagarajan R, Walter MJ, Link DC, Graubert TA, DiPersio JF, Wilson RK. DNA sequencing of a cytogenetically normal acute myeloid leukaemia genome. Nature. 2008;456:66–72.

60. Cancer Genome Atlas Research Network, Ley TJ, Miller C, Ding L, Raphael BJ, Mungall AJ, Robertson AG, Hoadley K, Eley G, et al. Genomic and epigenomic landscapes of adult de novo acute myeloid leukemia. N Engl J Med. 2013;368:2059–74.

61. Puente XS, Pinyol M, Quesada V, Conde L, Ordóñez GR, Villamor N, Escaramis G, Jares P, Campo E, et al. Whole-genome sequencing identifies recurrent mutations in chronic lymphocytic leukaemia. Nature. 2011;475:101–5.

62. Wang L, Lawrence MS, Wan Y, Stojanov P, Sougnez C, Stevenson K, Werner L, Sivachenko A, DeLuca DS, Zhang L, Zhang W, Vartanov AR, Fernandes SM, Goldstein NR, Folco EG, Cibulskis K, Tesar B, Sievers QL, Shefler E, Gabriel S,

Hacohen N, Reed R, Meyerson M, Golub TR, Lander ES, Neuberg D, Brown JR, Getz G, Wu CJ. SF3B1 and Other Novel Cancer Genes in Chronic Lymphocytic Leukemia. New England Journal of Medicine. Massachusetts Medical Society; 2011;365:2497–506.

63. Chapman MA, Lawrence MS, Keats JJ, Cibulskis K, Sougnez C, Schinzel AC, Harview CL, Brunet J-P, Ahmann GJ, Adli M, Anderson KC, Ardlie KG, Auclair D, Baker A, Bergsagel PL, Bernstein BE, Drier Y, Fonseca R, Gabriel SB, Hofmeister CC, Jagannath S, Jakubowiak AJ, Krishnan A, Levy J, Liefeld T, Lonial S, Mahan S, Mfuko B, Monti S, Perkins LM, Onofrio R, Pugh TJ, Rajkumar SV, Ramos AH, Siegel DS, Sivachenko A, Stewart AK, Trudel S, Vij R, Voet D, Winckler W, Zimmerman T, Carpten J, Trent J, Hahn WC, Garraway LA, Meyerson M, Lander ES, Getz G, Golub TR. Initial genome sequencing and analysis of multiple myeloma. Nature. 2011;471:467–72.

64. Tiacci E, Trifonov V, Schiavoni G, Holmes A, Kern W, Martelli MP, Pucciarini A, Bigerna B, Pacini R, Wells VA, Sportoletti P, Pettirossi V, Mannucci R, Elliott O, Liso A, Ambrosetti A, Pulsoni A, Forconi F, Trentin L, Semenzato G, Inghirami G, Capponi M, Di Raimondo F, Patti C, Arcaini L, Musto P, Pileri S, Haferlach C, Schnittger S, Pizzolo G, Foà R, Farinelli L, Haferlach T, Pasqualucci L, Rabadan R, Falini B. BRAF Mutations in Hairy-Cell Leukemia. New England Journal of Medicine. Massachusetts Medical Society; 2011;364:2305–15.

65. Jerez A, Clemente MJ, Makishima H, Koskela H, LeBlanc F, Ng KP, Olson T, Przychodzen B, Afable M, Gomez-Segui I, Guinta K, Durkin L, Hsi ED, McGraw K, Zhang D, Wlodarski MW, Porkka K, Sekeres MA, List A, Mustjoki S, Loughran TP, Maciejewski JP. STAT3 mutations unify the pathogenesis of chronic lymphoproliferative disorders of NK cells and T-cell large granular lymphocyte leukemia. Blood. 2012;120:3048–57.

66. Andersson EI, Rajala HLM, Eldfors S, Ellonen P, Olson T, Jerez A, Clemente MJ, Kallioniemi O, Porkka K, Heckman C, Loughran TP, Maciejewski JP, Mustjoki S. Novel somatic mutations in large granular lymphocytic leukemia affecting the STAT-pathway and T-cell activation. Blood Cancer Journal. 2013;3:e168.

67. Rajala HLM, Porkka K, Maciejewski JP, Loughran TP, Mustjoki S. Uncovering the pathogenesis of large granular lymphocytic leukemia-novel STAT3 and STAT5b mutations. Ann Med. 2014;46:114–22.

68. Koskela HLM, Eldfors S, Ellonen P, van Adrichem AJ, Kuusanmäki H, Andersson EI, Lagström S, Clemente MJ, Olson T, Jalkanen SE, Majumder MM, Almusa H, Edgren H, Lepistö M, Mattila P, Guinta K, Koistinen P, Kuittinen T, Penttinen K, Parsons A, Knowles J, Saarela J, Wennerberg K, Kallioniemi O, Porkka K, Loughran TP, Heckman CA, Maciejewski JP, Mustjoki S. Somatic STAT3 mutations in large granular lymphocytic leukemia. N Engl J Med. 2012;366:1905–13.

69. Andersson E, Kuusanmäki H, Bortoluzzi S, Lagström S, Parsons A, Rajala H, van Adrichem A, Eldfors S, Olson T, Clemente MJ, Laasonen A, Ellonen P, Heckman C, Loughran TP, Maciejewski JP, Mustjoki S. Activating somatic mutations outside the SH2-domain of STAT3 in LGL leukemia. Leukemia. 2016;30:1204–8.

70. Ishida F, Matsuda K, Sekiguchi N, Makishima H, Taira C, Momose K, Nishina S, Senoo N, Sakai H, Ito T, Kwong Y-L. STAT3 gene mutations and their association with pure red cell aplasia in large granular lymphocyte leukemia. Cancer Sci. 2014;105:342–6.

71. Qiu Z-Y, Fan L, Wang L, Qiao C, Wu Y-J, Zhou J-F, Xu W, Li J-Y. STAT3 mutations are frequent in T-cell large granular lymphocytic leukemia with pure red cell aplasia. J Hematol Oncol. 2013;6:82.

72. Kawakami T, Sekiguchi N, Kobayashi J, Imi T, Matsuda K, Yamane T, Nishina S, Senoo Y, Sakai H, Ito T, Koizumi T, Hirokawa M, Nakao S, Nakazawa H, Ishida F. Frequent STAT3 mutations in CD8+ T cells from patients with pure red cell aplasia. Blood Adv. 2018;2:2704–12.

73. Tanahashi T, Sekiguchi N, Matsuda K, Takezawa Y, Ito T, Kobayashi H, Ichikawa N, Nishina S, Senoo N, Sakai H, Nakazawa H, Ishida F. Cell size variations of large granular lymphocyte leukemia: Implication of a small cell subtype of granular lymphocyte leukemia with STAT3 mutations. Leuk Res. 2016;45:8–13.

74. Ohgami RS, Ma L, Monabati A, Zehnder JL, Arber DA. STAT3 mutations are present in aggressive B-cell lymphomas including a subset of diffuse large B-cell lymphomas with CD30 expression. Haematologica. 2014;99:e105.

75. Crescenzo R, Abate F, Lasorsa E, Tabbo' F, Gaudiano M, Chiesa N, Di Giacomo F, Spaccarotella E, Barbarossa L, Ercole E, Todaro M, Boi M, Acquaviva A, Ficarra E, Novero D, Rinaldi A, Tousseyn T, Rosenwald A, Kenner L, Cerroni L, Tzankov A, Ponzoni M, Paulli M, Weisenburger D, Chan WC, Iqbal J, Piris MA, Zamo' A, Ciardullo C, Rossi D, Gaidano G, Pileri S, Tiacci E, Falini B, Shultz LD, Mevellec L, Vialard JE, Piva R, Bertoni F, Rabadan R, Inghirami G, European T-Cell Lymphoma Study Group, T-Cell Project: Prospective Collection of Data in Patients with Peripheral T-Cell Lymphoma and the AIRC 5xMille Consortium "Genetics-Driven Targeted Management of Lymphoid Malignancies." Convergent mutations and kinase fusions lead to oncogenic STAT3 activation in anaplastic large cell lymphoma. Cancer Cell. 2015;27:516–32.

76. Nicolae A, Xi L, Pham TH, Pham T-A, Navarro W, Meeker HG, Pittaluga S, Jaffe ES, Raffeld M. Mutations in the JAK/STAT and RAS signaling pathways are common in intestinal T-cell lymphomas. Leukemia. 2016;30:2245–7.

77. Yan Y, Olson TL, Nyland SB, Feith DJ, Loughran TP. Emergence of a STAT3 mutated NK clone in LGL leukemia. Leuk Res Rep. 2014;4:4–7.

78. Rajala HLM, Eldfors S, Kuusanmäki H, Adrichem AJ van, Olson T, Lagström S, Andersson EI, Jerez A, Clemente MJ, Yan Y, Zhang D, Awwad A, Ellonen P, Kallioniemi O, Wennerberg K, Porkka K, Maciejewski JP, Loughran TP, Heckman C, Mustjoki S. Discovery of somatic STAT5b mutations in large granular lymphocytic leukemia. Blood. 2013;121:4541–50.

79. Rajala HLM, Mustjoki S. STAT5b in LGL leukemia – a novel therapeutic target? Oncotarget. 2013;4:808–9.

80. Gentile T, Uner A, Hutchinson R, Wright J, Ben-Ezra J, Russel E, Loughran T. CD3+, CD56+ aggressive variant of large granular lymphocyte leukemia. 1994;2315–21.

81. Andersson EI, Tanahashi T, Sekiguchi N, Gasparini VR, Bortoluzzi S, Kawakami T, Matsuda K, Mitsui T, Eldfors S, Bortoluzzi S, Coppe A, Binatti A, Lagström S, Ellonen P, Fukushima N, Nishina S, Senoo N, Sakai H, Nakazawa H, Kwong Y-L, Loughran TP, Maciejewski JP, Mustjoki S, Ishida F. High incidence of activating STAT5B mutations in CD4-positive T-cell large granular lymphocyte leukemia. Blood. 2016;128:2465–8.

82. Johansson P, Bergmann A, Rahmann S, Wohlers I, Scholtysik R, Przekopowitz M, Seifert M, Tschurtschenthaler G, Webersinke G, Jäger U, Siebert R, Klein-Hitpass L, Dührsen U, Dürig J, Küppers R. Recurrent alterations of TNFAIP3 (A20) in T-cell large granular lymphocytic leukemia. Int J Cancer. 2016;138:121–4.

83. Raess PW, Cascio MJ, Fan G, Press R, Druker BJ, Brewer D, Spurgeon SE. Concurrent STAT3, DNMT3A, and TET2 mutations in T-LGL leukemia with molecularly distinct clonal hematopoiesis of indeterminate potential. Am J Hematol. 2016;n/a-n/a.

84. Rajala HLM, Olson T, Clemente MJ, Lagström S, Ellonen P, Lundan T, Hamm DE, Zaman SAU, Lopez Marti JM, Andersson EI, Jerez A, Porkka K, Maciejewski JP, Loughran TP, Mustjoki S. The analysis of clonal diversity and therapy responses using STAT3 mutations as a molecular marker in large granular lymphocytic leukemia. Haematologica. 2015;100:91–9.

85. Lee JW, Jeong EG, Lee SH, Nam SW, Kim SH, Lee JY, Yoo NJ, Lee SH. Mutational analysis of PTPRT phosphatase domains in common human cancers. APMIS. 2007;115:47–51.

86. Ley TJ, Ding L, Walter MJ, McLellan MD, Lamprecht T, Larson DE, Kandoth C, Payton JE, Baty J, Welch J, Harris CC, Lichti CF, Townsend RR, Fulton RS, Dooling DJ, Koboldt DC, Schmidt H, Zhang Q, Osborne JR, Lin L, O'Laughlin M, McMichael JF, Delehaunty KD, McGrath SD, Fulton LA, Magrini VJ, Vickery TL, Hundal J, Cook LL, Conyers JJ, Swift GW, Reed JP, Alldredge PA, Wylie T, Walker J, Kalicki J, Watson MA, Heath S, Shannon WD, Varghese N, Nagarajan R, Westervelt P, Tomasson MH, Link DC, Graubert TA, DiPersio JF, Mardis ER, Wilson RK.

DNMT3A Mutations in Acute Myeloid Leukemia. New England Journal of Medicine. 2010;363:2424–33.

87. Hill PWS, Amouroux R, Hajkova P. DNA demethylation, Tet proteins and 5-hydroxymethylcytosine in epigenetic reprogramming: An emerging complex story. Genomics. 2014;104:324–33.

88. Teramo A, Gattazzo C, Passeri F, Lico A, Tasca G, Cabrelle A, Martini V, Frezzato F, Trimarco V, Ave E, Boscaro E, Piazza F, Facco M, Trentin L, Semenzato G, Zambello R. Intrinsic and extrinsic mechanisms contribute to maintain the JAK/STAT pathway aberrantly activated in T-type large granular lymphocyte leukemia. Blood. 2013;121:3843–54, S1.

89. Cismasiu VB, Ghanta S, Duque J, Albu DI, Chen H-M, Kasturi R, Avram D. BCL11B participates in the activation of IL2 gene expression in CD4+ T lymphocytes. Blood. 2006;108:2695–702.

90. Cismasiu VB, Adamo K, Gecewicz J, Duque J, Lin Q, Avram D. BCL11B functionally associates with the NuRD complex in T lymphocytes to repress targeted promoter. Oncogene. 2005;24:6753–64.

91. Gutierrez A, Kentsis A, Sanda T, Holmfeldt L, Chen S-C, Zhang J, Protopopov A, Chin L, Dahlberg SE, Neuberg DS, Silverman LB, Winter SS, Hunger SP, Sallan SE, Zha S, Alt FW, Downing JR, Mullighan CG, Look AT. The BCL11B tumor suppressor is mutated across the major molecular subtypes of T-cell acute lymphoblastic leukemia. Blood. 2011;118:4169–73.

92. Dunwell TL, Dickinson RE, Stankovic T, Dallol A, Weston V, Austen B, Catchpoole D, Maher ER, Latif F. Frequent epigenetic inactivation of the SLIT2 gene in chronic and acute lymphocytic leukemia. Epigenetics. 2009;4:265–9.

93. Waldmann TA, Conlon KC, Stewart DM, Worthy TA, Janik JE, Fleisher TA, Albert PS, Figg WD, Spencer SD, Raffeld M, Decker JR, Goldman CK, Bryant BR, Petrus MN, Creekmore SP, Morris JC. Phase 1 trial of IL-15 trans presentation blockade using humanized Mik-Beta-1 mAb in patients with T-cell large granular lymphocytic leukemia. Blood. 2013;121:476–84.

94. Dumitriu B, Ito S, Feng X, Stephens N, Yunce M, Kajigaya S, Melenhorst JJ, Rios O, Scheinberg P, Chinian F, Keyvanfar K, Battiwalla M, Wu CO, Maric I, Xi L, Raffeld M, Muranski P, Townsley DM, Young NS, Barrett AJ, Scheinberg P. Alemtuzumab in T-cell large granular lymphocytic leukaemia: interim results from a single-arm, open-label, phase 2 study. Lancet Haematol. 2016;3:e22-29.

95. Thomas S, Fisher KH, Snowden JA, Danson SJ, Brown S, Zeidler MP. Methotrexate Is a JAK/STAT Pathway Inhibitor. PLoS One [Internet]. 2015 [cited 2020 Mar 13];10. Available from: https://www.ncbi.nlm.nih.gov/pmc/articles/PMC4489434/

96. Watters RJ, Liu X, Loughran TP. T-cell and natural killer-cell large granular lymphocyte leukemia neoplasias. Leuk Lymphoma. 2011;52:2217–25.

97. Steinway SN, Leblanc F, Loughran TP. The pathogenesis and treatment of large granular lymphocyte leukemia. Blood Rev. 2014;28:87–94.

98. Hammarén HM, Virtanen AT, Raivola J, Silvennoinen O. The regulation of JAKs in cytokine signaling and its breakdown in disease. Cytokine. 2019;118:48–63.

99. Ward AC, Touw I, Yoshimura A. The Jak-Stat pathway in normal and perturbed hematopoiesis. Blood. 2000;95:19–29.

100. Vainchenker W, Constantinescu SN. JAK/STAT signaling in hematological malignancies. Oncogene. 2013;32:2601–13.

101. Li Q, Li B, Hu L, Ning H, Jiang M, Wang D, Liu T, Zhang B, Chen H. Identification of a novel functional JAK1 S646P mutation in acute lymphoblastic leukemia. Oncotarget. 2017;8:34687–97.

102. Flex E, Petrangeli V, Stella L, Chiaretti S, Hornakova T, Knoops L, Ariola C, Fodale V, Clappier E, Paoloni F, Martinelli S, Fragale A, Sanchez M, Tavolaro S, Messina M, Cazzaniga G, Camera A, Pizzolo G, Tornesello A, Vignetti M, Battistini A, Cavé H, Gelb BD, Renauld J-C, Biondi A, Constantinescu SN, Foà R, Tartaglia M. Somatically acquired JAK1 mutations in adult acute lymphoblastic leukemia. Journal of Experimental Medicine. 2008;205:751–8.

103. Jeong EG, Kim MS, Nam HK, Min CK, Lee S, Chung YJ, Yoo NJ, Lee SH. Somatic Mutations of JAK1 and JAK3 in Acute Leukemias and Solid Cancers. Clin Cancer Res. 2008;14:3716–21.

104. Zhang J, Ding L, Holmfeldt L, Wu G, Heatley SL, Payne-Turner D, Easton J, Chen X, Mullighan CG, et al. The genetic basis of early T-cell precursor acute lymphoblastic leukaemia. Nature. 2012;481:157–63.

105. Bellanger D, Jacquemin V, Chopin M, Pierron G, Bernard OA, Ghysdael J, Stern M-H. Recurrent JAK1 and JAK3 somatic mutations in T-cell prolymphocytic leukemia. Leukemia. 2014;28:417–9.

106. Kiel MJ, Velusamy T, Rolland D, Sahasrabuddhe AA, Chung F, Bailey NG, Schrader A, Li B, Li JZ, Ozel AB, Betz BL, Miranda RN, Medeiros LJ, Zhao L, Herling M, Lim MS, Elenitoba-Johnson KSJ. Integrated genomic sequencing reveals mutational landscape of T-cell prolymphocytic leukemia. Blood. 2014;124:1460–72.

107. Xiang Z, Zhao Y, Mitaksov V, Fremont DH, Kasai Y, Molitoris A, Ries RE, Miner TL, McLellan MD, DiPersio JF, Link DC, Payton JE, Graubert TA, Watson M, Shannon W, Heath SE, Nagarajan R, Mardis ER, Wilson RK, Ley TJ, Tomasson MH. Identification of somatic JAK1 mutations in patients with acute myeloid leukemia. Blood. 2008;111:4809–12.

108. Kan Z, Zheng H, Liu X, Li S, Barber TD, Gong Z, Gao H, Hao K, Willard MD, Xu J, Hauptschein R, Rejto PA, Fernandez J, Wang G, Zhang Q, Wang B, Chen R, Wang J, Lee NP, Zhou W, Lin Z, Peng Z, Yi K, Chen S, Li L, Fan X, Yang J, Ye R, Ju J, Wang K, Estrella H, Deng S, Wei P, Qiu M, Wulur IH, Liu J, Ehsani ME, Zhang C, Loboda A, Sung WK, Aggarwal A, Poon RT, Fan ST, Wang J, Hardwick J, Reinhard C, Dai H, Li Y, Luk JM, Mao M. Whole-genome sequencing identifies recurrent mutations in hepatocellular carcinoma. Genome Res. 2013;23:1422–33.

109. Ren Y, Zhang Y, Liu RZ, Fenstermacher DA, Wright KL, Teer JK, Wu J. JAK1 truncating mutations in gynecologic cancer define new role of cancer-associated protein tyrosine kinase aberrations. Scientific Reports. 2013;3:3042.

110. Küçük C, Jiang B, Hu X, Zhang W, Chan JKC, Xiao W, Lack N, Alkan C, Williams JC, Avery KN, Kavak P, Scuto A, Sen E, Gaulard P, Staudt L, Iqbal J, Zhang W, Cornish A, Gong Q, Yang Q, Sun H, d'Amore F, Leppä S, Liu W, Fu K, de Leval L, McKeithan T, Chan WC. Activating mutations of STAT5B and STAT3 in lymphomas derived from γδ-T or NK cells. Nat Commun. 2015;6:6025.

111. Maronpot RR, Nyska A, Foreman JE, Ramot Y. The legacy of the F344 rat as a cancer bioassay model (a retrospective summary of three common F344 rat neoplasms). Crit Rev Toxicol. 2016;46:641–75.

112. Stromberg PC. Large granular lymphocyte leukemia in F344 rats. Model for human T gamma lymphoma, malignant histiocytosis, and T-cell chronic lymphocytic leukemia. Am J Pathol. 1985;119:517–9.

113. Reynolds CW, Timonen T, Herberman RB. Natural killer (NK) cell activity in the rat. I. Isolation and characterization of the effector cells. The Journal of Immunology. 1981;127:282–7.

114. Losco PE, Ward JM. The Early Stage of Large Granular Lymphocyte Leukemia in the F344 Rat. Vet Pathol. 1984;21:286–91.

115. Thomas J, Haseman JK, Goodman JI, Ward JM, Loughran TP, Spencer PJ. A Review of Large Granular Lymphocytic Leukemia in Fischer 344 Rats as an Initial Step Toward Evaluating the Implication of the Endpoint to Human Cancer Risk Assessment. Toxicol Sci. 2007;99:3–19.

116. Ward JM, Reynolds CW. Large granular lymphocyte leukemia. A heterogeneous lymphocytic leukemia in F344 rats. Am J Pathol. 1983;111:1–10.

117. Reynolds CW, Bere EW, Ward JM. Natural killer activity in the rat. III. Characterization of transplantable large granular lymphocyte (LGL) leukemias in the F344 rat. The Journal of Immunology. 1984;132:534–40.

118. Ryan JC, Niemi EC, Nakamura MC. Functional analysis of natural killer cell receptors in the RNK-16 rat leukemic cell line. Methods Mol Biol. 2000;121:283–95.

119. Axberg I, Nose M, Reynolds CW, Wigzell H. Features of the in Vitro Established Rat Large Granular Lymphocyte Leukaemia RNK-16. Scandinavian Journal of Immunology. 1988;27:271–8.

120. Ishmael J, Dugard PH. A review of perchloroethylene and rat mononuclear cell leukemia. Regulatory Toxicology and Pharmacology. 2006;45:178–84.

121. Reynolds CW, Foon KA. T gamma-lymphoproliferative disease and related disorders in humans and experimental animals: a review of the clinical, cellular, and functional characteristics. Blood. 1984;64:1146–58.

122. Li H. Aligning sequence reads, clone sequences and assembly contigs with BWA-MEM. arXiv:13033997 [q-bio] [Internet]. 2013 [cited 2019 Sep 10]; Available from: http://arxiv.org/abs/1303.3997

123. Faust GG, Hall IM. SAMBLASTER: fast duplicate marking and structural variant read extraction. Bioinformatics. 2014;30:2503–5.

124. Li H, Handsaker B, Wysoker A, Fennell T, Ruan J, Homer N, Marth G, Abecasis G, Durbin R, 1000 Genome Project Data Processing Subgroup. The Sequence Alignment/Map format and SAMtools. Bioinformatics. 2009;25:2078–9.

125. Olshen AB, Venkatraman ES, Lucito R, Wigler M. Circular binary segmentation for the analysis of array-based DNA copy number data. Biostatistics. 2004;5:557–72.

126. Garrison E, Marth G. Haplotype-based variant detection from short-read sequencing. :20.

127. Chiang C, Layer RM, Faust GG, Lindberg MR, Rose DB, Garrison EP, Marth GT, Quinlan AR, Hall IM. SpeedSeq: Ultra-fast personal genome analysis and interpretation. Nat Methods. 2015;12:966–8.

128. Cingolani P, Platts A, Wang LL, Coon M, Nguyen T, Wang L, Land SJ, Lu X, Ruden DM. A program for annotating and predicting the effects of single nucleotide polymorphisms, SnpEff: SNPs in the genome of Drosophila melanogaster strain w1118; iso-2; iso-3. Fly (Austin). 2012;6:80–92.

129. Hermsen R, de Ligt J, Spee W, Blokzijl F, Schäfer S, Adami E, Boymans S, Flink S, van Boxtel R, van der Weide RH, Aitman T, Hübner N, Simonis M, Tabakoff B, Guryev V, Cuppen E. Genomic landscape of rat strain and substrain variation. BMC Genomics. 2015;16:357.

130. Ye J, Coulouris G, Zaretskaya I, Cutcutache I, Rozen S, Madden TL. Primer-BLAST: a tool to design target-specific primers for polymerase chain reaction. BMC Bioinformatics. 2012;13:134.

131. Sondka Z, Bamford S, Cole CG, Ward SA, Dunham I, Forbes SA. The COSMIC Cancer Gene Census: describing genetic dysfunction across all human cancers. Nat Rev Cancer. 2018;18:696–705.

132. Kim M, Rhee J-K, Choi H, Kwon A, Kim J, Lee GD, Jekarl DW, Lee S, Kim Y, Kim T-M. Passage-dependent accumulation of somatic mutations in mesenchymal stromal cells during in vitro culture revealed by whole genome sequencing. Sci Rep [Internet]. 2017 [cited 2019 Sep 12];7. Available from: https://www.ncbi.nlm.nih.gov/pmc/articles/PMC5674020/

133. Coppe A, Andersson EI, Binatti A, Gasparini VR, Bortoluzzi S, Clemente M, Herling M, Maciejewski J, Mustjoki S, Bortoluzzi S. Genomic landscape characterization of large granular lymphocyte leukemia with a systems genetics approach. Leukemia. 2017;31:1243–6.

134. Klein K, Witalisz-Siepracka A, Maurer B, Prinz D, Heller G, Leidenfrost N, Prchal-Murphy M, Suske T, Moriggl R, Sexl V. STAT5B N642H drives transformation of NKT cells: a novel mouse model for CD56 + T-LGL leukemia. Leukemia. 2019;33:2336–40.

135. Arulogun SO, Choong H-L, Taylor D, Ambrosoli P, Magor G, Irving IM, Keng T-B, Perkins AC. JAK1 somatic mutation in a myeloproliferative neoplasm. Haematologica. 2017;102:e324–7.

136. Gordon GM, Lambert QT, Daniel KG, Reuther GW. Transforming JAK1 mutations exhibit differential signalling, FERM domain requirements and growth responses to interferon-γ. Biochem J. 2010;432:255–65.

137. Liu KD, Gaffen SL, Goldsmith MA, Greene WC. Janus kinases in interleukin-2-mediated signaling: JAK1 and JAK3 are differentially regulated by tyrosine phosphorylation. Current Biology. 1997;7:817–26.

138. Haan S, Margue C, Engrand A, Rolvering C, Leur HS-V de, Heinrich PC, Behrmann I, Haan C. Dual Role of the Jak1 FERM and Kinase Domains in Cytokine Receptor Binding and in Stimulation-Dependent Jak Activation. The Journal of Immunology. 2008;180:998–1007.

139. Witalisz-Siepracka A, Klein K, Prinz D, Leidenfrost N, Schabbauer G, Dohnal A, Sexl V. Loss of JAK1 Drives Innate Immune Deficiency. Front Immunol. 2018;9:3108.

140. Cho J, Chang YH, Heo YJ, Kim S, Kim NK, Park JO, Kang WK, Lee J, Kim K-M. Four distinct immune microenvironment subtypes in gastric adenocarcinoma with special reference to microsatellite instability. ESMO Open [Internet]. 2018 [cited 2019 Sep 12];3. Available from: https://www.ncbi.nlm.nih.gov/pmc/articles/PMC5890063/

141. Gotthardt D, Sexl V. STATs in NK-Cells: The Good, the Bad, and the Ugly. Front Immunol [Internet]. 2017 [cited 2019 Sep 12];7. Available from: https://www.ncbi.nlm.nih.gov/pmc/articles/PMC5241313/

142. Bromberg JF, Wrzeszczynska MH, Devgan G, Zhao Y, Pestell RG, Albanese C, Darnell JE. Stat3 as an Oncogene. Cell. 1999;98:295–303.

143. Delgoffe GM, Vignali DAA. STAT heterodimers in immunity. JAKSTAT [Internet]. 2013 [cited 2018 Nov 27];2. Available from: https://www.ncbi.nlm.nih.gov/pmc/articles/PMC3670269/

144. Durant L, Watford WT, Ramos HL, Laurence A, Vahedi G, Wei L, Takahashi1 H, Sun H-W, Kanno Y, Powrie F, O'Shea JJ. Diverse Targets of the Transcription Factor STAT3 Contribute to T Cell Pathogenicity and Homeostasis. Immunity. 2010;32:605–15.

145. Forbes LR, Milner J, Haddad E. STAT3: A year in Review. Curr Opin Hematol. 2016;23:23–7.

146. Shi M, He R, Feldman AL, Viswanatha DS, Jevremovic D, Chen D, Morice WG. STAT3 mutation and its clinical and histopathologic correlation in T-cell large granular lymphocytic leukemia. Human Pathology. 2018;73:74–81.

147. Fasan A, Kern W, Grossmann V, Haferlach C, Haferlach T, Schnittger S. *STAT3* mutations are highly specific for large granular lymphocytic leukemia. Leukemia. 2013;27:1598–600.

148. Cibulskis K, Lawrence MS, Carter SL, Sivachenko A, Jaffe D, Sougnez C, Gabriel S, Meyerson M, Lander ES, Getz G. Sensitive detection of somatic point mutations in impure and heterogeneous cancer samples. Nat Biotechnol. Nature Publishing Group; 2013;31:213–9.

149. Saunders CT, Wong WSW, Swamy S, Becq J, Murray LJ, Cheetham RK. Strelka: accurate somatic small-variant calling from sequenced tumor-normal sample pairs. Bioinformatics. 2012;28:1811–7.

150. Cheng J, Zhang D, Zhou C, Marasco WA. Down-regulation of SHP1 and up-regulation of negative regulators of JAK/STAT signaling in HTLV-1 transformed cell lines and freshly transformed human peripheral blood CD4+ T-cells. Leuk Res. 2004;28:71–82.

151. Fan L-C, Teng H-W, Shiau C-W, Tai W-T, Hung M-H, Yang S-H, Jiang J-K, Chen K-F. Pharmacological Targeting SHP-1-STAT3 Signaling Is a Promising Therapeutic Approach for the Treatment of Colorectal Cancer. Neoplasia. 2015;17:687–96.

152. Liu C-Y, Tseng L-M, Su J-C, Chang K-C, Chu P-Y, Tai W-T, Shiau C-W, Chen K-F. Novel sorafenib analogues induce apoptosis through SHP-1 dependent STAT3 inactivation in human breast cancer cells. Breast Cancer Res. 2013;15:R63.

153. Palmer DC, Restifo NP. Suppressors of Cytokine Signaling (SOCS) in T cell differentiation, maturation, and function. Trends Immunol. 2009;30:592–602.

154. Dabir S, Kluge A, Dowlati A. The association and nuclear translocation of the PIAS3-STAT3 complex is ligand and time dependent. Mol Cancer Res. 2009;7:1854–60.

155. Yuan J, Zhang F, Niu R. Multiple regulation pathways and pivotal biological functions of STAT3 in cancer. Sci Rep [Internet]. 2015 [cited 2020 Apr 16];5. Available from: https://www.ncbi.nlm.nih.gov/pmc/articles/PMC4668392/

156. Abbas R, McColl KS, Kresak A, Yang M, Chen Y, Fu P, Wildey G, Dowlati A. PIAS3 expression in squamous cell lung cancer is low and predicts overall survival. Cancer Med. 2015;4:325–32.

157. Kluge A, Dabir S, Vlassenbroeck I, Eisenberg R, Dowlati A. Protein inhibitor of activated STAT3 expression in lung cancer. Molecular Oncology. 2011;5:256–64.

158. Kluge A, Dabir S, Kern J, Nethery D, Halmos B, Ma P, Dowlati A. Cooperative interaction between protein inhibitor of activated signal transducer and activator of transcription-3 with epidermal growth factor receptor blockade in lung cancer. Int J Cancer. 2009;125:1728–34.

159. Lai R, Rassidakis GZ, Medeiros LJ, Ramdas L, Goy AH, Cutler C, Fujio Y, Kunisada K, Amin HM, Gilles F. Signal Transducer and Activator of Transcription-3 Activation Contributes to High Tissue Inhibitor of Metalloproteinase-1 Expression in Anaplastic Lymphoma Kinase-Positive Anaplastic Large Cell Lymphoma. Am J Pathol. 2004;164:2251–8.

160. Han Y, Amin HM, Franko B, Frantz C, Shi X, Lai R. Loss of SHP1 enhances JAK3/STAT3 signaling and decreases proteosome degradation of JAK3 and NPM-ALK in ALK+ anaplastic large-cell lymphoma. Blood. 2006;108:2796–803.

161. Peyser ND, Freilino M, Wang L, Zeng Y, Li H, Johnson DE, Grandis JR. Frequent promoter hypermethylation of PTPRT increases STAT3 activation and sensitivity to STAT3 inhibition in head and neck cancer. Oncogene. 2016;35:1163–9.

162. Becker S, Groner B, Müller CW. Three-dimensional structure of the Stat3beta homodimer bound to DNA. Nature. 1998;394:145–51.

163. Huang G, Yan H, Ye S, Tong C, Ying Q-L. STAT3 Phosphorylation at Tyrosine 705 and Serine 727 Differentially Regulates Mouse ESC Fates. Stem Cells. 2014;32:1149–60.

164. Wakahara R, Kunimoto H, Tanino K, Kojima H, Inoue A, Shintaku H, Nakajima K. Phospho-Ser727 of STAT3 regulates STAT3 activity by enhancing dephosphorylation of phospho-Tyr705 largely through TC45. Genes Cells. 2012;17:132–45.

165. Qin HR, Kim H-J, Kim J-Y, Hurt EM, Klarmann GJ, Kawasaki BT, Duhagon Serrat MA, Farrar WL. Activation of signal transducer and activator of transcription 3

through a phosphomimetic serine 727 promotes prostate tumorigenesis independent of tyrosine 705 phosphorylation. Cancer Res. 2008;68:7736–41.

166. Chung CD, Liao J, Liu B, Rao X, Jay P, Berta P, Shuai K. Specific Inhibition of Stat3 Signal Transduction by PIAS3. Science. 1997;278:1803–5.

167. Jain N, Zhang T, Fong SL, Lim CP, Cao X. Repression of Stat3 activity by activation of mitogen-activated protein kinase (MAPK). Oncogene. 1998;17:3157–67.

168. Meier JA, Larner AC. Toward a new STATe: the role of STATs in mitochondrial function. Semin Immunol. 2014;26:20–8.

169. Waldmann TA. The interleukin-2 receptor. J Biol Chem. 1991;266:2681–4.

170. Nata T, Basheer A, Cocchi F, Besien R van, Massoud R, Jacobson S, Azimi N, Tagaya Y. Targeting the Binding Interface on a Shared Receptor Subunit of a Cytokine Family Enables the Inhibition of Multiple Member Cytokines with Selectable Target Spectrum. J Biol Chem. 2015;290:22338–51.

171. Yamagishi M, Watanabe T. Molecular Hallmarks of Adult T Cell Leukemia. Front Microbiol [Internet]. 2012 [cited 2017 Sep 12];3. Available from: http://www.ncbi.nlm.nih.gov/pmc/articles/PMC3444139/

172. Kips JC. Cytokines in asthma. European Respiratory Journal. 2001;18:24s–33s.

173. Wasik MA, Sackstein R, Novick D, Butmarc JR, Zhang Q, Vonderheid EC, Kadin ME. Cutaneous CD56+ large T-cell lymphoma associated with high serum concentration of IL-2. Hum Pathol. 1996;27:738–44.

174. Marzec M, Halasa K, Kasprzycka M, Wysocka M, Liu X, Tobias JW, Baldwin D, Zhang Q, Odum N, Rook AH, Wasik MA. Differential effects of interleukin-2 and interleukin-15 versus interleukin-21 on CD4+ cutaneous T-cell lymphoma cells. Cancer Res. 2008;68:1083–91.

175. Ribeiro ST, Ribot JC, Silva-Santos B. Five Layers of Receptor Signaling in γδ T-Cell Differentiation and Activation. Front Immunol [Internet]. 2015 [cited 2018 Mar 23];6. Available from: https://www.ncbi.nlm.nih.gov/pmc/articles/PMC4306313/

176. Ito M, Zhao N, Zeng Z, Zhou X, Chang C-C, Zu Y. Interleukin-2 Functions in Anaplastic Large Cell Lymphoma Cells through Augmentation of Extracellular Signal-Regulated Kinases 1/2 Activation. Int J Biomed Sci. 2011;7:181–90.

177. Mishra A, Liu S, Sams GH, Curphey DP, Santhanam R, Rush LJ, Schaefer D, Falkenberg LG, Sullivan L, Jaroncyk L, Yang X, Fisk H, Wu L-C, Hickey C, Chandler JC, Wu Y-Z, Heerema NA, Chan KK, Perrotti D, Zhang J, Porcu P, Racke FK, Garzon R, Lee RJ, Marcucci G, Caligiuri MA. Aberrant overexpression of IL-15 initiates large granular lymphocyte leukemia through chromosomal instability and DNA hypermethylation. Cancer Cell. 2012;22:645–55.

178. Tabbó F, Barreca A, Piva R, Inghirami G. ALK Signaling and Target Therapy in Anaplastic Large Cell Lymphoma. Front Oncol [Internet]. 2012 [cited 2018 Mar 22];2. Available from: https://www.ncbi.nlm.nih.gov/pmc/articles/PMC3355932/

179. Krejsgaard T, Ralfkiaer U, Clasen-Linde E, Eriksen KW, Kopp KL, Bonefeld CM, Geisler C, Dabelsteen S, Wasik MA, Ralfkiaer E, Woetmann A, Odum N. Malignant cutaneous T-cell lymphoma cells express IL-17 utilizing the Jak3/Stat3 signaling pathway. J Invest Dermatol. 2011;131:1331–8.

180. Dahmoush L, Hijazi Y, Barnes E, Stetler-Stevenson M, Abati A. Adult T-cell leukemia/lymphoma. Cancer. 2002;96:110–6.

181. Malamut G, El Machhour R, Montcuquet N, Martin-Lannerée S, Dusanter-Fourt I, Verkarre V, Mention J-J, Rahmi G, Kiyono H, Butz EA, Brousse N, Cellier C, Cerf-Bensussan N, Meresse B. IL-15 triggers an antiapoptotic pathway in human intraepithelial lymphocytes that is a potential new target in celiac disease-associated inflammation and lymphomagenesis. J Clin Invest. 2010;120:2131–43.

182. Shah MV, Zhang R, Loughran TP. Never Say Die: Survival Signaling in Large Granular Lymphocyte Leukemia. Clin Lymphoma Myeloma. 2009;9:S244–53.

183. Zhang D, Loughran TP. Large granular lymphocytic leukemia: molecular pathogenesis, clinical manifestations, and treatment. Hematology. 2012;2012:652–9.

184. Chen J, Petrus M, Bryant BR, Nguyen VP, Goldman CK, Bamford R, Morris JC, Janik JE, Waldmann TA. Autocrine/paracrine cytokine stimulation of leukemic cell proliferation in smoldering and chronic adult T-cell leukemia. Blood. 2010;116:5948–56.

185. Tendler CL, Greenberg SJ, Blattner WA, Manns A, Murphy E, Fleisher T, Hanchard B, Morgan O, Burton JD, Nelson DL. Transactivation of interleukin 2 and its receptor induces immune activation in human T-cell lymphotropic virus type I-associated myelopathy: pathogenic implications and a rationale for immunotherapy. Proc Natl Acad Sci USA. 1990;87:5218–22.

186. Mariner JM, Lantz V, Waldmann TA, Azimi N. Human T cell lymphotropic virus type I Tax activates IL-15R alpha gene expression through an NF-kappa B site. J Immunol. 2001;166:2602–9.

187. Ju W, Zhang M, Jiang J, Thomas CJ, Oh U, Bryant BR, Chen J, Sato N, Tagaya Y, Morris JC, Janik JE, Jacobson S, Waldmann TA. CP-690,550, a therapeutic agent, inhibits cytokine-mediated Jak3 activation and proliferation of T cells from patients with ATL and HAM/TSP. Blood. 2011;117:1938–46.

188. Waldmann TA, White JD, Goldman CK, Top L, Grant A, Bamford R, Roessler E, Horak ID, Zaknoen S, Kasten-Sportes C. The interleukin-2 receptor: a target for monoclonal antibody treatment of human T-cell lymphotrophic virus I-induced adult T-cell leukemia. Blood. 1993;82:1701–12.

189. Dubois S, Shou W, Haneline LS, Fleischer S, Waldmann TA, Müller JR. Distinct pathways involving the FK506-binding proteins 12 and 12.6 underlie IL-2-versus IL-15-mediated proliferation of T cells. Proc Natl Acad Sci USA. 2003;100:14169–74.

190. Berkowitz JL, Janik JE, Stewart DM, Jaffe ES, Stetler-Stevenson M, Shih JH, Fleisher TA, Turner M, Urquhart NE, Wharfe GH, Figg WD, Peer CJ, Goldman CK, Waldmann TA, Morris JC. Safety, efficacy, and pharmacokinetics/pharmacodynamics of daclizumab (anti-CD25) in patients with adult T-cell leukemia/lymphoma. Clin Immunol. 2014;155:176–87.

191. Waldmann TA. JAK/STAT pathway directed therapy of T-cell leukemia/lymphoma: Inspired by functional and structural genomics. Mol Cell Endocrinol. 2017;451:66–70.

192. Massoud R, Enose-Akahata Y, Tagaya Y, Azimi N, Basheer A, Jacobson S. Common γ-chain blocking peptide reduces in vitro immune activation markers in HTLV-1-associated myelopathy/tropical spastic paraparesis. PNAS. 2015;112:11030–5.

193. Frohna P, Tagaya Y, Ratnayake A, Doerr N, Basheer A, Al-Mawsawi L, Kim WJ, Zapata J, Wu X, Azimi N. Results from a First-in-Human Study with Bnz-1: A Novel Peptide Inhibitor of IL-2, IL-9 and IL-15 for the Treatment of T-Cell Malignancies That Safely and Selectively Decreases Regulatory T-Cells, Natural Killer Cells, and CD8+ Central Memory T-Cells. Blood. 2017;130:695–695.

194. Robertson MJ, Cochran KJ, Cameron C, Le JM, Tantravahi R, Ritz J. Characterization of a cell line, NKL, derived from an aggressive human natural killer cell leukemia. Exp Hematol. 1996;24:406–15.

195. Otani H, Siegel JP, Erdos M, Gnarra JR, Toledano MB, Sharon M, Mostowski H, Feinberg MB, Pierce JH, Leonard WJ. Interleukin (IL)-2 and IL-3 induce distinct but overlapping responses in murine IL-3-dependent 32D cells transduced with human IL-2 receptor beta chain: involvement of tyrosine kinase(s) other than p56lck. Proc Natl Acad Sci USA. 1992;89:2789–93.

196. Maeda M, Shimizu A, Ikuta K, Okamoto H, Kashihara M, Uchiyama T, Honjo T, Yodoi J. Origin of human T-lymphotrophic virus I-positive T cell lines in adult T cell leukemia. Analysis of T cell receptor gene rearrangement. J Exp Med. 1985;162:2169–74.

197. Olson KC, Kulling PM, Olson TL, Tan S-F, Rainbow RJ, Feith DJ, Loughran TP. Vitamin D decreases STAT phosphorylation and inflammatory cytokine output in T-LGL leukemia. Cancer Biol Ther. 2017;18:290–303.

198. Nicot C, Mahieux R, Takemoto S, Franchini G. Bcl-XL is up-regulated by HTLV-I and HTLV-II in vitro and in ex vivo ATLL samples. Blood. 2000;96:275–81.

199. Zhang M, Mathews Griner LA, Ju W, Duveau DY, Guha R, Petrus MN, Wen B, Maeda M, Shinn P, Ferrer M, Conlon KD, Bamford RN, O'Shea JJ, Thomas CJ, Waldmann TA. Selective targeting of JAK/STAT signaling is potentiated by Bcl-xL blockade in IL-2–dependent adult T-cell leukemia. Proc Natl Acad Sci U S A. 2015;112:12480–5.

200. Sato N, Sabzevari H, Fu S, Ju W, Petrus MN, Bamford RN, Waldmann TA, Tagaya Y. Development of an IL-15-autocrine CD8 T-cell leukemia in IL-15-transgenic mice requires the cis expression of IL-15Rα. Blood. 2011;117:4032–40.

201. Matsuda T, Muromoto R, Sekine Y, Togi S, Kitai Y, Kon S, Oritani K. Signal transducer and activator of transcription 3 regulation by novel binding partners. World J Biol Chem. 2015;6:324–32.

202. Togi S, Muromoto R, Hirashima K, Kitai Y, Okayama T, Ikeda O, Matsumoto N, Kon S, Sekine Y, Oritani K, Matsuda T. A New STAT3-binding Partner, ARL3, Enhances the Phosphorylation and Nuclear Accumulation of STAT3. J Biol Chem. 2016;291:11161–71.

203. Huang G, Lu H, Hao A, Ng DCH, Ponniah S, Guo K, Lufei C, Zeng Q, Cao X. GRIM-19, a cell death regulatory protein, is essential for assembly and function of mitochondrial complex I. Mol Cell Biol. 2004;24:8447–56.

204. Steinway SN, Loughran TP. Targeting IL-15 in large granular lymphocyte leukemia. Expert Rev Clin Immunol. 2013;9:405–8.

205. Gloss BS, Dinger ME. Realizing the significance of noncoding functionality in clinical genomics. Experimental & Molecular Medicine. Nature Publishing Group; 2018;50:1–8.

206. LeBlanc F, Zhang D, Liu X, Loughran TP. Large granular lymphocyte leukemia: from dysregulated pathways to therapeutic targets. Future Oncology. Future Medicine; 2012;8:787–801.

207. Verma K, Ogonek J, Varanasi P, Luther S, Buenting I, Thomay K, Behrens YL, Mischak-Weissinger E, Hambach L. Human CD8+ CD57- TEMRA cells: Too young to be called "old." PloS one. 2017.

208. Harty JT, Badovinac VP. Shaping and reshaping CD8+ T-cell memory. Nat Rev Immunol. 2008;8:107–19.

209. Buenrostro J, Wu B, Chang H, Greenleaf W. ATAC-seq: A Method for Assaying Chromatin Accessibility Genome-Wide. Curr Protoc Mol Biol. 2015;109:21.29.1-21.29.9.

210. Davie K, Jacobs J, Atkins M, Potier D, Christiaens V, Halder G, Aerts S. Discovery of Transcription Factors and Regulatory Regions Driving In Vivo Tumor

Development by ATAC-seq and FAIRE-seq Open Chromatin Profiling. PLOS Genet. 2015;11:e1004994.

211. Buenrostro JD, Giresi PG, Zaba LC, Chang HY, Greenleaf WJ. Transposition of native chromatin for fast and sensitive epigenomic profiling of open chromatin, DNA-binding proteins and nucleosome position. Nat Meth. 2013;10:1213–8.

212. Quinlan AR, Hall IM. BEDTools: a flexible suite of utilities for comparing genomic features. Bioinformatics. Oxford Academic; 2010;26:841–2.

213. Zhang Y, Liu T, Meyer CA, Eeckhoute J, Johnson DS, Bernstein BE, Nusbaum C, Myers RM, Brown M, Li W, Liu XS. Model-based Analysis of ChIP-Seq (MACS). Genome Biol. 2008;9:R137.

214. Love MI, Huber W, Anders S. Moderated estimation of fold change and dispersion for RNA-seq data with DESeq2. Genome Biology. 2014;15:550.

215. McLean CY, Bristor D, Hiller M, Clarke SL, Schaar BT, Lowe CB, Wenger AM, Bejerano G. GREAT improves functional interpretation of cis-regulatory regions. Nat Biotechnol. 2010;28:495–501.

216. Viny AD, Lichtin A, Pohlman B, Loughran T, Maciejewski J. Chronic B-cell dyscrasias are an important clinical feature of T-LGL leukemia. Leuk Lymphoma. 2008;49:932–8.